UNIVERSITÀ DEGLI STUDI FIRENZE

DOTTORATO DI RICERCA IN

Scienze Agrarie e Ambientali

CICLO XXXV

COORDINATORE Prof. Pietramellara Giacomo

Assessing grassland development by means of modelling and remote sensing approaches: current situation and future projections

Settore Scientifico Disciplinare AGR/02

Dottorando
Dott. Bellini Edoardo

Tutore
Prof. Argenti Giovanni

Cotutori
Dott. Moriondo Marco

Dott.ssa Dibari Camilla

Coordinatore
Prof. Pietramellara Giacomo

Anni 2019/2022

Supervisor

Prof. Argenti Giovanni

Department of Agriculture, Food, Environment and Forestry (DAGRI)

University of Florence

Piazzale delle Cascine 18, 50144, Florence, Italy

Phone: +39 0552755747

Email: giovanni.argenti@unifi.it

Co-supervisors

Dr. Dibari Camilla

Department of Agriculture, Food, Environment and Forestry (DAGRI)

University of Florence

Piazzale delle Cascine 18, 50144, Florence, Italy

Phone: +39 0552755703

Email: camilla.dibari@unifi.it

Dr. Moriondo Marco

Institute of BioEconomy, Italian National Research Council (IBE-CNR)

Via Caproni 8, 50145, Florence, Italy

Department of Agriculture, Food, Environment and Forestry (DAGRI)

University of Florence

Piazzale delle Cascine 18, 50144, Florence, Italy

Phone: +39 0553288257

Email: marco.moriondo@cnr.it

Table of Contents

Abstract

Grasslands, covering about 70% of agricultural land and 15% of the non-water area on a global scale, represent a key food source for animal production systems and provide a wide range of ecosystem benefits, including water and nutrient regulation, biodiversity conservation, and carbon storage. However, the provisioning of these functions is dependent on the efficient use of the herbaceous resources through agronomic management and, at the same time, is influenced by current and future climate changes (forage production, quality, phenology, botanical composition, biodiversity, etc.). Thus, proper management and the assessment of possible current and future risks related to climate change appear necessary in order to preserve the production and ecosystem functionality of grasslands.

In this sense, the potential offered by methodologies such as remote sensing and crop modelling represent a great opportunity to analyze the status of grasslands and predict their future trends.

The main objective of this research was to test, validate and assess different approaches, namely modelling and remote sensing technologies, to monitor growth of grassland vegetation in its current state and according to future projections.

Specifically, the aims of this PhD thesis were: 1) the development of a simplified simulation model for reproducing grassland system growth and production; 2) the evaluation of climate change-induced phenological changes of grassland ecosystems along the recent decades by using remote sensing technologies; 3) the assessment of potential changes caused by future climate and the identification of possible adaptation strategies for grassland management through the application of a biogeochemical process-based simulation model.

With particular reference to objective 1, Chapter 3 presents the structure of a simulation model that uses the Normalized Difference Vegetation Index as proxy to estimate structural characteristics of vegetation (i.e. Leaf Are Index), thus simplifying the calibration of numerous parameters. Through the use of specific equations for reproducing the physiological, chemical and biological processes of the system and the adoption of NDVI from proximal and remote sensing data, the model provides, as output, forage production (above ground biomass) and water conditions of the system along the season. The simplified model, calibrated and validated in different environments, obtained robust results in simulating grassland aboveground biomass, as well as water dynamics (fraction of transpirable soil water and evapotranspiration), under different management, with few input required (e.g. minimum and maximum daily temperature, precipitation, solar radiation and soil texture). It can therefore represent an important tool for optimizing grassland management.

Chapter 4 answers the questions of objective 2, investigating, through long time series of MODIS satellite imagery, the impacts of climate change already visible in European grassland phenology over the period 2001-2021. The study offers a comprehensive methodological analysis regarding the optimal procedure to use for extracting the dates of the start (SOS), peak (POS) and end (EOS) of growing season from remote sensing data and, then, quantify the phenological changes observed from MODIS satellite imagery. The extent of these changes was then evaluated in light of the specific characteristics of the test sites, specifically average winter and spring temperatures during the years 2001-2021, altitude and latitude of the analysed grasslands. Results of the study highlight a significant advance of SOS and POS in most of the tested grassland, while EOS proved to be difficult to detect. Finally, the impacts of future climate on grazing systems and the evaluation of specific management strategies are reported in Chapter 5. In this section, future projections in two pastures of the central Italian Apennines were performed by using a grassland simulation model (Pasture Simulation Model, PaSim, Riedo et al., 1998) under two time slices (i.e. 2011-2040 and 2041-2070) and future scenarios (RCP4.5 and 8.5). The simulations analyzed future forage production, length of growing season, hydrological status and green-house gas emissions. Alternative management strategies, involving changing of grazing season length and animal stocking rate, were tested to cope with future changes in extensive grazing systems simulated by the model. Results showed a significant increase in future grassland aboveground biomass in studied forage systems, allowing higher stocking rate and grazing period as adaptation strategies.

The evaluation of growth development at the present time with remote sensing and modelling technologies proved to be a fundamental step to better understanding the state of the system under the growing season. The gathered information highlighted the potential of these technologies to optimize grassland management. On the other hand, the assessment of the climate change-induced impacts, at the current moment and in future projections, represent the prerequisite for the adoption of adaptation and mitigation strategies that can cope with the difficulties resulting from changes in the grassland system.

Riassunto

Le praterie, vocabolo con il quale è stato tradotto in questa tesi il termine inglese “grassland”, coprono circa il 70% dei terreni agricoli e il 15% della superficie terrestre su scala globale, rappresentando una fonte di alimentazione chiave per i sistemi di produzione animale e fornendo un'ampia gamma di benefici ecosistemici, tra i quali, ad esempio, la regolazione delle acque e dei nutrienti, la conservazione della biodiversità e lo stoccaggio del carbonio. Tuttavia, le funzionalità di questi sistemi dipendono da un uso efficiente della risorsa erbacea, ottenibile attraverso una gestione agronomica ottimale. Parallelamente, queste funzionalità sono, e saranno, influenzate dai cambiamenti climatici attuali e futuri, che agiscono su questi sistemi sotto diversi aspetti, come ad esempio la produzione e la qualità di foraggio, la fenologia della vegetazione, la composizione botanica e la biodiversità. Pertanto, una corretta gestione e la valutazione dei possibili rischi, già visibili e futuri, legati al cambiamento climatico appaiono azioni necessarie per preservare le funzionalità produttive ed ecosistemiche delle praterie.

In questo senso, le potenzialità offerte da due metodologie come il telerilevamento e la modellistica rappresentano una grande opportunità per l’analisi delle praterie al momento attuale e secondo proiezioni future.

L'obiettivo principale di questo dottorato di ricerca è stato dunque lo studio e l’analisi di varie tecnologie di telerilevamento e modellistica per la valutazione dell’andamento di crescita della vegetazione nel presente e nel futuro, in un’ottica di cambiamento climatico.

In particolare, gli obiettivi specifici di questa tesi di dottorato sono stati: 1) lo sviluppo di un modello di simulazione semplificato per la riproduzione del sistema prateria; 2) la valutazione dei cambiamenti fenologici, già visibili, indotti dai cambiamenti climatici negli ultimi decenni; 3) la valutazione dei potenziali impatti sulla vegetazione causati dal clima futuro e l'identificazione di possibili strategie di adattamento per la gestione delle praterie.

Con particolare riferimento all'obiettivo 1, il capitolo 3 della tesi presenta la struttura di un modello di simulazione, basato sul concetto di light-use efficiency, che utilizza l'indice di vegetazione Normalized Difference Vegetation Index (NDVI) per stimare le caratteristiche strutturali della vegetazione (Leaf Area Index), in modo da semplificare la simulazione e, conseguentemente, la calibrazione di numerosi parametri. Attraverso l'uso di equazioni specifiche per riprodurre i processi fisiologici, chimici e biologici del sistema e l'adozione dell'NDVI da dati prossimali e telerilevati, il modello è stato in grado di fornire importanti indicazioni sulla produzione foraggera e sulle condizioni idriche del sistema (frazione di acqua traspirabile ed evapotraspirazione). Il modello semplificato, calibrato e validato in diversi ambienti, ha ottenuto risultati ottimali nella simulazione

della biomassa foraggera dei pascoli, nonché delle dinamiche idriche, in diverse tipologie di gestione utilizzando un numero limitato di input (temperatura minima e massima giornaliera, precipitazioni, radiazione solare e tessitura del terreno). Il modello sviluppato nell'ambito del dottorato di ricerca può dunque rappresentare uno strumento importante per la gestione efficiente dei pascoli.

Il capitolo 4 risponde alle domande dell'obiettivo 2, indagando, attraverso lunghe serie temporali di immagini satellitari MODIS, gli impatti dei cambiamenti climatici già visibili nella fenologia delle praterie europee nel corso del periodo 2001-2021. Lo studio offre un'analisi metodologica completa sulla procedura ottimale da utilizzare per estrarre le date di inizio (SOS), picco (POS) e fine (EOS) della stagione vegetativa da dati telerilevati. La metodologia individuata è stata successivamente utilizzata per quantificare i cambiamenti fenologici osservabili dalle immagini satellitari MODIS. L'entità di questi cambiamenti è stata poi valutata alla luce delle caratteristiche specifiche dei siti di prova, in particolare delle temperature medie invernali e primaverili negli anni 2001-2021, dell'altitudine e della latitudine delle praterie analizzate. I risultati dello studio evidenziano un significativo avanzamento nelle date di SOS e POS nella maggior parte delle praterie analizzate, mentre la data di EOS si è rivelata difficile da rilevare.

Infine, nel Capitolo 5 sono stati analizzati gli impatti del clima futuro sui sistemi estensivi di pascolamento e le possibili strategie gestionali di adattamento. In questa sezione, le proiezioni future in due pascoli dell'Appennino centrale italiano sono state effettuate attraverso l'utilizzo di un modello di simulazione specifico per i prati o pascoli (PaSim, Riedo et al., 1998), in diverse finestre temporali (2011-2040 e 2041-2070) e scenari (RCP4.5 e 8.5). Le simulazioni future hanno preso in condizione la produzione futura di foraggio, la durata della stagione di crescita, lo stato idrologico e le emissioni di gas serra. Per far fronte ai futuri cambiamenti simulati da PaSim sono state testate diverse strategie di gestione, incentrate principalmente sulla modifica della durata della stagione di pascolo e/o del carico animale. I risultati della simulazione hanno evidenziato un aumento significativo di biomassa nei pascoli nell'Appennino centrale italiano per le diverse finestre temporali e per i diversi scenari. L'incremento produttivo stimato si è dimostrato sufficientemente elevato per l'adozione di strategie di adattamento basate su un carico animale e un periodo di pascolo maggiori.

La valutazione dello sviluppo di crescita con tecnologie di telerilevamento e modellistica si è dimostrata un passaggio fondamentale per la comprensione dello stato dei pascoli, mentre le informazioni raccolte ne hanno evidenziato il potenziale utilizzo per una gestione efficiente del sistema. Parallelamente, la stima degli impatti indotti dai cambiamenti climatici, allo stato attuale e nelle proiezioni future, rappresenta il prerequisito necessario per l'adozione di strategie di adattamento e di mitigazione che possano far fronte alle difficoltà derivanti dai cambiamenti futuri.

Chapter 1.

General background

Chapter 1 shows a general background on grasslands and describes the possible potential of two methodologies (i.e. remote sensing and simulation modelling) in assessing the current state and possible impacts of climate change on grassland systems.

PhD candidate's contribution:

Edoardo Bellini wrote all sections of the chapter.

1. General background

Grassland systems

The term grassland refers to a series of systems that are principally used for forage production. These environments can range from natural ecosystems (i.e. natural grasslands) characterised by the presence of indigenous and natural herbaceous species to imposed grazing-land systems (i.e. pastureland) in which vegetation is managed with sowing, grazing, cutting or the combination of the latter two (Allen et al., 2011). Consequently, grasslands play a key role in animal systems (e.g. milk and meat) (Ertl et al., 2015; Herrero et al., 2013), providing the feed necessary for protein-rich food production (Barbour et al., 2022) in the context of a steadily increasing population (UN, 2019). In addition to food and other secondary production (Boval and Dixon, 2012), grasslands can also provide a wide range of ecosystem functions: water and nutrients (e.g. nitrate and phosphorus) regulation, biodiversity conservation, landscape preservation, areas for wild animals protection, soil fertility increase and carbon storage (Tamburini et al., 2022; Wepking et al., 2022). The importance of these systems is also given by the area they cover on a global scale: about 25% of the non-water surface area (Lemaire et al., 2011) and 75% of the agricultural surface area (FAO, 2013).

In order to ensure the maintenance of these ecosystem benefits, how the pastoral resources are managed is utmost crucial. In the case of animal grazing, for example, it is necessary to properly balance the forage supply with the animal stocking rate in order to avoid cases of over- or undergrazing. Specifically, management that favours overgrazing leads to pasture degradation and desertification (Hilker et al., 2014), loss of SOC and change in botanical composition (Liu et al., 2022), seed bank reduction (Gonzalez and Ghermandi, 2021), nitrate loss (Eriksen et al., 2015) and soil compaction (Krzic et al., 2014). On the other hand, undergrazing, or land abandonment can lead to soil degradation (Quaranta et al., 2020), increased fire risk (Bajocco et al., 2011) and, above all, reduced production of the grassland-livestock system (Fernandes et al., 2022). At the same time, high-intensity mowing can also lead to changes in forage productivity (Reinhart et al., 2022), botanical composition (Piseddu et al., 2021) and a general reduction in biodiversity (Hannappel and Fischer, 2020).

It is evidence based that grasslands ecosystems are vulnerable to climate change (Dibari et al., 2020), especially when located in marginal areas. Studies analysing the observed and future impacts of climate on grassland ecosystems evidenced changes in forage production (Insua et al., 2019; Nandintsetseg et al., 2021; Zarrineh et al., 2020) which in turn altered and/or will alter dynamics in livestock systems (Fust and Schlecht, 2022; Ghahramani et al., 2019; Scocco et al., 2016), plant and

microbial biodiversity (Petriccione and Bricca, 2019; Wu et al., 2022), botanical composition (Dibari et al., 2020; Stanisci et al., 2016) and phenology (Gong et al., 2015; Ren et al., 2020; Stöckli and Vidale, 2004).

The implementation of proper management and the assessment of possible current and future risks due to climate change is pivotal to preserve forage production and ecosystem functionality.

In these contexts, approaches widely used in precision agriculture systems such as crop modelling and remote sensing may be considered also in analysing and predicting current and future grasslands ecosystems dynamics.

Remote sensing

The monitoring of grassland status, through the quantification of various production, physical, chemical or biological parameters, requires the collection of reliable data as a starting point. Traditional methods, based on ground surveys, represent a methodology capable of providing data of excellent quality, but as a disadvantage, they are cost and time-consuming, as well as generally applicable on a limited spatial scale, not suitable for regional or global analyses (Wang et al., 2022).

In this sense, remote sensing, defined as "the acquisition of information about the land, sea and atmosphere by sensors located at some distance from the target of study" (Haines-Young, 1994), has been proved to be a consistent, cost-effective, and reliable methodology to acquire data and observe vegetation growth and development (Ali et al., 2016), providing useful indications in decision-making processes of agricultural management (Hatfield et al., 2019). Remote sensing applications are generally based on the use of vegetation indices (VIs, such as NDVI), strongly related to vegetation features (e.g. LAI, standing biomass, health, height, forage quality, etc.), derived from the combination of different waveband reflectance values captured from specific sensors (Xue and Su, 2017; Bannari et al., 1995). Remote sensing images from specific optical sensors are obtained through multispectral or hyperspectral sensors (Wang et al. 2022). The former, generally more widely used, provide greater product availability and high temporal resolution, while the latter, relying on the use of a much higher number of spectral bands, enable more accurate analysis of vegetation dynamics.

Various studies on grasslands have been carried out by using multispectral satellite images obtained from different types of satellites, such as MODIS (Ding et al., 2022; Gong et al., 2015), Sentinel (Andreatta et al., 2022; Guerini Filho et al., 2020), SPOT (He et al., 2020) and LANDSAT (Guo et al., 2019), each with its own technical characteristics in terms of spatial and temporal resolution. At the same time, hyperspectral sensors have also been used in the analysis of grassland characteristics (Ling et al., 2019; Lyu et al., 2020). Furthermore, another possible application of remote sensing data for the study of grasslands is the use of satellite radar sensors, based on synthetic aperture radar (SAR)

images, for the estimation of vegetation parameters or for grassland monitoring (Braun et al., 2018; Zalite et al., 2016).

Satellite imagery has been widely applied in grassland studies to assess several aspects: forage production and quality (Askari et al., 2019; Edirisinghe et al., 2011; Lugassi et al., 2019; Serrano et al., 2019), phenology (Li et al., 2021; Tian et al., 2021), biodiversity (Bayle et al., 2019; Ma et al., 2019) or water dynamics (Xia et al., 2014). The remotely acquired images can then be used to make estimates of the status (e.g. biomass, phenology, vegetation type, etc.) of the grasslands being analysed (Shoko and Mutanga, 2017; Wang et al., 2019; Wang et al., 2019). Otherwise, especially for certain types of satellites, the long-time series of images collected by optical sensors can be analysed to estimate the extent of changes occurred over the time frame under consideration, especially to assess the impacts of climate change that are already visible (Hou et al., 2014; Huang et al., 2018; Li et al., 2021).

The spatial resolution of satellite-sensors may be considered a critical issue in remote sensing analysis, especially when satellite imageries are applied to monitor herbaceous vegetation characteristics at paddock-scale (Wu and Li, 2009). To overcome this issue, alongside satellite imageries, remote data can be collected from Unmanned Aerial Vehicle (UAV) equipped with different sensors and cameras: standard RGB cameras, multispectral and NIR cameras, hyperspectral cameras, thermal sensors and depth sensors (Hassler and Baysal-Gurel, 2019). In recent years these systems proved to be effective in analysing grassland production and quality at a finer spatial resolution (Askari et al., 2019; Murphy et al., 2019; Vong et al., 2019). Furthermore, indications on plant phenology and status conditions, in form of colour (e.g. green chromatic coordinate) or vegetation indices, can be obtained with good results from sensing instruments, such as digital cameras, settled in proximity of the target (Filippa et al., 2018; Inoue et al., 2015; Petach et al., 2014). Finally, the information collected from remote sensing techniques can also be integrated into crop growth models by forcing factors and/or model input data (Jin et al., 2018), so as to increase the accuracy of the simulation process (Huang et al., 2019) and reduce field data acquisition, well noted as time-consuming and expensive. With regard to grassland studies, major improvements concerning this issue can be foreseen in above ground biomass simulation through modelling by data assimilation from satellite imageries (He et al., 2015).

Grassland system modelling

Over last decades, crop simulation models have been widely utilized to understand and predict biophysical processes through a mechanistic representation of agricultural systems (Ehrhardt et al., 2018b; Snow et al., 2014), including grazing land systems (Ma et al., 2019). Compared to generic

crop models, those focused on grasslands entail some challenges, such as simulating processes related to plants diversity, animal-plant interactions and animal mobility. An important application of these tools is their use in estimating the changes in the grassland system caused by future climate change, as this assessment can be performed through modelling exercises (Morales et al., 2007; Petersen et al., 2021) or by setting up long-run experiments (Brookshire and Weaver, 2015; Evangelista et al., 2016). For instance, forage production, a basic requirement for all grazing land models, has been simulated in several studies to assess future climate impacts on pasture productivity and possible adaptation strategies in grasslands (Ghahramani and Moore, 2016; Harrison et al., 2016; Moore and Ghahramani, 2013). To perform such long-term predictions, grazing land models require data on future climate that are based on the results of climate models (Flato et al., 2013), in different possible scenarios of GHGs emissions and concentrations (e.g. Representative Concentration Pathways, IPCC, 2014). In addition to this purpose, outputs of grazing land models are also useful for identifying proper management techniques, through comparisons of different agricultural practises and field conditions (Christie et al., 2018; Insua et al., 2019b; Vogeler et al., 2019). Although pasture biomass is generally well simulated on a seasonal basis (Pulina et al., 2018), improvements on forage production simulation are required in terms of temporal and spatial distribution, plant phenology and forage quality (Ma et al., 2019). Parameters needed in simulation runs are adjusted as a result of calibration processes in order to reduce model uncertainties. Currently, this is mainly achieved through a last square approach, a Bayesian approach or trial-and-error search (Seidel et al., 2018); also, sensitivity analysis has been often applied so as to identify the most influencing parameters in the simulation runs (Touhami et al., 2013). Considering model's structure, one of the most commonly used types of models is based on the concept of light use efficiency (Monteith, 1972), in which GPP is elaborated considering the incoming photosynthetically active radiation (PAR), the fraction of radiation absorbed by the vegetation (FPAR), the maximum light use efficiency, and possible environmental stress factors (Pei et al., 2022). This type of approach is also used with remote data integration, often applied for large-scale simulations (Yu et al., 2020).

Grassland simulation models can be successfully employed to evaluate different management practises and assess the effect of climate on grassland system under current state and future projections. As suggested by Ma et al. (2019) three possible actions can be adopted to improve the application of these model as decision supporting tool: increase user-friendliness, improve simulation on ecosystem services and grazing activity; enhance the cooperation between modelers, experimentalists, and stakeholders.

In fact, the use of crop modelling for scientific and management purposes may remain limited due to the complex structure of these models. Calibration, which requires detailed field-collected data, can

therefore be time-consuming and can often result in a site-specific parameterization (i.e. overparameterization, Kirchner et al., 1996) that is then difficult to apply in other areas without performing a new calibration (Sinclair and Seligman, 2000). The possible use of crop modelling may also be partially limited by the requirement for very accurate input data needed for adequate system simulation, which are often available at the local scale but not for high spatial scale precision farming applications (Jin et al., 2018) in pastoral systems that are acknowledged to be very heterogeneous in terms of botanical composition and productive features.

Moreover, recent studies have investigated the possibility of using a multi-model ensemble to improve model simulation efficiency as well as better define uncertainties in models' outcomes (Ehrhardt et al., 2018b; Fitton et al., 2019; R. Sándor et al., 2017) or the integration into models of data collected from remote sensing (Maselli et al., 2013).

References

Ali, I., Cawkwell, F., Dwyer, E., Barrett, B., Green, S., 2016. Satellite remote sensing of grasslands: From observation to management. J. Plant Ecol. 9, 649–671. https://doi.org/10.1093/jpe/rtw005

Allen, V.G., Batello, C., Berretta, E.J., Hodgson, J., Kothmann, M., Li, X., McIvor, J., Milne, J., Morris, C., Peeters, A., Sanderson, M., 2011. An international terminology for grazing lands and grazing animals. Grass Forage Sci. 66, 2–28. https://doi.org/10.1111/j.1365-2494.2010.00780.x

Andreatta, D., Gianelle, D., Scotton, M., Vescovo, L., Dalponte, M., 2022. Detection of grassland mowing frequency using time series of vegetation indices from Sentinel-2 imagery. GIScience Remote Sens. 59, 481–500. https://doi.org/10.1080/15481603.2022.2036055

Askari, M.S., McCarthy, T., Magee, A., Murphy, D.J., 2019. Evaluation of grass quality under different soil management scenarios using remote sensing techniques. Remote Sens. 11, 1–23. https://doi.org/10.3390/rs11151835

Bajocco, S., Salvati, L., Ricotta, C., 2011. Land degradation versus fire: A spiral process? Prog. Phys. Geogr. 35, 3–18. https://doi.org/10.1177/0309133310380768

Bannari, A.; Morin, D.; Bonn, F.; Huete, A. A review of vegetation indices. Remote Sens. Rev. 1995, 13, 95–120.

Barbour, R., Young, R.H., Wilkinson, J.M., 2022. Production of Meat and Milk from Grass in the United Kingdom. Agronomy 12, 1–9. https://doi.org/10.3390/agronomy12040914

Bayle, A., Carlson, B.Z., Thierion, V., Isenmann, M., Choler, P., 2019. Improved mapping of mountain shrublands using the sentinel-2 red-edge band. Remote Sens. 11. https://doi.org/10.3390/rs11232807

Boval, M., Dixon, R.M., 2012. The importance of grasslands for animal production and other functions: A review on management and methodological progress in the tropics. Animal 6,

748–762. https://doi.org/10.1017/S1751731112000304

Braun, A., Wagner, J., Hochschild, V., 2018. Above-ground biomass estimates based on active and passive microwave sensor imagery in low-biomass savanna ecosystems. J. Appl. Remote Sens. 12, 1. https://doi.org/10.1117/1.jrs.12.046027

Brookshire, E.N.J., Weaver, T., 2015. Long-term decline in grassland productivity driven by increasing dryness. Nat. Commun. 6. https://doi.org/10.1038/ncomms8148

Christie, K.M., Smith, A.P., Rawnsley, R.P., Harrison, M.T., Eckard, R.J., 2018. Simulated seasonal responses of grazed dairy pastures to nitrogen fertilizer in SE Australia: Pasture production. Agric. Syst. https://doi.org/10.1016/j.agsy.2018.07.010

Dibari, C., Costafreda-Aumedes, S., Argenti, G., Bindi, M., Carotenuto, F., Moriondo, M., Padovan, G., Pardini, A., Staglianò, N., Vagnoli, C., Brilli, L., 2020. Expected changes to alpine pastures in extent and composition under future climate conditions. Agronomy 10, 1–21. https://doi.org/10.3390/agronomy10070926

Ding, L., Li, Z., Shen, B., Wang, X., Xu, D., Yan, R., Yan, Y., Xin, X., Xiao, J., Li, M., Wang, P., 2022. Spatial patterns and driving factors of aboveground and belowground biomass over the eastern Eurasian steppe. Sci. Total Environ. 803, 149700. https://doi.org/10.1016/j.scitotenv.2021.149700

Edirisinghe, A., Hill, M.J., Donald, G.E., Hyder, M., 2011. Quantitative mapping of pasture biomass using satellite imagery. Int. J. Remote Sens. 32, 2699–2724. https://doi.org/10.1080/01431161003743181

Ehrhardt, F., Soussana, J.F., Bellocchi, G., Grace, P., McAuliffe, R., Recous, S., Sándor, R., Smith, P., Snow, V., de Antoni Migliorati, M., Basso, B., Bhatia, A., Brilli, L., Doltra, J., Dorich, C.D., Doro, L., Fitton, N., Giacomini, S.J., Grant, B., Harrison, M.T., Jones, S.K., Kirschbaum, M.U.F., Klumpp, K., Laville, P., Léonard, J., Liebig, M., Lieffering, M., Martin, R., Massad, R.S., Meier, E., Merbold, L., Moore, A.D., Myrgiotis, V., Newton, P., Pattey, E., Rolinski, S., Sharp, J., Smith, W.N., Wu, L., Zhang, Q., 2018a. Assessing uncertainties in crop and pasture ensemble model simulations of productivity and N2O emissions. Glob. Chang. Biol. 24, e603–e616. https://doi.org/10.1111/gcb.13965

Ehrhardt, F., Soussana, J.F., Bellocchi, G., Grace, P., McAuliffe, R., Recous, S., Sándor, R., Smith, P., Snow, V., de Antoni Migliorati, M., Basso, B., Bhatia, A., Brilli, L., Doltra, J., Dorich, C.D., Doro, L., Fitton, N., Giacomini, S.J., Grant, B., Harrison, M.T., Jones, S.K., Kirschbaum, M.U.F., Klumpp, K., Laville, P., Léonard, J., Liebig, M., Lieffering, M., Martin, R., Massad, R.S., Meier, E., Merbold, L., Moore, A.D., Myrgiotis, V., Newton, P., Pattey, E., Rolinski, S., Sharp, J., Smith, W.N., Wu, L., Zhang, Q., 2018b. Assessing uncertainties in crop and pasture ensemble model simulations of productivity and N2O emissions. Glob. Chang. Biol. 24, e603–e616. https://doi.org/10.1111/gcb.13965

Eriksen, J., Askegaard, M., Rasmussen, J., Søegaard, K., 2015. Nitrate leaching and residual effect in dairy crop rotations with grass-clover leys as influenced by sward age, grazing, cutting and fertilizer regimes. Agric. Ecosyst. Environ. 212, 75–84. https://doi.org/10.1016/j.agee.2015.07.001

Ertl, P., Klocker, H., Hörtenhuber, S., Knaus, W., Zollitsch, W., 2015. The net contribution of dairy production to human food supply: The case of austrian dairy farms. Agric. Syst. 137, 119–125. https://doi.org/10.1016/j.agsy.2015.04.004

Evangelista, Alberto, Frate, L., Carranza, M.L., Attorre, F., Pelino, G., Stanisci, A., 2016. Changes in composition, ecology and structure of high-mountain vegetation: A re-visitation study over 42 years. AoB Plants 8, 1–11. https://doi.org/10.1093/aobpla/plw004

FAO, 2013. FAO Statistical Yearbook 2013. World food and Agriculture Food and Agriculture Organisation for the United Nations, Rome.

Fernandes, M.H.M.R., Cardoso, A.S., Lima, L.O., Berça, A.S., Reis, R.A., 2022. Human-edible protein contribution of tropical beef cattle production systems at different levels of intensification. Animal 16, 100538. https://doi.org/10.1016/j.animal.2022.100538

Filippa, G., Cremonese, E., Migliavacca, M., Galvagno, M., Sonnentag, O., Humphreys, E., Hufkens, K., Ryu, Y., Verfaillie, J., Morra di Cella, U., Richardson, A.D., 2018. NDVI derived from near-infrared-enabled digital cameras: Applicability across different plant functional types. Agric. For. Meteorol. 249, 275–285. https://doi.org/10.1016/j.agrformet.2017.11.003

Fitton, N., Bindi, M., Brilli, L., Cichota, R., Dibari, C., Fuchs, K., Huguenin-Elie, O., Klumpp, K., Lieffering, M., Lüscher, A., Martin, R., McAuliffe, R., Merbold, L., Newton, P., Rees, R.M., Smith, P., Topp, C.F.E., Snow, V., 2019. Modelling biological N fixation and grass-legume dynamics with process-based biogeochemical models of varying complexity. Eur. J. Agron. 106, 58–66. https://doi.org/10.1016/j.eja.2019.03.008

Flato, G., J. Marotzke, B. Abiodun, P. Braconnot, S.C. Chou, W. Collins, P. Cox, F. Driouech, S. Emori, V. Eyring, C. Forest, P. Gleckler, E. Guilyardi, C. Jakob, V. Kattsov, C. Reason and M. Rummukainen, 2013: Evaluation of Climate Models. In: Climate Change 2013: The Physical Science Basis. Contribution of Working Group I to the Fifth Assessment Report of the Intergovernmental Panel on Climate Change [Stocker, T.F., D. Qin, G.-K. Plattner, M. Tignor, S.K. Allen, J. Boschung, A. Nauels, Y. Xia, V. Bex and P.M. Midgley (eds.)]. Cambridge University Press, Cambridge, United Kingdom and New York, NY, USA.Fox, D.G., 1981. Judging air quality model performance. Bull. Am. Meteorol. Soc. 62, 599-609

Fust, P., Schlecht, E., 2022. Importance of timing : Vulnerability of semi-arid rangeland systems to increased variability in temporal distribution of rainfall events as predicted by future climate change. Ecol. Modell. 468, 109961. https://doi.org/10.1016/j.ecolmodel.2022.109961

Ghahramani, A., Howden, S.M., Prado, A., Thomas, D.T., Moore, A.D., Ji, B., Ates, S., n.d. Climate Change Impact , Adaptation , and Mitigation in Temperate Grazing Systems : A Review 1–30.

Ghahramani, A., Moore, A.D., 2016. Impact of climate changes on existing crop-livestock farming systems. Agric. Syst. 146, 142–155. https://doi.org/10.1016/j.agsy.2016.05.011

Gong, Z., Kawamura, K., Ishikawa, N., Goto, M., Wulan, T., Alateng, D., Yin, T., Ito, Y., 2015. MODIS normalized difference vegetation index (NDVI) and vegetation phenology dynamics in the Inner Mongolia grassland. Solid Earth 6, 1185–1194. https://doi.org/10.5194/se-6-1185-2015

Gonzalez, S.L., Ghermandi, L., 2021. Overgrazing causes a reduction in the vegetation cover and seed bank of Patagonian grasslands. Plant Soil 464, 75–87. https://doi.org/10.1007/s11104-021-04931-y

Guerini Filho, M., Kuplich, T.M., Quadros, F.L.F.D., 2020. Estimating natural grassland biomass by vegetation indices using Sentinel 2 remote sensing data. Int. J. Remote Sens. 41, 2861–2876. https://doi.org/10.1080/01431161.2019.1697004

Guo, J., Yang, X., Niu, J., Jin, Y., Xu, B., Shen, G., Zhang, W., Zhao, F., Zhang, Y., 2019. Remote sensing monitoring of green-up dates in the Xilingol grasslands of northern China and their correlations with meteorological factors. Int. J. Remote Sens. 40, 2190–2211. https://doi.org/10.1080/01431161.2018.1506185

Haines-Young R (1994) Remote sensing of environmental change. In: Roberts N (ed) The changing global environment. Blackwell, Oxford, pp 22–43

Hannappel, I., Fischer, K., 2020. Grassland intensification strongly reduces butterfly diversity in the Westerwald mountain range, Germany. J. Insect Conserv. 24, 279–285. https://doi.org/10.1007/s10841-019-00195-1

Harrison, M.T., Cullen, B.R., Rawnsley, R.P., 2016. Modelling the sensitivity of agricultural systems to climate change and extreme climatic events. Agric. Syst. https://doi.org/10.1016/j.agsy.2016.07.006

Hassler, S.C., Baysal-Gurel, F., 2019. Unmanned aircraft system (UAS) technology and applications in agriculture. Agronomy 9. https://doi.org/10.3390/agronomy9100618

Hatfield, J.L., Prueger, J.H., Sauer, T.J., Dold, C., Brien, P.O., Wacha, K., 2019. Applications of Vegetative Indices from Remote Sensing to Agriculture : Past and Future 1–17.

He, B., Li, X., Quan, X., Qiu, S., 2015. Estimating the aboveground dry biomass of grass by assimilation of retrieved LAI into a crop growth model. IEEE J. Sel. Top. Appl. Earth Obs. Remote Sens. 8, 550–561. https://doi.org/10.1109/JSTARS.2014.2360676

He, Y., Yang, J., Guo, X., 2020. Green vegetation cover dynamics in a heterogeneous grassland: Spectral unmixing of landsat time series from 1999 to 2014. Remote Sens. 12, 1–20. https://doi.org/10.3390/rs12223826

Herrero, M., Havlík, P., Valin, H., Notenbaert, A., Rufino, M.C., Thornton, P.K., Blümmel, M., Weiss, F., Grace, D., Obersteiner, M., 2013. Biomass use, production, feed efficiencies, and greenhouse gas emissions from global livestock systems. Proc. Natl. Acad. Sci. U. S. A. 110, 20888–20893. https://doi.org/10.1073/pnas.1308149110

Hilker, T., Natsagdorj, E., Waring, R.H., Lyapustin, A., Wang, Y., 2014. Satellite observed widespread decline in Mongolian grasslands largely due to overgrazing. Glob. Chang. Biol. 20, 418–428. https://doi.org/10.1111/gcb.12365

Hou, X., Gao, S., Niu, Z., Xu, Z., 2014. Extracting grassland vegetation phenology in North China based on cumulative SPOT-VEGETATION NDVI data. Int. J. Remote Sens. 35, 3316–3330. https://doi.org/10.1080/01431161.2014.903437

Huang, J., Gómez-Dans, J.L., Huang, H., Ma, H., Wu, Q., Lewis, P.E., Liang, S., Chen, Z., Xue, J.H., Wu, Y., Zhao, F., Wang, J., Xie, X., 2019. Assimilation of remote sensing into crop growth models: Current status and perspectives. Agric. For. Meteorol. 276–277, 107609. https://doi.org/10.1016/j.agrformet.2019.06.008

Huang, N., He, J.S., Chen, L., Wang, L., 2018. No upward shift of alpine grassland distribution on the Qinghai-Tibetan Plateau despite rapid climate warming from 2000 to 2014. Sci. Total Environ. 625, 1361–1368. https://doi.org/10.1016/j.scitotenv.2018.01.034

Inoue, T., Nagai, S., Kobayashi, H., Koizumi, H., 2015. Utilization of ground-based digital photography for the evaluation of seasonal changes in the aboveground green biomass and

foliage phenology in a grassland ecosystem. Ecol. Inform. 25, 1–9. https://doi.org/10.1016/j.ecoinf.2014.09.013

Insua, J.R., Utsumi, S.A., Basso, B., 2019a. Assessing and modelling pasture growth under different nitrogen fertilizer and defoliation rates in argentina and the united states. Agron. J. 111, 702–713. https://doi.org/10.2134/agronj2018.07.0438

Insua, J.R., Utsumi, S.A., Basso, B., 2019b. Estimation of spatial and temporal variability of pasture growth and digestibility in grazing rotations coupling unmanned aerial vehicle (UAV) with crop simulation models. PLoS One 14, 1–21. https://doi.org/10.1371/journal.pone.0212773

Jin, X., Kumar, L., Li, Z., Feng, H., Xu, X., Yang, G., Wang, J., 2018. A review of data assimilation of remote sensing and crop models. Eur. J. Agron. 92, 141–152. https://doi.org/10.1016/j.eja.2017.11.002

Kirchner, J.W., Hooper, R.P., Kendall, C., Neal, C., Leavesley, G., 1996. Testing and validating environmental models. Sci. Total Environ. 183, 33–47. https://doi.org/10.1016/0048-9697(95)04971-1

Krzic, M., Lamagna, S.F., Newman, R.F., Bradfield, G., Wallace, B.M., 2014. Long-term grazing effects on rough fescue grassland soils in southern British Columbia. Can. J. Soil Sci. 94, 337–345. https://doi.org/10.4141/CJSS2013-019

Lemaire, G., Hodgson, S., Chabbi, A., 2011. Grassland Productivity and Ecosystems Services.

Li, X., Guo, W., Li, S., Zhang, J., Ni, X., 2021. The different impacts of the daytime and nighttime land surface temperatures on the alpine grassland phenology. Ecosphere 12. https://doi.org/10.1002/ecs2.3578

Lieth, H., 1974. Phenology and Seasonality Modelling. Springer-Verlag, New York.

Ling, B., Raynor, E.J., Goodin, D.G., Joern, A., 2019. Effects of fire and large herbivores on canopy nitrogen in a tallgrass prairie. Remote Sens. 11, 1–21. https://doi.org/10.3390/rs11111364

Liu, J., Isbell, F., Ma, Q., Chen, Y., Xing, F., Sun, W., Wang, L., Li, J., Wang, Y., Hou, F., Xin, X., Nan, Z., Eisenhauer, N., Wang, D., 2022. Overgrazing, not haying, decreases grassland topsoil organic carbon by decreasing plant species richness along an aridity gradient in Northern China. Agric. Ecosyst. Environ. 332, 107935. https://doi.org/10.1016/j.agee.2022.107935

Lugassi, R., Zaady, E., Goldshleger, N., Shoshany, M., Chudnovsky, A., 2019. Spatial and temporal monitoring of pasture ecological quality: Sentinel-2-based estimation of crude protein and neutral detergent fiber contents. Remote Sens. 11. https://doi.org/10.3390/rs11070799

Lyu, X., Li, X., Dang, D., Dou, H., Xuan, X., Liu, S., Li, M., Gong, J., 2020. A new method for grassland degradation monitoring by vegetation species composition using hyperspectral remote sensing. Ecol. Indic. 114, 106310. https://doi.org/10.1016/j.ecolind.2020.106310

Ma, X., Mahecha, M.D., Migliavacca, M., van der Plas, F., Benavides, R., Ratcliffe, S., Kattge, J., Richter, R., Musavi, T., Baeten, L., Barnoaiea, I., Bohn, F.J., Bouriaud, O., Bussotti, F., Coppi, A., Domisch, T., Huth, A., Jaroszewicz, B., Joswig, J., Pabon-Moreno, D.E., Papale, D., Selvi, F., Laurin, G.V., Valladares, F., Reichstein, M., Wirth, C., 2019. Inferring plant functional diversity from space: the potential of Sentinel-2. Remote Sens. Environ. 233, 111368. https://doi.org/10.1016/j.rse.2019.111368.

Maselli, F., Argenti, G., Chiesi, M., Angeli, L., Papale, D., 2013. Simulation of grassland productivity by the combination of ground and satellite data. Agric. Ecosyst. Environ. 165, 163–172. https://doi.org/10.1016/j.agee.2012.11.006.

Monteith, 1972. Solar Radiation and Productivity in Tropical Ecosystems Author (s): J . L . Monteith Source : Journal of Applied Ecology , Vol . 9 , No . 3 (Dec ., 1972), pp . 747-766 Published by : British Ecological Society Stable URL : http://www.jstor.org/stable/. Society 9, 747–766.

Moore, A.D., Ghahramani, A., 2013. Climate change and broadacre livestock production across southern Australia. 1. Impacts of climate change on pasture and livestock productivity, and on sustainable levels of profitability. Glob. Chang. Biol. 19, 1440–1455. https://doi.org/10.1111/gcb.12150

Morales, P., Hickler, T., Rowell, D.P., Smith, B., Sykes, M.T., 2007. Changes in European ecosystem productivity and carbon balance driven by regional climate model output. Glob. Chang. Biol. 13, 108–122. https://doi.org/10.1111/j.1365-2486.2006.01289.x

Murphy, D.J., O' Brien, B., O' Donovan, M., Condon, T., Claffey, A., Murphy, M.D., 2019. A preliminary near infrared spectroscopy calibration for the prediction of undried fresh grass quality. Precis. Livest. Farming 2019 - Pap. Present. 9th Eur. Conf. Precis. Livest. Farming, ECPLF 2019 199–203.

Nandintsetseg, B., Boldgiv, B., Chang, J., Ciais, P., 2021. Risk and vulnerability of Mongolian grasslands under climate change OPEN ACCESS Risk and vulnerability of Mongolian grasslands under climate change.

Pei Y., Dong J., Zhang Y., Yuan W., Doughty R., Yang J., Zhou D., Zhang L., Xiao X., 2022. Evolution of light use efficiency models: Improvement, uncertainties, and implications. Agricultural and Forest Meteorology, 317, 108905. https://doi.org/10.1016/j.agrformet.2022.108905.

Petach, A.R., Toomey, M., Aubrecht, D.M., Richardson, A.D., 2014. Monitoring vegetation phenology using an infrared-enabled security camera. Agric. For. Meteorol. 195–196, 143–151. https://doi.org/10.1016/j.agrformet.2014.05.008

Petersen, K., Kraus, D., Calanca, P., Semenov, M.A., Butterbach-Bahl, K., Kiese, R., 2021. Dynamic simulation of management events for assessing impacts of climate change on pre-alpine grassland productivity. Eur. J. Agron. 128, 126306. https://doi.org/10.1016/j.eja.2021.126306

Petriccione, B., Bricca, A., 2019. Thirty years of ecological research at the Gran Sasso d'Italia LTER site: Climate change in action. Nat. Conserv. 34, 9–39. https://doi.org/10.3897/natureconservation.34.30218

Piseddu, F., Bellocchi, G., Picon-Cochard, C., 2021. Mowing and warming effects on grassland species richness and harvested biomass: meta-analyses. Agron. Sustain. Dev. 41, 1–21. https://doi.org/10.1007/s13593-021-00722-y

Pulina, A., Lai, R., Salis, L., Seddaiu, G., Roggero, P.P., Bellocchi, G., 2018. Modelling pasture production and soil temperature, water and carbon fluxes in Mediterranean grassland systems

with the Pasture Simulation model. Grass Forage Sci. 73, 272–283. https://doi.org/10.1111/gfs.12310

Quaranta, G., Salvia, R., Salvati, L., Paola, V. De, Coluzzi, R., Imbrenda, V., Simoniello, T., 2020. Long-term impacts of grazing management on land degradation in a rural community of Southern Italy: Depopulation matters. L. Degrad. Dev. 31, 2379–2394. https://doi.org/10.1002/ldr.3583

Reinhart, K.O., Komatsu, K.J., Vermeire, L.T., 2022. Effects of mowing, spring precipitation, soil nutrients, and enzymes on grassland productivity. Agrosystems, Geosci. Environ. 5, 1–11. https://doi.org/10.1002/agg2.20320

Ren, S., Li, Y., Peichl, M., 2020. Diverse effects of climate at different times on grassland phenology in mid-latitude of the Northern Hemisphere. Ecol. Indic. 113. https://doi.org/10.1016/j.ecolind.2020.106260

Scocco, P., Piermarteri, K., Malfatti, A., Tardella, F.M., Catorci, A., 2016. Increase of drought stress negatively affects the sustainability of extensive sheep farming in sub-Mediterranean climate. J. Arid Environ. 128, 50–58. https://doi.org/10.1016/j.jaridenv.2016.01.006

Serrano, J., Shahidian, S., da Silva, J.M., 2019. Evaluation of normalized difference water index as a tool for monitoring pasture seasonal and inter-annual variability in a Mediterranean agro-silvo-pastoral system. Water (Switzerland) 11. https://doi.org/10.3390/w11010062

Shoko, C., Mutanga, O., 2017. Examining the strength of the newly-launched Sentinel 2 MSI sensor in detecting and discriminating subtle differences between C3 and C4 grass species. ISPRS J. Photogramm. Remote Sens. 129, 32–40. https://doi.org/10.1016/j.isprsjprs.2017.04.016

Sinclair, T.R., Seligman, N., 2000. Criteria for publishing papers on crop modelling. F. Crop. Res. 68, 165–172. https://doi.org/10.1016/S0378-4290(00)00105-2

Snow, V.O., Rotz, C.A., Moore, A.D., Martin-Clouaire, R., Johnson, I.R., Hutchings, N.J., Eckard, R.J., 2014. The challenges - and some solutions - to process-based modelling of grazed agricultural systems. Environ. Model. Softw. 62, 420–436. https://doi.org/10.1016/j.envsoft.2014.03.009

Stanisci, A., Frate, L., Morra Di Cella, U., Pelino, G., Petey, M., Siniscalco, C., Carranza, M.L., 2016. Short-term signals of climate change in Italian summit vegetation: observations at two GLORIA sites. Plant Biosyst. 150, 227–235. https://doi.org/10.1080/11263504.2014.968232

Stöckli, R., Vidale, P.L., 2004. European plant phenology and climate as seen in a 20-year AVHRR land-surface parameter dataset. Int. J. Remote Sens. 25, 3303–3330. https://doi.org/10.1080/01431160310001618149

Tamburini, G., Aguilera, G., Öckinger, E., 2022. Grasslands enhance ecosystem service multifunctionality above and below-ground in agricultural landscapes. J. Appl. Ecol. 3061–3071. https://doi.org/10.1111/1365-2664.14302

Tian, F., Cai, Z., Jin, H., Hufkens, K., Scheifinger, H., Tagesson, T., Smets, B., Van Hoolst, R., Bonte, K., Ivits, E., Tong, X., Ardö, J., Eklundh, L., 2021. Calibrating vegetation phenology from Sentinel-2 using eddy covariance, PhenoCam, and PEP725 networks across Europe. Remote Sens. Environ. 260. https://doi.org/10.1016/j.rse.2021.112456

Touhami, H. Ben, Lardy, R., Barra, V., Bellocchi, G., 2013. Screening parameters in the Pasture

Simulation model using the Morris method. Ecol. Modell. 266, 42–57. https://doi.org/10.1016/j.ecolmodel.2013.07.005

UN, 201 and d. World population prospects 2019: Highlights | multimedia library - united nations department of economic and social affairs [WWW document].

Vogeler, I., Thomas, S., van der Weerden, T., 2019. Effect of irrigation management on pasture yield and nitrogen losses. Agric. Water Manag. https://doi.org/10.1016/j.agwat.2019.01.022

Vong, C.N., Zhou, J., Tooley, J.A., Naumann, H.D., Lory, J.A., 2019. Estimating forage dry matter and nutritive value using UAV- And ground-based sensors - A preliminary study. 2019 ASABE Annu. Int. Meet. 2–15. https://doi.org/10.13031/aim.201900556

Wang, Z.; Ma, Y.; Zhang, Y.; Shang, J. Review of Remote Sensing Applications in Grassland Monitoring. Remote Sens. 2022, 14, 2903. https://doi.org/10.3390/rs14122903

Wang, G., Liu, S., Liu, T., Fu, Z., Yu, J., 2019. Modelling above-ground biomass based on vegetation indexes : a modified approach for biomass estimation in semi-arid grasslands. Int. J. Remote Sens. 40, 3835–3854. https://doi.org/10.1080/01431161.2018.1553319

Wang, J., Xiao, X., Bajgain, R., Starks, P., Steiner, J., Doughty, R.B., Chang, Q., 2019. Estimating leaf area index and aboveground biomass of grazing pastures using Sentinel-1, Sentinel-2 and Landsat images. ISPRS J. Photogramm. Remote Sens. 154, 189–201. https://doi.org/10.1016/j.isprsjprs.2019.06.007

Wang, Z., Ma, Y., Zhang, Y., Shang, J., 2022. Review of remote sensing applications in grassland monitoring. Remote Sens. 14.

Wepking, C., Mackin, H.C., Raff, Z., Shrestha, D., Orfanou, A., Booth, E.G., Kucharik, C.J., Gratton, C., Jackson, R.D., 2022. Perennial grassland agriculture restores critical ecosystem functions in the U.S. Upper Midwest. Front. Sustain. Food Syst. 6. https://doi.org/10.3389/fsufs.2022.1010280

Wu, H., Li, Z.L., 2009. Scale issues in remote sensing: A review on analysis, processing and modelling. Sensors 9, 1768–1793. https://doi.org/10.3390/s90301768

Wu, Linwei, Zhang, Y., Guo, X., Ning, D., Zhou, X., Feng, J., Yuan, M.M., Liu, S., Guo, J., Gao, Z., Ma, J., Kuang, J., Jian, S., Han, S., Yang, Z., Ouyang, Y., Fu, Y., Xiao, N., Liu, X., Wu, Liyou, Zhou, A., Yang, Y., Tiedje, J.M., Zhou, J., n.d. Reduction of microbial diversity in grassland soil is driven by long-term climate warming. https://doi.org/10.1038/s41564-022-01147-3

Xia, J., Liang, S., Chen, J., Yuan, W., Liu, Shuguang, Li, L., Cai, W., Zhang, L., Fu, Y., Zhao, T., Feng, J., Ma, Z., Ma, M., Liu, Shaomin, Zhou, G., Asanuma, J., Chen, S., Du, M., Davaa, G., Kato, T., Liu, Q., Liu, Suhong, Li, S., Shao, C., Tang, Y., Zhao, X., 2014. Satellite-based analysis of evapotranspiration and water balance in the grassland ecosystems of Dryland East Asia. PLoS One 9, 1–11. https://doi.org/10.1371/journal.pone.0097295

Xue, J., Su, B., 2017. Significant remote sensing vegetation indices: A review of developments and applications. J. Sensors 2017. https://doi.org/10.1155/2017/1353691

Yu, R. (2020). An improved estimation of net primary productivity of grassland in the Qinghai-Tibet region using light use efficiency with vegetation photosynthesis model. Ecological Modelling 431.

Zalite, K., Antropov, O., Praks, J., Voormansik, K., Noorma, M., 2016. Monitoring of Agricultural Grasslands with Time Series of X-Band Repeat-Pass Interferometric SAR. IEEE J. Sel. Top. Appl. Earth Obs. Remote Sens. 9, 3687–3697. https://doi.org/10.1109/JSTARS.2015.2478120

Zarrineh, N., Abbaspour, K.C., Holzkämper, A., 2020. Integrated assessment of climate change impacts on multiple ecosystem services in Western Switzerland. Sci. Total Environ. 708, 135212. https://doi.org/10.1016/j.scitotenv.2019.135212

Chapter 2.

Aim and outline

Chapter 2 shows the objectives and structure of the thesis.

PhD candidate's contribution:

Edoardo Bellini wrote the entire chapter.

2. Aim and outline of the research

The main objective of this research was to test, validate and assess different approaches, namely modelling and remote sensing technologies, to monitor growth of grassland vegetation under different climate and managements.
The evaluation of growth development at the present time with these technologies represents a fundamental step in understanding the state of the system with the resulting information that can be used for optimal and effective management. On the other hand, the assessment of the changes of grasslands growth and production caused by current and future climate changes is a prerequisite for the identification and promotion of adaptation strategies to cope with the future climatic projections.

In particular, the specific objectives of the thesis pursued as part of the PhD are:

1) Development of a simplified simulation model, integrated with satellite-based vegetation indexes, to reproduce grassland systems dynamics and soil water balance;

2) Evaluation of the impacts caused by climate change on grassland phenology in recent decades;

3) Assessment of potential changes caused by future climate in grassland systems and identification of possible adaptation strategies.

With particular reference to objective 1, **Chapter 3** presents the development of a simplified simulation model based on the concept of light-use efficiency (Monteith, 1972) that uses specific vegetation indices (i.e. Normalized Difference Vegetation Index, NDVI) to estimate structural characteristics of vegetation (i.e. LAI). Through the use of specific equations for reproducing the physiological, chemical and biological processes of the system and the adoption of NDVI from proximal or remote sensing instruments, the model provides important information on the status of forage production (above ground biomass) and water conditions of the system with few input required (e.g. minimum and maximum daily temperature, precipitation, solar radiation and soil texture). The simplified model, calibrated and validated in different environments, can therefore represent an important tool for optimal grassland management.
Chapter 4 answers the questions of the specific objective 2, investigating the changes that occurred in grassland phenology on the European continent over the period 2001-2021 through the analysis of a long time series of MODIS satellite images. The study offers a comprehensive analysis of the methodology to be used to effectively extract the phenological dates of the start, peak and end of

growing season and then reports in detail the phenological changes observed from the satellite imagery. The extent of these changes was then evaluated in light of the specific characteristics of the test sites, specifically average winter and spring temperatures during the years 2001-2021, altitude and latitude of the analysed grasslands.

In conclusion, the impacts of future climate on grazing systems and the evaluation of specific management strategies are analysed in **Chapter 5**. This section reports the results of future projections carried out within two pastures in the central Italian Apennines with a specific simulation model (i.e. Pasture Simulation Model, Riedo et al., 1998) under different time windows (i.e. 2011-2040 and 2041-2070) and future scenarios (RCP4.5 and 8.5). The simulations took into account the future forage production, growing season length, water conditions and climate-altering gas emissions. Alternative management strategies (grazing season length and animal stocking rate) are tested to cope with future changes in extensive grazing systems simulated by the model.

References

Monteith, 1972. Solar Radiation and Productivity in Tropical Ecosystems Author (s): J . L . Monteith Source : Journal of Applied Ecology , Vol . 9 , No . 3 (Dec ., 1972), pp . 747-766 Published by : British Ecological Society Stable URL : http://www.jstor.org/stable/. Society 9, 747–766.

Riedo, M., Grub, A., Rosset, M., 1998. A pasture simulation model for dry matter production , and fluxes of carbon , nitrogen , water and energy 105, 141–183.

Chapter 3.

VISTOCK: A simplified model for simulating grassland systems

Chapter 3 has been based on the study:
Bellini, E., Moriondo M., Dibari C., Bindi M., Staglianò N., Cremonese E., Filippa G., Galvagno M. and Argenti G. 2023. VISTOCK: A Simplified Model for Simulating Grassland Systems. (*Published*) *European Journal of Agronomy* 142 (January). doi:10.1016/j.eja.2022.126647.

PhD candidate's contribution:

Edoardo Bellini developed the model for simulating grass growth with the collaboration of Moriondo M. He collected on-field data with co-authors, produced the results and wrote the sections of the chapter under the supervision of the other co-authors.

3. VISTOCK: A simplified model for simulating grassland systems

Edoardo Bellini[a], Marco Moriondo[b] *, Camilla Dibari[a], Marco Bindi[a], Nicolina Staglianò[a], Edoardo Cremonese[c], Gianluca Filippa[c], Marta Galvagno[c], Giovanni Argenti[a]

[a] Department of Agriculture, Food, Environment and Forestry (DAGRI), University of Florence, Florence (Italy)
[b] Institute of BioEconomy, Italian National Research Council (IBE-CNR), Florence (Italy)
[c] Environmental Protection Agency of Aosta Valley - Climate Change Unit, Saint-Christophe (Italy)
* Corresponding author: marco.moriondo@cnr.it

Keywords: grazing; aboveground biomass; NDVI; LAI; FAPAR

Abstract

This article presents the structure and results of a simplified model (VISTOCK) for simulating grass growth and water dynamics of grassland systems. The model, based on a process-based approach coupled with proximal (SKR 1800 2-Channel Light Sensor) and remote (Sentinel-2) NDVI-derived data for estimating LAI, simulates aboveground biomass (AGB), net primary production *(*NPP), evapotranspiration (ET), and the fraction of total transpirable water in soil (FTSW). VISTOCK simulated a grassland system with few meteorological data (i.e., minimum and maximum daily temperatures, precipitation, global solar radiation), considering limitations to vegetation growth due to thermal and water stresses. It was calibrated for a natural alpine grassland in Italy (site T) during the most contrasting meteorological seasons of the dataset (2012, 2017, and 2018). It was then evaluated for the remaining years at site T (2013, 2014, 2015, and 2016) and for other two sites in Italy (sites B1, B2 and M) with different soil and climate conditions and diverse management strategies (2020 and 2021). VISTOCK accurately predicted AGB during the growing season (RMSE = 445, 240, 219, 365 kg DM ha^{-1} for T, M, B1, and B2, respectively) as well as for NPP, ET, and FSTW at site T. Simulation results suggest the ability of the model to simulate grassland in diverse environments with few inputs and parameters to be calibrated. The model's simplified structure, combined with easy-to obtain input data and easy applicability, encourages its wider use for out- and/or upscaling and decision making.

1. Introduction

Grasslands, which cover ca. 25% of the world's land area (Lemaire et al., 2011) and ca. 70% of the world's total agricultural area (FAO, 2013), provide a wide range of ecosystem services, such as erosion protection, water regulation, food for wildlife and aesthetic and recreational functions (Bengtsson et al., 2019; Hao et al., 2017; Ponzetta et al., 2010). Grazing land, defined as "any vegetated land that is grazed or has the potential to be grazed by animals" (Allen et al., 2011), plays a major role in animal production systems. Due to climate change, however, livestock systems based on grazing are facing variability in grassland production (Insua et al., 2019a) and changes in forage quality and quantity (Scocco et al., 2016; Dibari et al., 2021). This is particularly evident in mountain pastures, where these impacts are already visible on the botanical composition and as a decrease in suitable grazing areas (Dibari et al., 2015; A. Evangelista et al., 2016; Petriccione and Bricca, 2019). These effects are expected to increase even more in the future (Dibari et al., 2020).

To properly balance grassland production with animal intake needs in these uncertain and variable conditions (Holechek et al., 2011), prompt and spatial information about vegetation growth would help farmers make decisions. Such monitoring would facilitate the adoption of management strategies (e.g., rotational grazing) that use forage better than other grazing systems (e.g., continuous grazing, Boavista et al., 2019) during the growing season.

In this respect, simulation models are considered effective tools for predicting biophysical processes of agricultural systems (Brilli et al., 2013; Leolini et al., 2018; Maselli et al., 2012; Stöckle et al., 2003), including grasslands (Ehrhardt et al., 2018a; L. Ma et al., 2019; Snow et al., 2014). However, using simulation models to identify strategies for optimising animal intake remains limited, mainly due to their complex architecture, which often requires detailed observed data to calibrate them and thus ensure that they reproduce local conditions as well as possible. In contrast, a model calibrated too strongly for a local situation would be difficult to extrapolate to another site without readjusting its parameters (Sinclair and Seligman, 2000), sometimes risking overparameterization (Kirchner et al., 1996). Furthermore, to predict growth processes accurately, simulation models require detailed input data (e.g., meteorological data, soil type, management practices) (Holzworth et al., 2014; Riedo et al., 1998) that are generally available at the field scale but often not readily available for precision-agriculture applications at a larger scale (Jin et al., 2018).

Hence, to overcome these issues we developed a grassland model that can simulate grass growth using a process-based approach and integrating remote sensing data as a proxy for canopy-intercepted radiation. This approach implies having a simplified architecture, which in turn reduces the number of processes that are simulated and thus the number of parameters that must be calibrated. This increases model robustness and applicability in different environments (Sinclair and Seligman, 2000)

as observed by Maselli et al. (2013), whose simplified model integrated with remote sensing data provided reliable simulation of grasslands with contrasting soil and climate conditions.

This article presents a new simplified model for simulating grassland systems – VISTOCK – as a robust and effective tool to overcome some of the problems experienced by complex process-based crop models when used for grazing systems (i.e., input data availability and time-consuming calibration) (Graux et al., 2011; Parton et al., 1994; Simionesei et al., 2018). VISTOCK simulates potential grass biomass accumulation on a daily time step as a function of canopy-intercepted radiation that is reduced to actual biomass depending on the effects of thermal and water stresses. Leaf Area Index (LAI), derived from remote sensing platforms or proximal sensing tools, was used to drive simulations during the growing season. Along with grassland production, VISTOCK estimates grassland evapotranspiration (ET) fluxes and soil water content, which provides detailed information about water dynamics of the system.

VISTOCK's performance was evaluated for three sites with contrasting climates, soils and grass management practices to test its applicability to conditions different from those for which it had been calibrated. The results are discussed to highlight the flexibility of our approach in reproducing grassland systems, considering the potential to integrate model predictions into an automated system for optimizing the efficiency of rotational grazing systems and simplifying farm management.

2. Materials and methods

2.1 VISTOCK model description

VISTOCK simulates daily dry matter (DM) production and biomass dynamics of grasslands, considering thermal and water stress as limiting factors for growth (Figure 1). The information gathered from proximal (i.e., field spectroradiometer) and remote sensing (i.e., satellite) Normalized Difference Vegetation Index (NDVI) is integrated in the model through LAI, which is estimated using empirical relationships between LAI and the specific vegetation index (section 2.3.3). The model is based on the light-use efficiency-model developed by Monteith (1972, 1977) and used in many studies (Maselli et al., 2013; Migliavacca et al., 2011; Rossini et al., 2014, 2012), in which grassland production is estimated as a function of the fraction of absorbed photosynthetically active radiation (fAPAR,%) and radiation-use efficiency (RUE, g MJ^{-1}), considering limiting factors and meteorological variables.

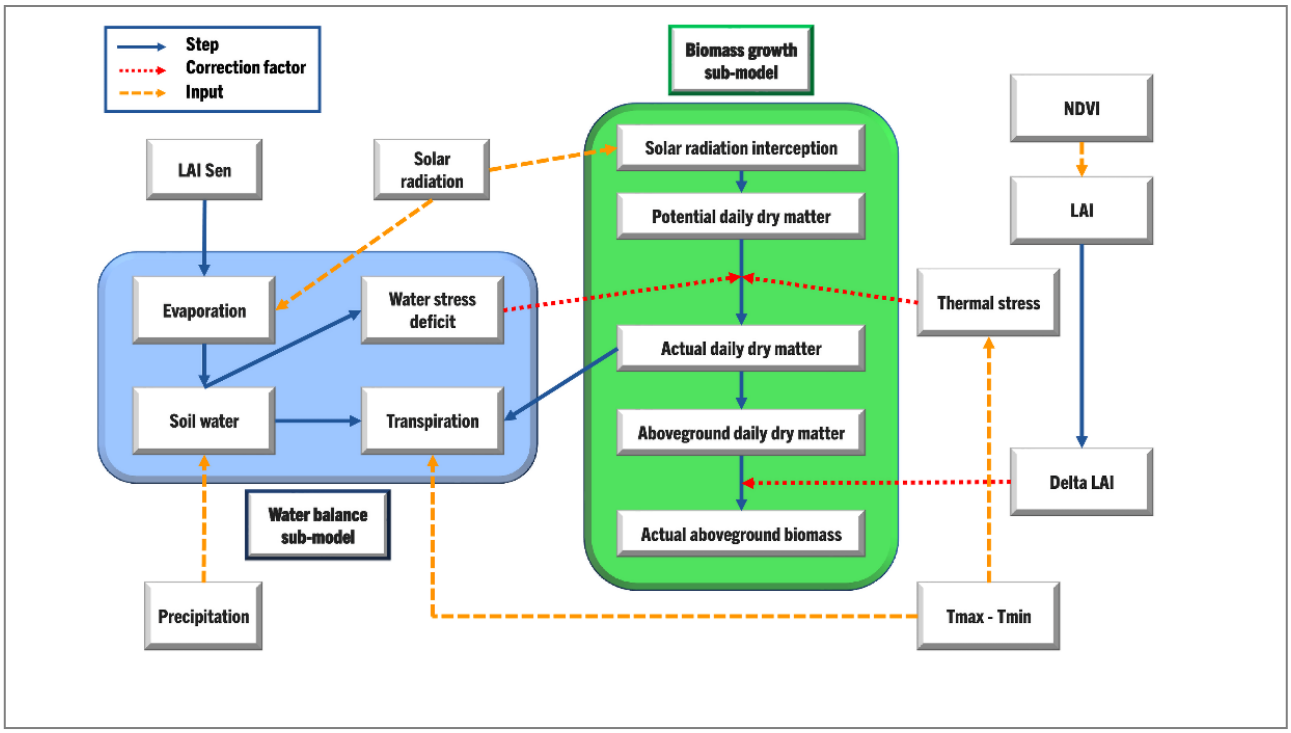

Figure 1. Flow diagram of the VISTOCK model including biomass growth sub-model and water balance sub-model. Tmax and Tmin are the daily maximum and minimum temperatures, respectively, NDVI the Normalized Difference Vegetation Index, LAI the leaf area index, LAI Sen the LAI of senescent biomass, and Delta LAI the difference between LAI on day n and n-1. See Table 1 for variable and parameter descriptions.

2.1.1 Grass growth model

VISTOCK first calculates potential net primary production (NPP) of the grassland at a daily time step (pNPP, g·m^{-2}·day^{-1}) as:

$$pNPP = fAPAR \cdot PAR \cdot RUE \quad (1)$$

where PAR (MJ·m^{-2}·day^{-1}) is photosynthetically active radiation, which is calculated from global solar radiation.

Next, fAPAR is calculated according to Sinclair (2006) as:

$$fAPAR = 1 - e^{-k \cdot LAI} \quad (2)$$

where k represents the extinction coefficient of the vegetation cover, and LAI is the mean grassland LAI (m^2·m^{-2}). Coefficient k is assumed to increase linearly as LAI increases during the growing season, according to the relation found for grassland ecosystems by Zhang et al. (2014).

LAI on day n is calculated as follows:

$$LAI_n = c \cdot e^{d \cdot NDVI} \quad (3)$$

where *c* and *d* are coefficients derived from the empirical relationship between LAI and NDVI developed from proximal or remote sensing instruments (section 2.3.3).

RUE of vegetation was estimated through calibration (section 2.4). Next, *p*NPP is rescaled as actual NPP (*a*NPP, $g \cdot m^{-2} \cdot day^{-1}$), considering thermal and water factors that limit grass growth:

$$aNPP = pNPP \cdot T_{COR} \cdot WS_{COR} \cdot SNOW \quad (4)$$

where T_{COR} (proportion) is the factor for thermal stress, WS_{COR} (proportion) is the factor for water stress, and SNOW indicates the presence (0) or absence (1) of snow.

T_{COR} is a function of daily minimum temperature, which varies from 0, for the temperature at which vegetation stops growing (GT_{MIN}), to 1, for the temperature at which plant growth is optimal (GT_{OPT}) (Heinsch et al., 2003). This approach based on minimum temperatures was used in other studies (Jolly et al., 2005; Migliavacca et al., 2011). The temperatures used for GT_{MIN} and GT_{OPT} depend on the botanical composition of a grassland, as grass species have different optimal temperatures for growth, as highlighted for forage mixtures by Movedi et al. (2019). WS_{COR} is calculated from the water balance sub-model (section 2.1.2), as a function of transpirable soil water. If snow is present, SNOW is set to 0, to represent vegetation growth stopping due to the interception of PAR. If not, SNOW is set to 1.

Next, the daily production of aboveground DM (ADM, $kg \cdot DM \cdot ha^{-1} \cdot day^{-1}$) is estimated as:

$$ADM = aNPP \cdot r \cdot 10 \quad (5)$$

Where r is the proportion of $aNPP_{daily}$ allocated aboveground and 10 is the factor to convert $g \cdot m^{-2} \cdot day^{-1}$ to $kg \cdot ha^{-1} \cdot day^{-1}$. According to Xu et al. (2013), *r* is set to a fixed value of 0.5.

Finally, ADM is used to estimate grassland aboveground biomass on day *n* (AGB_n), whose change is driven by the difference in LAI between day *n* and day *n-1* ($DELTA_{LAI}$).

$$DELTA_{LAI} = LAI_n - LAI_{n-1} \quad (6)$$

If $DELTA_{LAI}$ is positive, AGB is assumed to increase by the value of ADM, and AGB_n is calculated as:

$$AGB_n = AGB_{n-1} + ADM \quad (7)$$

If $DELTA_{LAI}$ is negative, AGB is assumed to decrease in linear proportion to the decrease in LAI, and AGB_n is calculated as:

$$AGB_n = AGB_{n-1} + AGB_{n-1} \cdot \left(\frac{DELTA_{LAI}}{LAI_{n-1}}\right) \quad (8)$$

2.1.2 Water balance

VISTOCK simulates daily water dynamics in the system in two soil layers, the first from the surface to the rooting depth of grasses (L_{GRASS}), and the second from L_{GRASS} to the maximum soil depth, which is assumed to equal 1 m (L_{TOT}). Each layer is defined by the most relevant hydrological constants: field capacity (%), wilting point (%), available water content (AWC, i.e., the water between field capacity and wilting point), and total transpirable soil water (TTSW, mm) (i.e., AWC × layer depth [mm]).

The water actually available (available soil water, ATSW (mm)) is calculated daily for each layer. ATSW for L_{GRASS} depends on the amount of precipitation (PRC, mm) and irrigation (I, mm) on day *n* and $ATSW_g$ on day *n-1*:

$$ATSW_{g\,n} = ATSW_{g\,n-1} + PRC + I \tag{9}$$

If $ATSW_g$ exceeds the TTSW of this layer, the excess enters the next layer.

Assuming that plant growth is influenced by the ratio of ATSW to TTSW in the layer explored by plant roots (Sinclair et al., 1998) we used this ratio, called the fraction of transpirable soil water, FTSW (%, Eq. 10), to rescale potential RUE to its actual value according to the general equation of Sinclair (1986) and Bindi et al. (2005) (Eq. 11):

$$FTSW_g = \frac{ATSW_g}{TTSW_g} \tag{10}$$

$$WS_{COR} = \frac{1}{1+a\cdot e^{-b\cdot FTSWg}} \tag{11}$$

where WS_{COR} quantifies the decrease in RUE due to water stress, while *a* and *b* are empirical parameters that shape WS_{COR} as a function of $FTSW_g$.

At the end of the *n*-day simulation, $ATSW_g$ is re-calculated by subtracting soil evaporation (SEVP, mm) and grass transpiration (TR, mm):

$$ATSW_{g\,n} = ATSW_{g\,n} - SEVP - TR \tag{12}$$

According to Soltani and Sinclair (2012), TR is calculated as:

$$TR = \frac{aNPP\cdot VPD}{TEC} \tag{13}$$

where VPD is the effective daily vapour pressure deficit for transpiration (kPa), and TEC is the transpiration efficiency coefficient (Pa) of the grass.

According to Tanner and Sinclair (1983), VPD is calculated from the difference between vapour pressure at maximum and minimum daily temperatures (VP_{Tmax} and VP_{Tmin}):

$$VPD = VPDf \cdot (VP_{Tmax} - VP_{Tmin}) \quad (14)$$

where VPDf is a coefficient that ranges from 0.65 (humid and sub-humid climate) to 0.75 (arid and semi-arid climate), and VP_{Tmax} and VP_{Tmin} are calculated as:

$$VP_{Tmax} = 0.6108 \cdot exp\left(\frac{17.27 \cdot Tmax}{237.3 + Tmax}\right) \quad (15)$$

$$VP_{Tmin} = 0.6108 \cdot exp\left(\frac{17.27 \cdot Tmin}{237.3 + Tmin}\right) \quad (16)$$

SEVP is determined from a two-stage model (Amir and Sinclair, 1991). The first occurs when water is freely evaporated and soil is considered wet (i.e., $FTSW_g$ higher than a specific threshold, $FTSW_{g\,THR}$). Under these conditions, SEVP is calculated as potential SEVP ($SEVP_{pot}$) using the equation of Moriondo et al. (2019):

$$SEVP_{pot} = RAD \cdot (1 - sALB) \cdot (1 - fAPAR_{TOT}) \cdot \frac{DELT}{DELT + 68} \cdot \frac{293}{583} \quad (17)$$

where RAD is global solar radiation (MJ m^{-2} day^{-1}), sALB is the soil albedo, $fAPAR_{TOT}$ is the amount of solar radiation intercepted by total grass cover (%), DELT (mbar $°K^{-1}$) is the slope of saturated vapour pressure vs. temperature, and the last ratio converts energy to mm of water evaporated.

$fAPAR_{TOT}$ represents the proportion of radiation intercepted by the vegetation, a value that differs from fAPAR as, in this case, LAI in (Eq. 2) is replaced with LAI_{TOT}.

$$LAI_{TOT} = LAI + LAI_{SEN} \quad (18)$$

where LAI_{SEN} is the LAI of senescent leaves. LAI_{SEN} is not considered in fAPAR as it is not photosynthetically active, although it does influence evaporation by covering the soil. Assuming an inversely proportional relation between LAI and LAI_{SEN}, LAI_{TOT} is set to a fixed value. For pasture and meadow-pasture, LAI_{TOT} is assumed equal to LAI, as grazing and mowing do not allow senescent leaves to accumulate as they do in natural grassland.

DELT is calculated as a function of maximum daily temperature (T_{max}, °C), according to Soltani and Sinclair (2012):

$$DELT = exp \cdot \left(21.255 - \frac{5304}{273 + TMP}\right) \cdot \frac{5304}{(273 + TMP)^2} \quad (19)$$

The second stage occurs when the evaporation in L_{GRASS} is not equivalent to the evaporation of a wet surface ($SEVP_{pot}$), as in the first stage. Under these conditions ($FTSW_g < FTSW_{g\ THR}$), SEVP is rescaled from SEV_{pot} as follows:

$$SEVP = SEVP_{pot} \cdot (\sqrt{(DYSE + 1)} + \sqrt{DYSE}) \quad (20)$$

where DYSE represents the number of days since the last water supply (precipitation or irrigation) higher than a specific threshold ($DYSE_{THR}$, mm). Daily evapotranspiration (ET, mm) is then calculated as:

$$ET = SEVP + TR \quad (21)$$

Table 1. Variables and parameters used in the VISTOCK model for sites T, M and B.

Type	Name	Description	Units/value	Reference
Biomass	*p*NPP	Potential net primary production	g m^{-2} day^{-1}	
	*a*NPP	Actual net primary production	g m^{-2} day^{-1}	
	ADM	Daily dry matter production allocated above ground	MJ m^{-2} day^{-1}	
	LAI	Leaf area index of green biomass	m^2 m^{-2}	
	AGB	Aboveground biomass	kg DM ha^{-1}	
	AGB_{MIN}	Minimum AGB	150 kg DM ha^{-1}	Fixed
	$DELTA_{LAI}$	Daily difference in LAI	m^2 m^{-2}	
	LAI_{TOT}	Total LAI	2.5 m^2 m^{-2}	Fixed
	LAI_{SEN}	LAI of senescent biomass	m^2 m^{-2}	Fixed
Rate	fAPAR	Fraction of absorbed photosynthetically active radiation intercepted by green grass cover	proportion (0-1)	
	$fAPAR_{TOT}$	Fraction of absorbed photosynthetically radiation intercepted by total grass cover	proportion (0-1)	
	SEVP	Daily actual soil evaporation	mm day^{-1}	
	$SEVP_{pot}$	Potential soil evaporation	mm day^{-1}	
	ET	Daily evapotranspiration	mm day^{-1}	
	$FTSW_g$	Fraction of transpirable water in the upper soil layer (L_{GRASS})	proportion (0-1)	
	$FTSW_{gr\ THR}$	$FTSW_g$ threshold for estimating SEVP	0.35	Fixed
	WS_{COR}	Factor for water stress	proportion (0-1)	
	T_{COR}	Factor for thermal stress	proportion (0-1)	
	$ATSW_g$	Available transpirable soil water in L_{GRASS}	mm	
	$ATSW_{TOT}$	Available transpirable soil water in L_{TOT}	mm	

	r	Proportion of *a*NPP allocated aboveground	0.5	Xu et al. (2013)
	a	Coefficient for estimating WS_{COR}	9.49	Calibrated
	b	Coefficient for estimating WS_{COR}	-15.69	Calibrated
	c	Coefficient of the empirical relation between NDVI and LAI	0.0034 T; 0.0767 M-B	Calculated
	d	Coefficient of the empirical relation between NDVI and LAI	4.2965 T; 8.6362 M-B	Calculated
	VPDf	Vapour pressure deficit coefficient	0.75	Fixed
	DELT	Slope of saturated vapour pressure vs. temperature	mbar $°K^{-1}$	
Plant	RUE	Radiation-use efficiency	1.39 g MJ^{-1}	Calibrated
	k	Extinction coefficient of the vegetation cover	0.5	Zhang et al. (2014)
	TEC	Transpiration efficiency coefficient	3.0 Pa	Calibrated
	GT_{MIN}	Minimum daily temperature at which growth stops	-5.66°C T; 2°C M-B	Migliavacca et al. (2011); Calibrated
	GT_{OPT}	Minimum daily temperature of optimal growth	7.24°C T; 10°C M-B	Migliavacca et al. (2011); Calibrated
Soil	AWC	Available water content in the soil	mm	
	$TTSW_g$	Total transpirable water in the upper soil layer (L_{GRASS})	mm	
	$TTSW_{TOT}$	Total transpirable water in the lower soil layer (L_{TOT})	mm	
	AWAFC	Amount of water that can be retained on the soil surface	mm	
	$DEPTH_g$	Depth of the upper soil layer (L_{GRASS})	m	
	$DEPTH_{TOT}$	Depth of the lower soil layer (L_{TOT})	m	
	sALB	Soil albedo	0.9	Fixed
Environment	T_{MAX}	Daily maximum temperature	°C	Input
	T_{MIN}	Daily minimum temperature	°C	Input
	PAR	Photosynthetic active radiation	MJ m^{-2} day^{-1}	Input
	RAD	Global solar radiation	MJ m^{-2} day^{-1}	Input
	PRC	Daily cumulative precipitation	mm	Input
	SNOW	Snow presence	0 (present) or 1 (absent)	Input

VPD	Effective daily vapour pressure deficit for transpiration	kPa	
VP_{MAX}	Vapour pressure at maximum daily temperature	kPa	
VP_{MIN}	Vapour pressure at minimum daily temperature	kPa	
DYSE	Days since the last water supply	days	
$DYSE_{THR}$	DYSE threshold for estimating SEVP	6 mm	Fixed

2.2 Study sites

Data for model calibration and evaluation were collected for three test sites in Italy (Figure 2): Torgnon (T), Marradi (M) and Borgo San Lorenzo (B). To test the model under diverse conditions and obtain a more robust evaluation, these study sites were chosen for their elevations, botanical composition, soil and climate characteristics, and management.

Site T is an abandoned natural sub-alpine grassland located at 2160 m a.s.l. in the north-western Italian Alps (45.8444°N; 7.5781°E). The site has mean annual temperature of 3.1°C and mean annual precipitation of 880 mm (2008-2020, Oddi et al., 2021). Snow usually covers the grassland from October to May (Galvagno et al., 2013). Since 2007, the last time it was grazed, the site can be considered as a permanent grassland dominated by *Nardus stricta*, with the presence of *Poa alpina*, *Trifolium alpinum*, *Arnica montana*, and *Ranunculus pyrenaeus* (Pintaldi et al., 2016).

Site M is a pasture at 600 m a.s.l. in the Tuscan Apennines (44.0810°N; 11.6327°E), with mean annual temperature of 12.4°C (2016, 2017, 2020) and mean annual precipitation of 1330 mm (2001-2020). Site M is a sown pasture tending to a rewilding process, with a predominance of *Dactylis glomerata*, *Lolium* spp., *Festuca arundinacea*, *Phleum pratense*, and *Onobrychis viciifolia*, with other minor forbs and the presence of many shrubs in some sectors, such as *Rubus ulmifolius*. The pasture is usually continuously grazed by Limousin cattle from May to July.

Site B is a pasture located at 200 m a.s.l. in the Sieve River plain (43.9536°N; 11.3487°E), with mean annual temperature of 13.4°C (1951-2020) and mean annual precipitation of 990 mm (2001-2020). Site B is a sown pasture with grassland species generally present in commercial mixtures, such as *Lolium* spp., *D. glomerata*, *Trifolium pratense*, *Trifolium repens*, *Lotus corniculatus*, and *F. arundinacea*, with other minor forbs. For the purpose of the experiment, in 2020 site B was further divided into two areas with different management approaches: B1 and B2. Specifically, B1 was grazed by Limousin cattle from April to late October, while B2 was managed as a meadow-pasture, with mowing in May and grazing from June to late October. In 2021, both B1 and B2 were managed as pasture under continuous grazing.

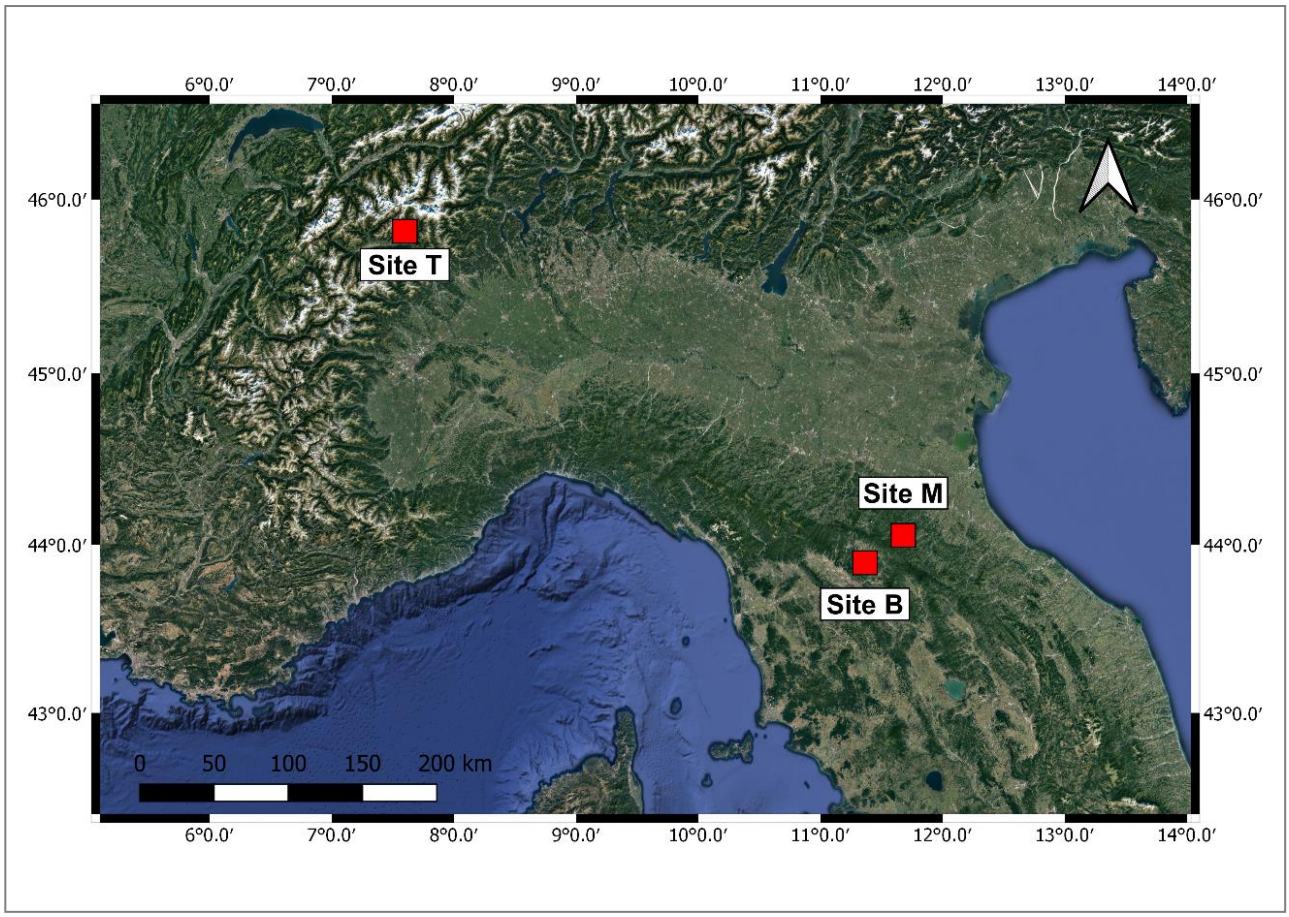

Figure 2. Locations of the experimental sites in Italy: Torgnon (site T), Marradi (site M) and Borgo San Lorenzo (site B).

2.3 Data collection

2.3.1 Ground-based observed data

Soil texture was collected by Pintaldi et al. (2016) for site T, while it was retrieved from the Soilgrids^{TM} dataset (https://soilgrids.org/) for sites B and M. Field capacity, wilting point, and AWC of L_{TOT} and L_{GRASS} were calculated according to Saxton et al. (1986). At site T, information on soil water content (i.e., daily $FTSW_g$) were calculated from data collected by a soil moisture sensor (CS-616, Campbell Scientific) installed at a depth of 30 cm.

Grassland production throughout the growing season (i.e., AGB (kg DM ha^{-1}) and LAI) was measured during field surveys conducted from 2012-2018 at site T (58 field samplings), and in spring/summer 2020 and 2021 at sites B and M (15 and 11 field samplings, respectively). Specifically, at site T, AGB and LAI were measured on each sampling date from 12 (2012-2013) and 9 (2013-2018) 30 × 30 cm samples located at the corners of 3 separate rectangular plots (40 × 15 m). LAI was measured with an area meter (model LI-3100, LI-COR, Inc., Lincoln, Nebraska, USA), while fresh grass samples were dried in an oven at 60°C and weighed (Filippa et al., 2015) . At sites B and M, AGB was

measured from 8 randomly located 1 m^2 samples per site, further subdivided at site B according to the two management approaches (4 in B1 and 4 in B2). Grass was cut with scissors at ground level and the fresh grass samples were dried in a forced-air oven at 60°C. LAI was measured using an AccuPAR PAR/LAI Ceptometer Model LP-80.

Daily gross primary production (GPP, g C m^{-2} day^{-1}) and ET (mm day^{-1}) were derived from eddy-covariance measurements taken at site T (IT-Tor ICOS site, https://meta.icos-cp.eu/resources/stations/ES_IT-Tor). Details of instrument setup, measurements, and data processing are provided by Galvagno et al. (2017, 2013). To estimate daily *a*NPP, GPP was converted to NPP (g C m^{-2} day^{-1}) by multiplying it by a fixed conversion factor of 0.53 (Chen et al., 2003; Zhang et al., 2009) and then by 2 to convert g C to g DM (White et al., 2000).

2.3.2 Meteorological data

As mentioned, VISTOCK requires daily data on minimum and maximum temperatures, precipitation, and global solar radiation. Daily temperature, precipitation and solar radiation data at site T were measured by a meteorological station installed at the study site, as described in detail by Galvagno et al. (2013). For sites B and M, temperature and precipitation data were collected from weather stations operated by the Tuscany region (SIR, Servizio Idrologico Regionale, https://www.sir.toscana.it/) located near the study sites. Daily solar radiation data were calculated using the "sirad" package (Bojanowski, 2016) of R software (R Core Team, 2021) based on the model of Bristow and Campbell (1984).

2.3.3 Remote and proximal sensing data

NDVI (Tucker, 1979), used to estimate LAI, was calculated as follows:

$$NDVI = \frac{R_{NIR} - R_{RED}}{R_{NIR} + R_{RED}} \quad (22)$$

where R_{NIR} and R_{RED} are reflectance in near-infrared and red wavelengths, respectively.

NDVI was calculated from proximal devices (site T) and satellite-derived observations (sites B and M). Specifically, for site T, NDVI (Skye-NDVI) was calculated using reflectances at 640 and 860 nm in red and near-infrared wavelengths, respectively (Eq. 22), measured by a SKR 1800 2-Channel Light Sensor (Skye Instruments). For sites B and M, NDVI (S2-NDVI) was calculated remotely from band 4 (red, central wavelength of 665 nm) and band 8 (near-infrared, central wavelength of 842 nm) of Sentinel-2 L2A images. Given the latter's 5-day temporal resolution and the unavailability of some satellite images due to atmospheric conditions, processed S2-NDVI data were linearly interpolated to obtain daily data.

LAI was measured in the field at all test sites at different vegetation stages. Observed LAI and NDVI were correlated using an exponential function (Fan et al., 2009) to obtain a specific empirical relationship:

$$LAI_n = c \cdot e^{d \cdot NDVI_n} \quad (23)$$

where LAI_n and $NDVI_n$ are LAI and NDVI on day *n*, respectively, and *c* and *d* are empirical parameters.

As proximal and remote sensing instruments operate with different specific central wavelengths and spatial resolutions, the LAI-NDVI relationships were kept separate. Hence, *c* and *d* for site T (Skye-NDVI) differed from those for sites B and M (S2-NDVI).

2.4 Model calibration and evaluation

The parameters calibrated during model calibration were RUE, TEC, and the empirical parameters *a* and *b* that determine WS_{COR}. Because site T provided daily data for *a*NPP, ET and $FTSW_g$, it was selected for the calibration process. Subsequently, the parameters were optimized using the *estim_param* function of the R package *CroptimizR* (Buis et al., 2018) by minimizing the difference between observed and predicted values of *a*NPP, ET, and $FTSW_g$ using the log transformation of the concentrated version of weighted sum of squares (Wallach et al., 2011). Calibration using *estim_param* required setting a range of values for each parameter: 1.3-2.0 g MJ^{-1} for RUE (Maselli et al., 2013), 3.0-4.5 Pa for TEC (Soltani and Sinclair, 2012), 9-30 for *a*, and -17 to -8 for *b*. During the minimization process, the options of the *estim_param* function were set to 20, 200, and 0.001 for the number of replicates, maximum number of evaluations of the minimized criterion, and the tolerance criterion between two iterations, respectively.

Calibration was performed for site T for three years (2012, 2017, and 2018), which were chosen because they had the most diverse meteorological characteristics in the dataset, in order to capture the meteorological variability in the calibration. Specifically, for an approximate grassland growing season (i.e., day of year (DOY) 130-300), mean daily temperature varied slightly in 2012, 2017, and 2018 (9.2, 9.6 and 9.8°C, respectively), while snow melt date (DOY 129, 131 and 142 for 2012, 2017 and 2018, respectively) and cumulative precipitation (761, 694 and 1156 mm $year^{-1}$, respectively) varied greatly.

Once calibrated, VISTOCK was evaluated using the observed *a*NPP, ET, and $FTSW_g$ for the remaining 4 years of data (2013, 2014, 2015 and 2016) to predict grass growth (AGB_n) at site T (2012-2018). The calibrated model was also applied to sites M and B (approximate season from DOY

60 to 300) using the same parameters as those for site T, except for GT_{MIN} and GT_{OPT}, as site M and B had plant species with different thermal requirements, which yielded different values of GT_{MIN} and GT_{OPT} than those set for the alpine conditions of site T (Migliavacca et al., 2011). To find optimal values for sites M and B, we applied the optimization procedure to the thermal requirements using observed AGB data at site M (2020) to minimize the error, varying GT_{MIN} and GT_{OPT} from 0-9°C and 9-20°C, respectively. The temperatures obtained were then applied to sites M, B1, and B2 for 2020 and 2021. The AGB at the beginning of each simulation (i.e., DOY 1) was initialized both for calibration and evaluation using a spin-up procedure in which the model iteratively tests initial AGB in the range of 100-1500 kg DM ha^{-1} with a step of 50 kg DM ha^{-1} to provide the best match between predicted AGB and the AGB measured at the first destructive sampling.

2.5 Assessing the accuracy of predicted aNPP, ET, $FTSW_g$, and AGB

VISTOCK's ability to predict *a*NPP, ET, $FTSW_g$ and AGB of the grasslands was evaluated using the coefficient of variation (R^2), Root Mean Square Error (RMSE), and relative RMSE (RRMSE, %) (Moriondo et al., 2019), calculated as follows:

$$R^2 = 1 - \frac{\sum_{i=1}^{n}(y_i - f_i)^2}{\sum_{1=1}^{n}(y_i - \underline{y})^2} \quad (24)$$

$$RMSE = \sqrt{\frac{1}{n}\sum_{i}^{n}(y_i - f_i)^2} \quad (25)$$

$$RRMSE = \frac{RMSE}{\underline{y}} \quad (26)$$

where y_i is the observed value, f_i is the predicted value, and $\underline{y}$ is the mean of the observed data.

For observed AGB data, we used means calculated from AGB measured on the same sampling date. Statistical indicators were calculated for site T for the daily variables NPP, ET, and $FTSW_g$ only for the days on which there was no snow cover, which yielded a total of 555 points for the calibration and 743 for the evaluation. For observed AGB, the total number of evaluation points was 84 (51, 9, 13, and 11 for sites T, M, B1, and B2, respectively). The first observed AGB value of each year was not considered in the statistical analyses as these points were used in the spin-up process to initialise the model.

3. Results

3.1 Calibration

From the optimization, RUE, TEC, *a,* and *b* used to simulate grass growth were set at 1.39 g MJ^{-1}, 3.0 Pa, 9.50, and -15.69, respectively, while GT_{MIN} and GT_{OPT} were set at 2°C and 10°C, respectively, for sites M and B. Empirical relationships between Skye-NDVI, S2-NDVI, and LAI had an R^2 of 0.77 (RMSE = 0.22, RRMSE = 25.6%) for site T (*c*= 0.0767 and *d*= 4.2965) and 0.76 (RMSE = 0.63, RRMSE = 40.0%) for sites B_1, B_2, M (*c*= 0.0034 and *d* = 8.6362). All the inputs and model parameters used to predict *a*NPP, ET, $FTSW_g$ (site T), and AGB_n (sites T, B1, B2, and M) are shown in Table 1. The calibration for site T yielded good predictions under the diverse meteorological conditions (2012, 2017, and 2018) (Table 2). VISTOCK generally predicted *a*NPP well, except for a slight overestimation during the peak of grassland production (ca. DOY 170-230) (Figure 3). The calibration showed a strong relationship between observed and predicted 10-day cumulative values of *a*NPP, with an $R^2 > 0.94$ and RRMSE < 25% for all calibration years (Table 2).

VISTOCK tended to underpredict ET, especially for 2017 (RMSE = 15.1 mm 10 d^{-1}, RRMSE = 47.8%) and 2018 (RMSE = 11.5 mm 10 d^{-1}, RRMSE = 43.8%), but it predicted ET more accurately for 2012 (RMSE = 6.6 m 10 d^{-1}, RRMSE = 26.7%) (Figure 4). Despite this bias, the model correctly predicted ET dynamics over the growing season, as highlighted by R^2 equal to 0.86, 0.94, and 0.86 for 2012, 2017, and 2018, respectively.

For soil water content, the calibration provided optimal predictions of $FTSW_g$ (Figure 5). VISTOCK predicted water dynamics in the soil layer explored by roots well for 2012, 2017, and 2018 (R^2 = 0.91, 0.70, and 0.92, respectively), with robust quantitative accuracy as well (RRMSE = 12.0%, 18.4% and 13.5%, respectively).

3.2 Evaluation

3.2.1 Site T

When the calibrated model was applied to the remaining years for site T (2013, 2014, 2015 and 2016), it adequately reproduced *a*NPP dynamics during their growing seasons, thus capturing grassland growth dynamics at a daily time step (Figure 3). Moreover, 10-day cumulative values of *a*NPP showed a good fit between observed and predicted values ($R^2 > 0.84$) for all evaluation years (Table 2). At the same time, the quantitative accuracy was similar to that for the calibration results for 2013

and 2014 (RRMSE = 18.3% and 21.8%, respectively), but slightly lower for 2015 and 2016 (RRMSE = 30.9% and 33.5%, respectively), due to specific water-stress periods simulated by the model.

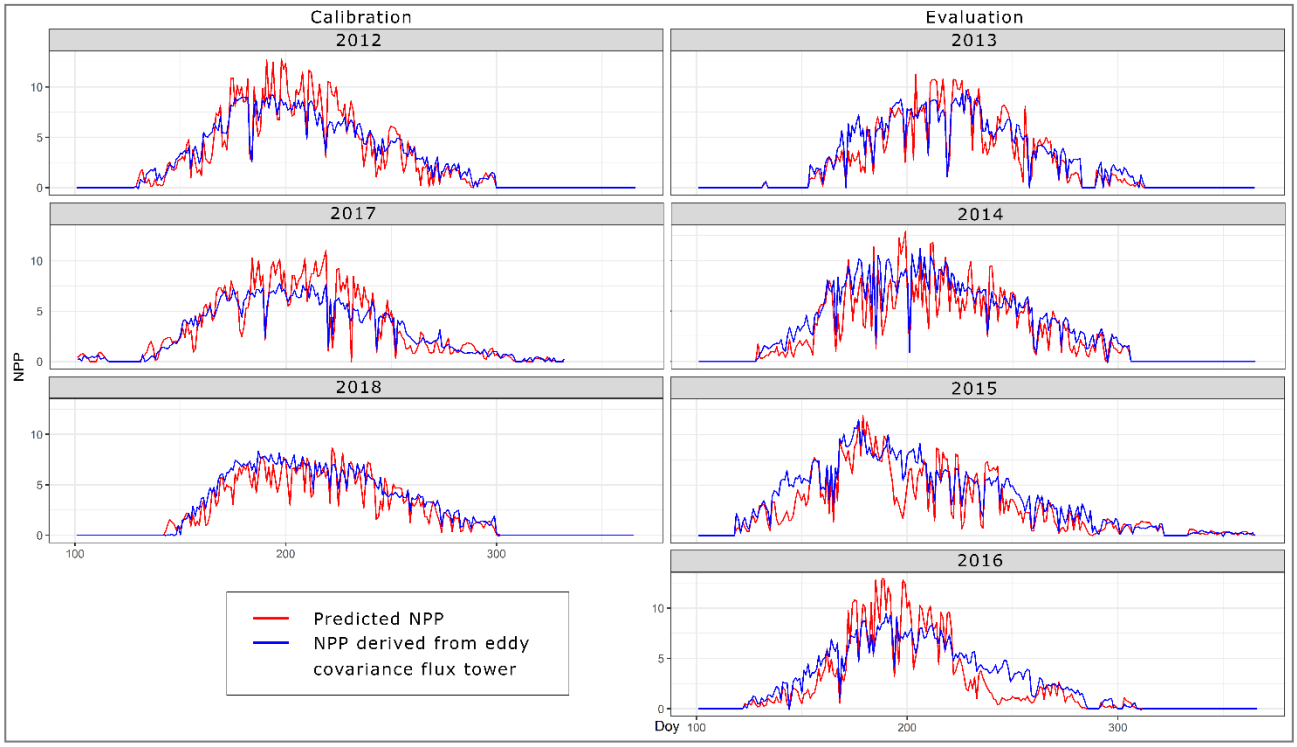

Figure 3. Daily values of predicted actual net primary production (aNPP, g m^{-2} d^{-1}) and NPP derived from eddy covariance method in 2012-2018 at site T, divided between (left) calibration and (right) evaluation years.

VISTOCK generally underestimated ET (RMSE > 10.0 mm 10 d^{-1} for all evaluation years), which resulted in high RRMSE (> 35%) (Figure 4). Nevertheless, it generally captured ET dynamics well, especially in 2013 and 2014 (R^2 = 0.95 and 0.93, respectively). As observed for *a*NPP, R^2 was lower in 2015 and 2016 (R^2 = 0.73 and 0.52, respectively) due to a period of decreased ET (ca. DOY 190-210 and 230-260, respectively) predicted by the model during a drought, but which was not observed in the ET measured by the eddy covariance tower.

Overall, VISTOCK reproduced $FTSW_g$ beneath grassland vegetation well. Specifically, the dynamics and quantitative accuracy of daily $FTSW_g$ were adequately reproduced (Figure 5, Table 2). Hence, $FTSW_g$ was correctly predicted in 2013 (R^2 = 0.72, RMSE = 11.9%, RRMSE = 14.0%) and 2014 (R^2 = 0.51, RMSE = 6.0%, RRMSE = 6.3%), which usually had transpirable soil water available in the layer explored by grass roots. Soil water was also predicted well during extended periods of decreased $FTSW_g$, as in 2016 (R^2 = 0.95, RMSE = 10.6%, RRMSE = 15.9%), as well as in years with one brief period of decreased $FTSW_g$ during the growing season (i.e., 2015, R^2 = 0.91, RMSE = 8.5%, RRMSE = 10.0%).

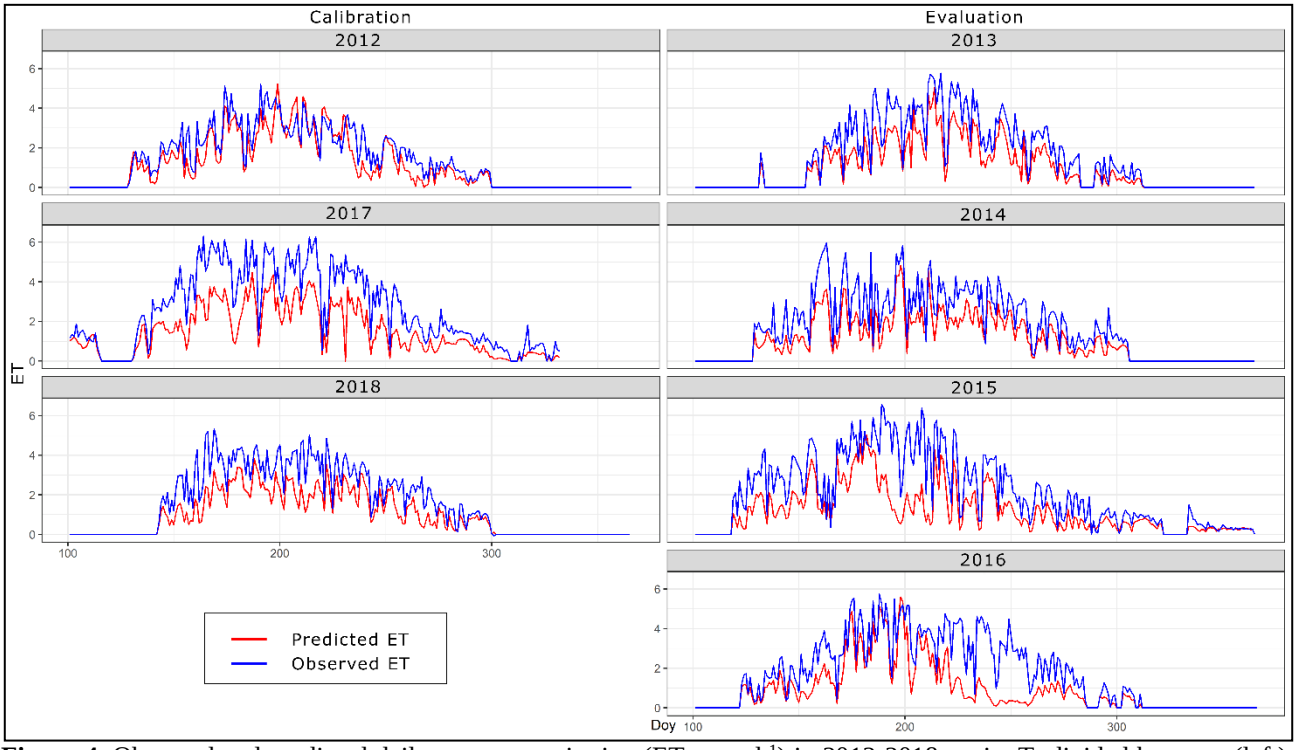

Figure 4. Observed and predicted daily evapotranspiration (ET, mm d^{-1}) in 2012-2018 at site T, divided between (left) calibration and (right) evaluation years.

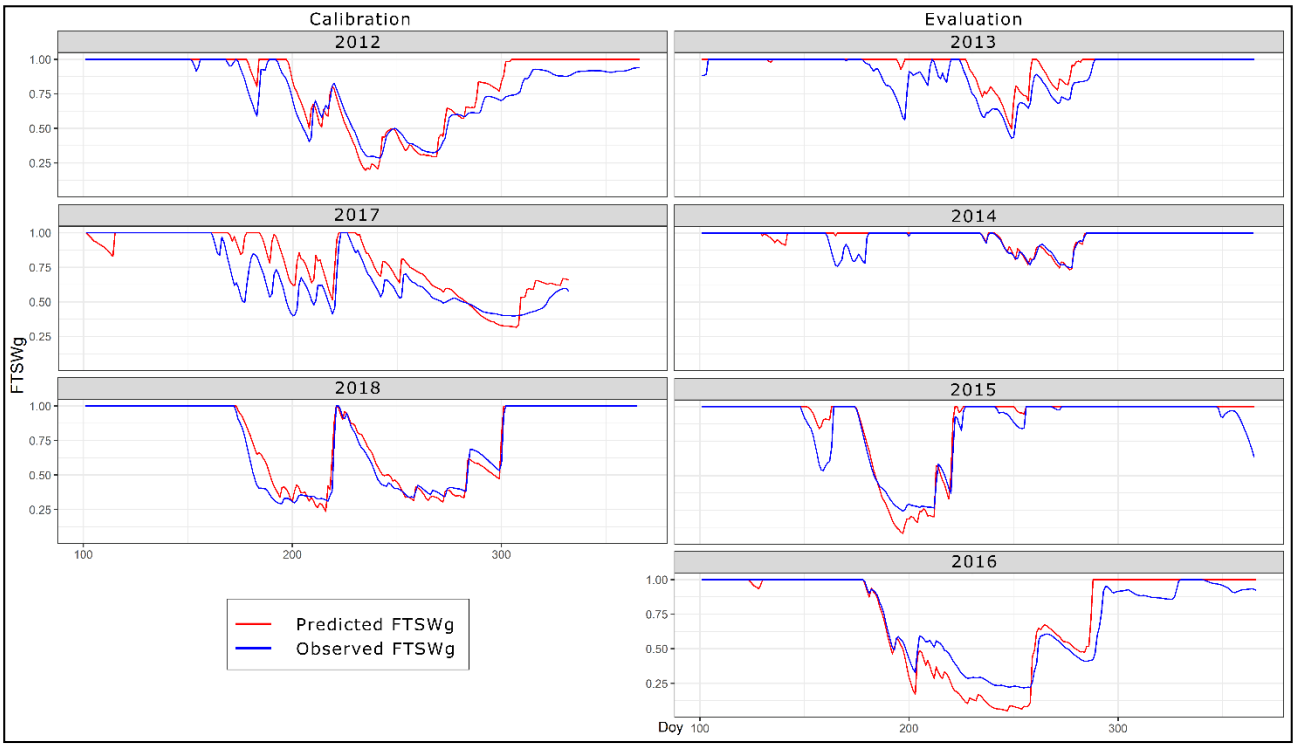

Figure 5. Observed and predicted fraction of total transpirable soil water ($FTSW_g$, %) in 2012-2018 at site T, divided between (left) calibration and (right) evaluation years.

VISTOCK reproduced AGB well during the growing season of each evaluation year (R^2 = 0.68, RMSE = 444.5 kg DM ha^{-1}, RRMSE = 23.6%), capturing well the peak of AGB and the start of the decrease in green AGB due to senescence (Figure 6, Table 2).

3.2.2 Site M

Despite estimating LAI for sites M and B using S2-NDVI instead of Skye-NDVI, VISTOCK robustly reproduced AGB production in 2020 and 2021 (Table 2). Specifically, predicted AGB at site M accurately followed observed AGB from its peak to the end of the growing season (R^2 = 0.81, RMSE = 240.4 kg DM ha^{-1}, RRMSE = 32.1%), which captured well the impact of grazing animals on AGB (Figure 7).

3.2.3 Site B1

Using site M parameters and LAI estimates in site B1simulation, VISTOCK reproduced AGB dynamics well during the growing seasons 2020 and 2021 according to R^2 (0.70), although the RRMSE was relatively high (42.8%). Despite having the lowest RMSE (219.4 kg DM ha^{-1}) among all evaluation sites, small differences between observed and predicted AGB had a high RRMSE, due to the small proportion of AGB left on the pasture by the cattle at the end of the grazing period.

3.2.4 Site B2

Using site M parameters and LAI estimates in site B2 simulation, VISTOCK reproduced well the combined effect of mowing (DOY 130), followed by vegetation regrowth, and then grazing on DOY 180 in 2020 and continuous grazing in 2021 (R^2 = 0.79, RMSE = 364.9 kg DM ha^{-1}, RRMSE = 33.9%).

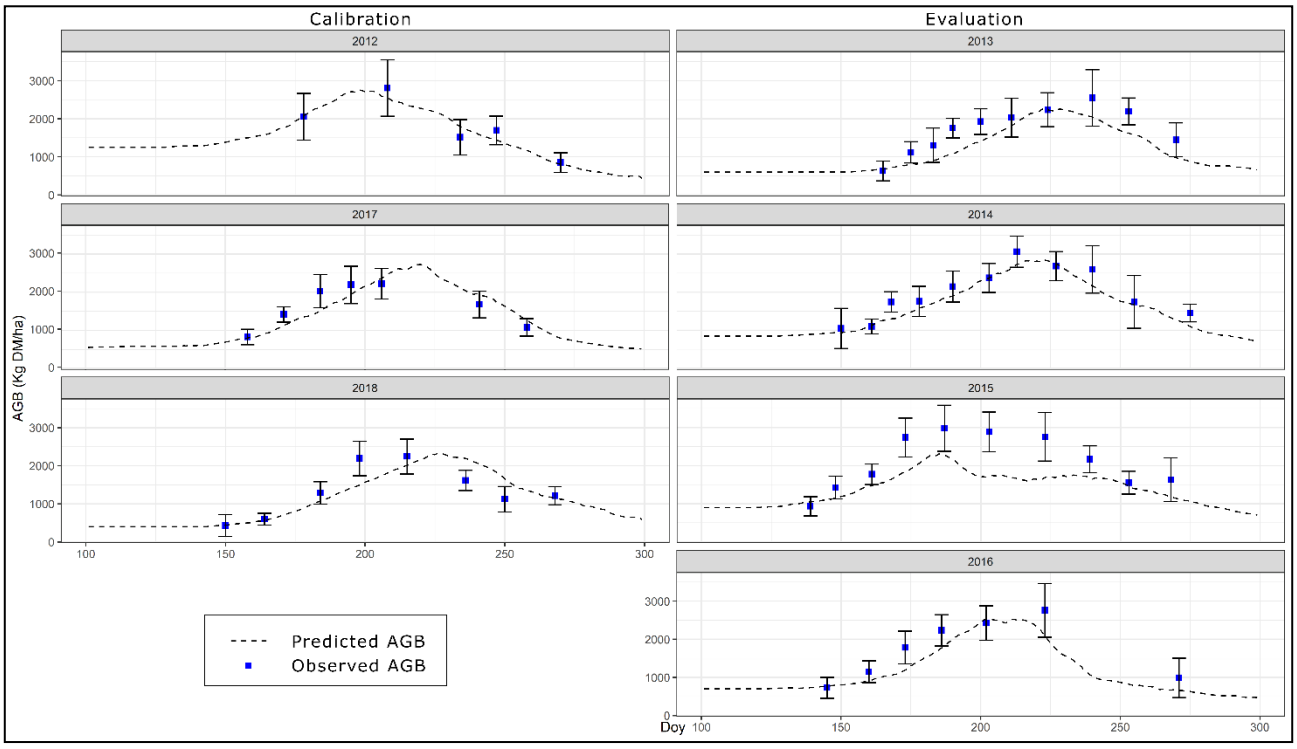

Figure 6. Predicted and mean (±1 standard deviation) observed aboveground biomass (AGB, kg DM ha^{-1}) at site T in 2012-2018, divided between (left) calibration and (right) evaluation years.

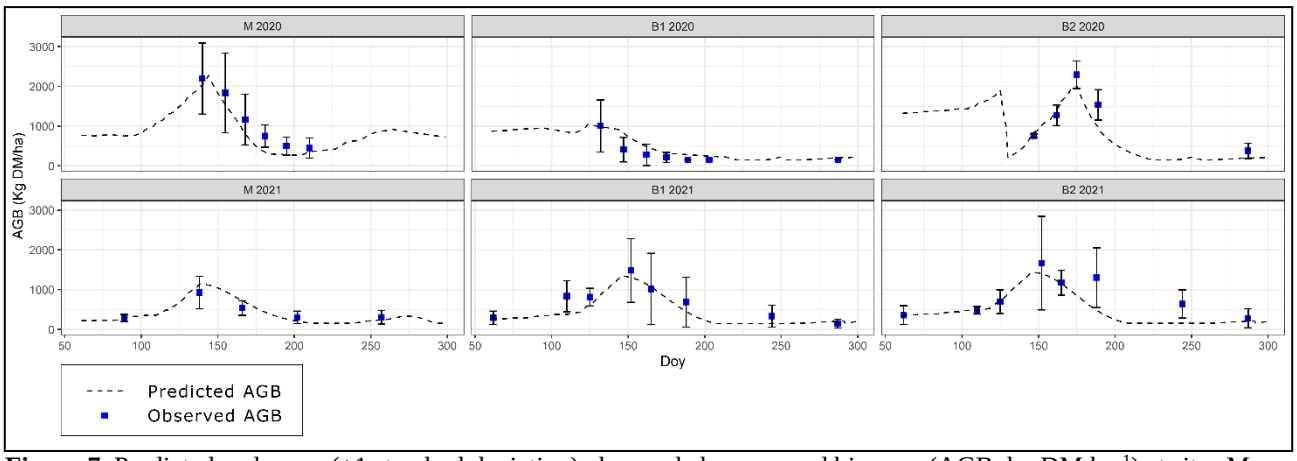

Figure 7. Predicted and mean (±1 standard deviation) observed aboveground biomass (AGB, kg DM ha^{-1}) at sites M, B1, and B2 in 2020 and 2021.

Table 2. Goodness-of-fit indicators (i.e., coefficient of variation (R^2), root mean square error (RMSE), and relative RMSE (RRMSE)) of actual net primary production (*a*NPP), evapotranspiration (ET), fraction of transpirable soil water ($FTSW_g$), and aboveground biomass (AGB) between observations and VISTOCK predictions for model calibration and evaluation. A 10 days-aggregation level was chosen for *a*NPP and ET to reduce the effect of daily fluctuations.

Variable	Site	Simulation	Year	Aggregation	R^2	RMSE	RRMSE
*a*NPP	T	Calibration	2012	10 days	0.94	10.9 g m^{-2} $10d^{-1}$	21.0%
	T	Evaluation	2013	10 days	0.84	10.2 g m^{-2} $10d^{-1}$	18.3%
	T	Evaluation	2014	10 days	0.90	12.0 g m^{-2} $10d^{-1}$	21.8%
	T	Evaluation	2015	10 days	0.87	12.8 g m^{-2} $10d^{-1}$	30.9%
	T	Evaluation	2016	10 days	0.88	15.3 g m^{-2} $10d^{-1}$	33.5%
	T	Calibration	2017	10 days	0.94	8.5 g m^{-2} $10d^{-1}$	23.0%
	T	Calibration	2018	10 days	0.96	8.1 g m^{-2} $10d^{-1}$	18.3%
ET	T	Calibration	2012	10 days	0.86	6.6 mm $10d^{-1}$	26.7%
	T	Evaluation	2013	10 days	0.95	10.8 mm $10d^{-1}$	35.7%
	T	Evaluation	2014	10 days	0.93	10.3 mm $10d^{-1}$	39.2%
	T	Evaluation	2015	10 days	0.73	14.2 mm $10d^{-1}$	55.9%
	T	Evaluation	2016	10 days	0.52	15.3 mm $10d^{-1}$	53.3%
	T	Calibration	2017	10 days	0.94	15.1 mm $10d^{-1}$	47.8%
	T	Calibration	2018	10 days	0.85	11.5 mm $10d^{-1}$	43.8%
$FTSW_g$	T	Calibration	2012	daily	0.91	8.4%	12.0%
	T	Evaluation	2013	daily	0.72	11.9%	14.0%
	T	Evaluation	2014	daily	0.51	6.0%	6.3%
	T	Evaluation	2015	daily	0.91	8.5%	10.0%

	T	Evaluation	2016	daily	0.95	10.6%	15.9%
	T	Calibration	2017	daily	0.70	15.6%	18.4%
	T	Calibration	2018	daily	0.92	8.0%	13.5%
AGB	T	Evaluation	2012-2018	-	0.68	444.5 kg ha^{-1}	23.6%
	M	Evaluation	2020 and 2021	-	0.81	240.4 kg ha^{-1}	32.1%
	B1	Evaluation	2020 and 2021	-	0.70	219.4 kg ha^{-1}	42.8%
	B2	Evaluation	2020 and 2021	-	0.79	364.9 kg ha^{-1}	33.9%

4. Discussion

Once calibrated, VISTOCK simulated the grassland system well (Table 2). The model's potentially wide applicability, due to optimizing a few important parameters (i.e., RUE, TEC, *a*, and *b*) that are kept constant, is confirmed by its predictions for different environments (sites T, B1, B2 and M).

As highlighted by Maselli et al. (2013) and Moriondo et al. (2019), simplifying the system increased the applicability of the model, which provided encouraging results, even for sites with diverse soil, climate, botanical, and management conditions. For VISTOCK, this simplification was to estimate LAI directly from NDVI data obtained from proximal and remote sensing techniques. It is well known that LAI is a key parameter for estimating carbon and energy fluxes between plants and the atmosphere, photosynthetic activity, and AGB production (Prieto-Blanco et al., 2009; Swain et al., 2016; Verrelst et al., 2016; Yu et al., 2018). The importance of LAI for assessing these processes is also reflected in process-based models (Liu et al., 2018), in which LAI and related parameters (e.g., fAPAR) play a major role in simulating growth processes in agro-ecosystems (Touhami et al., 2013). Using NDVI during the growing season to estimate LAI, which is influenced by biotic (pests and disease, Baròn et al., 2013), abiotic (water or nitrogen stresses, Bahrani et al., 2010; Knops and Reinhart, 2000), and ecological factors (Westoby et al., 2004), is therefore of paramount importance for determining crop growth processes. The use of a strict relationship between LAI and remote sensing vegetation indexes observed for many crop systems (Liu et al., 2012; Xie et al., 2015), including grasslands (Fan et al., 2009; Palmer et al., 2017; Wylie et al., 2002), supports simplification of a crop growth model that no longer needs to estimate effects of limiting factors on leaf area growth and thus to calibrate relevant parameters, but rather relies on conservative relationships such as RUE or water-use efficiency (Sinclair and Seligman, 2000). Effects of thermal and water stresses related to these parameters were explicitly considered, as in other light-use-efficiency models (e.g., Maselli et al., 2013), to quantify effects of these factors and monitor plant conditions during the simulated growing season. This was especially important for reproducing water dynamics in the soil with the water balance sub-model, as plant transpiration influences them.

In addition, estimating LAI using remote sensing data also avoided the need to adjust model parameters to effectively simulate grassland systems with different types of management (i.e., natural grassland, pasture, meadow-pasture). Using NDVI to estimate LAI thus increases the robustness of the model, which can be potentially applied to contexts other than those for which it was calibrated and opens up the potential to simulate very local scales, thus exploiting the high spatial and temporal resolutions of currently available satellite data (Wakulińska and Marcinkowska-Ochtyra, 2020). At the same time, using satellite data in models may overcome possible uncertainties in process-based models due to spatial variability in agricultural systems over large regions (Jin et al., 2018).

In the present study, Skye-NDVI and S2-NDVI were equally effective at detecting grassland LAI during the growing season, thus confirming the results of Van Cleemput et al. (2018), who observed similar estimates of grassland biophysical traits for satellite and ground-based spectral measurements. The present study provided relationships between NDVI measured by different sensors and the LAI of generic multi-species grasslands. Using VISTOCK's current structure, estimates of LAI based vegetation indices could be improved by using new empirical relationships using new ground-based data, especially when the botanical conditions differ greatly from those of this study (e.g., single-species grasslands or grasslands dominated by species very different from those of this study), or using a variety of vegetation indices.

Because a vegetation index was used to estimate LAI, model calibration was limited to parameters directly related to crop biomass accumulation (i.e., RUE), crop water loss (i.e., TEC), and effects of thermal and water stresses on RUE. The adjustment of only a few coefficients highlights VISTOCK's good performance when evaluated for a variety of climate conditions; adjusting more coefficients would have likely made the model more accurate at local scale but less applicable to other contexts (Sinclair and Seligman, 2000). Hence, this simplification increases the model's robustness, which makes it applicable to different contexts (Maselli et al., 2013), and at the same time may solve the problem of estimating spatial variability in grass growth and development by using the high spatial and temporal resolution of Sentinel-2 data.

Four parameters (i.e., RUE, TEC, *a*, and *b*) were calibrated for three years (i.e., 2012, 2017, and 2018) for site T based on the most contrasting temperature and precipitation conditions. The model provided satisfactory predictions of NPP, ET, and $FTSW_g$ at a high temporal scale (i.e., 10 days for NPP and ET, daily for $FTSW_g$) for the calibration years. The calibrated model showed reliable predictions when applied to the evaluation years of site T. Model generality is corroborated by predictions of AGB for sites M and B, which had climatic conditions very different from those used for calibration (site T).

Predictions of NPP were in line with those of other studies (Liang et al., 2015; Zhang et al., 2016) that used light-use efficiency with auxiliary remote sensing data to simulate NPP on a yearly basis. VISTOCK's ability to predict NPP during different vegetative stages during the growing season of different study years, which had different thermal and water conditions, indicated the ability of the T_{COR} and WS_{COR} limiting factors to reproduce the influence of thermal and water stresses on NPP production, further supporting the findings that thermal and water regimes are the main drivers of grassland NPP dynamics during a growing season (Zhang et al., 2016).

Indications of VISTOCK's ability to reproduce water dynamics in the grassland system were provided by comparing observed and predicted ET and $FTSW_g$. Although the model slightly underestimate ET dynamics of site T, it generally reproduced them well during the growing season, as reported in other studies of alpine grassland ecosystems (Liu et al., 2015). Differences between observed and predicted ET may have been influenced by i) the quality of input data (Battista et al., 2018), ii) the partitioning between evaporation and transpiration (Wang et al., 2016), and iii) spatial and temporal variability in topography and snow cover in alpine grasslands (Gurtz et al., 1999).

Along with ET, information on soil water content, expressed as $FTSW_g$ indicated the model's ability to reproduce water dynamics in the grassland system at a daily time step under diverse conditions of soil water availability. Specifically, $FTSW_g$ during the growing season was correctly predicted, whether the grassland experienced general water availability (i.e., 2013 and 2014), an extended period of decreased $FTSW_g$ (i.e., 2012, 2016, and 2017), or one (i.e., 2015) or two (i.e., 2018) brief periods of decreased $FTSW_g$.

Due to the reliable simulation of LAI and fAPAR for predicting daily NPP, the calibrated model provided encouraging results for predicting grassland AGB using both proximal (site T) and remote sensing techniques (sites B and M). Specifically, when properly initialized with biomass on DOY 1, the model generally reproduced AGB well for different environments (i.e., mountains, hills, and plains) and types of management (i.e., natural grassland, semi-natural pasture, sown pasture, and meadow-pasture) with only a few parameters to calibrate and inputs to include.

Regarding possible limitations, the presence of clouds, aerosols, or shadows in remote sensing data with high temporal and spatial solution during specific periods can limit the use of VISTOCK; however, methods to reconstruct time series of vegetation indices can be used to fill data gaps, for example by using additional sources of information, such as Synthetic Aperture Radar (Garioud et al., 2021; Moreno-Martínez et al., 2020).

For future calibrations, the only varying parameters are those related to thermal requirements (GT_{MIN} and GT_{OPT}), which need specific consideration because they differ among species in diverse environments. To this end, we evaluated the model for two contrasting environments (sub-alpine (site

T) and hills and plains with a Mediterranean influence (sites M and B)), which provided a range of temperatures for GT_{MIN} and GT_{OPT}.

The influence of nitrogen on plant growth (e.g., possible limitation) is not explicitly considered in VISTOCK, a simplification made considering that LAI estimated from NDVI already include information on N concentration, since NDVI can be related to plants' nitrogen concentration or nitrogen-related characteristics (e.g., crude protein content) (Adjorlolo C., 2014; Vong et al., 2019).

One source of error in model evaluation may have been the simplification of deriving NPP from GPP, which is not actually observed, but derived from the flux tower with the eddy covariance method. A fixed coefficient is usually used in the literature to convert GPP to NPP (Chen et al., 2003; Zhang et al., 2009), but this approach is theoretically less correct than methods based on estimating autotrophic respiration (Maselli et al., 2013). Concerning the model initialization, a spin-up process based on the first biomass sample of the season is required to properly initialize VISTOCK at the beginning of each year.

Notwithstanding the limitations, this modelling approach represents an advance in simulation models that integrate remote sensing data by providing results at a potentially higher spatial resolution than those of previous studies (Liu et al., 2015; Maselli et al., 2013) and adding a more detailed water balance sub-model for simulating water dynamics than those in Liang et al. (2015) and Zhang et al. (2016). Model predictions at high temporal and spatial resolutions, especially for a future pixel-level analysis, may represent a valuable tool for grassland management for farmers (Ding et al., 2020). Specifically, data collected by satellites such as Sentinel-2 offer the potential to upscale predictions to larger areas, which allows stakeholders to monitor grassland growth and, in turn, identify management strategies for optimization at a regional scale (Wang et al., 2019).

Furthermore, the potential future use of VISTOCK at high resolutions combined with technologies/strategies that can increase grazing efficiency, such as rotational grazing (Li et al., 2020), may represent a valuable tool for developing a new integrated system to support grazing management. Grassland AGB and its spatio-temporal variability could be monitored and predicted throughout the grazing season to determine the best extent and location of pasture for grazing in a context of rotational grazing.

Concerning future prospects, application of VISTOCK will be investigated at the pixel level of Sentinel-2, instead of using mean values of NDVI at the field level. Furthermore, Sentinel-2 data may be supplemented with additional information (e.g., Sentinel-1, Landsat) to decrease the number of gaps in the remote sensing data and increase the accuracy of estimated LAI (Wang et al., 2019), thus improving grassland AGB predictions during the growing season. At the same time, to increase the information provided by the model, the potential of satellites to detect chemical and nutritional

properties of vegetation (Fernández-Habas et al., 2021) might be explored and included in the model structure.

5. Conclusions

The main aim of this study was to develop and test a new simplified model (VISTOCK) for simulating grassland growth and development under different bioclimatic zones and management. The model, based on process-based equations that require few input data and integrated with Skye-NDVI and S2-NDVI, yielded robust and reliable predictions that can be used for out- and/or upscaling. Despite its simple structure, VISTOCK was generally able to reproduce processes of the grassland system, considering effects of thermal and water stresses on grass growth. Except for slightly underestimating ET, VISTOCK was able to effectively predict NPP, $FTSW_g$, and AGB of grassland. The model's applicability to different environments and management types, combined with the few inputs required and parameters to be calibrated, makes it an effective tool for farmers to support the optimization of grassland grazing systems. Future perspectives to enhance the model's performances and potential include using additional remote sensing data and adding a specific sub-model to simulate the quality of AGB.

Funding

Project "Virtual Fencing for precision management of beef cattle farms (precision livestock) – VISTOCK": funded by GAL-START Mugello (Tuscany Region), grant no. 853175.

CrediT author statement

Edoardo Bellini: Conceptualization, Methodology, Software, Validation, Formal analysis, Investigation, Writing – Original Draft, Visualization; **Marco Moriondo:** Conceptualization, Methodology, Software, Validation, Formal analysis, Investigation, Writing – Review & Editing; **Camilla Dibari:** Data Curation, Writing – Review & Editing, Project administration, Funding acquisition; **Marco Bindi**: : Writing – Review & Editing, **Nicolina Staglianò**: Writing – Review & Editing, Investigation; **Edoardo Cremonese**: Writing – Review & Editing, Investigation; **Gianluca Filippa:** Writing – Review & Editing, Investigation; **Marta Galvagno**: Writing – Review & Editing, Investigation; **Giovanni Argenti**: Conceptualization ,Writing – Review & Editing, Investigation, Project administration, Funding acquisition, Supervision

Declaration of interests

The authors declare that they have no known competing financial interests or personal relationships that could have appeared to influence the work reported in this paper.

References

Adjorlolo, C., M.O, C.M.A, 2014. Estimation of canopy nitrogen concentration across C3 and C4 grasslands using worldview-2 multispectral data. IEEE J. Sel. Top. Appl. Earth Obs. Remote Sens. 7, 4385–4392. https://doi.org/10.1109/ JSTARS.2014.2320601.

Allen, V.G., Batello, C., Berretta, E.J., Hodgson, J., Kothmann, M., Li, X., McIvor, J., Milne, J., Morris, C., Peeters, A., Sanderson, M., 2011. An international terminology for grazing lands and grazing animals. Grass Forage Sci. 66, 2–28. https://doi.org/ 10.1111/j.1365-2494.2010.00780.x.

Amir, J., Sinclair, T.R., 1991. A model of water limitation on spring wheat growth and yield. F. Crop. Res. 28, 59–69.

Bahrani, M.J., Bahrami, H., Haghighi, A.A.K., 2010. Effect of water stress on ten forage grasses native or introduced to Iran. Grassl. Sci. 56, 1–5. https://doi.org/10.1111/ j.1744-697X.2009.00165.x.

Bar`on, M., Flexas, J., DeLucia, E.H., 2013. Photosynthetic responses to biotic stress. Terrestrial Photosynthesis in a Changing Environment, pp. 331–350.

Battista, P., Chiesi, M., Fibbi, L., Gardin, L., Rapi, B., Romanelli, S., Romani, M., Sabatini, F., Salerni, E., Perini, C., Maselli, F., 2018. Simulation of soil water content in Mediterranean ecosystems by biogeochemical and remote sensing models. Water (Switzerland) 10. https://doi.org/10.3390/w10050665.

Bengtsson, J., Bullock, J.M., Egoh, B., Everson, C., Everson, T., O'Connor, T., O'Farrell, P. J., Smith, H.G., Lindborg, R., 2019. Grasslands—more important for ecosystem services than you might think. Ecosphere 10, 1–20. https://doi.org/10.1002/ ecs2.2582.

Bindi, M., Bellesi, S., Orlandini, S., Fibbi, L., Moriondo, M., Sinclair, T.R., 2005. Influence of water deficit stress on leaf area development and transpiration of Sangiovese grapevines grown in pots. Am. J. Enol. Vitic. 56, 68–72.

Boavista, L. da R., Trindade, J.P.P., Overbeck, G.E., Müller, S.C., 2019. Effects of grazing regimes on the temporal dynamics of grassland communities. Appl. Veg. Sci. 22, 326–335. https://doi.org/10.1111/avsc.12432.

Bojanowski, J.S., 2016. sirad: functions for calculating daily solar radiation and evapotranspiration. R. Package Version 2, 3-3.

Brilli, L., Chiesi, M., Maselli, F., Moriondo, M., Gioli, B., Toscano, P., Zaldei, A., Bindi, M., 2013. Simulation of olive grove gross primary production by the combination of ground and multi-sensor satellite data. Int. J. Appl. Earth Obs. Geoinf. 23, 29–36. https://doi.org/10.1016/j.jag.2012.11.006.

Bristow, K.L., Campbell, G.S., 1984. On the relationship between incoming solar radiation and daily maximum and minimum temperature. Agric. . Meteorol. 31, 159–166. https://doi.org/10.1016/0168-1923(84)90017-0.

Buis, S., Giner, M., Lecharpentier, P., Stics Rpacks, 2018. CroptimizR: A Package for Parameter Estimation, Uncertainty and Sensitivity Analysis for the Stics Model.R package version 0.2.0.9000.

Chen, X., Hutley, L.B., Eamus, D., 2003. Carbon balance of a tropical savanna of northern Australia. Oecologia 137, 405–416. https://doi.org/10.1007/s00442-003-1358-5.

Dibari, C., Argenti, G., Catolfi, F., Moriondo, M., Staglian`o, N., Bindi, M., 2015. Pastoral suitability driven by future climate change along the apennines. Ital. J. Agron. 10, 109–116. https://doi.org/10.4081/ija.2015.659.

Dibari, C., Pulina, A., Argenti, G., Aglietti, C., Bindi, M., Moriondo, M., Mula, L., Pasqui, M., Seddaiu, G., Roggero, P.P., 2021. Climate change impacts on the alpine, continental and mediterranean grassland systems of italy: a review. Ital. J. Agron. 16, 1843.

Dibari, C., Costafreda-Aumedes, S., Argenti, G., Bindi, M., Carotenuto, F., Moriondo, M., Padovan, G., Pardini, A., Staglian`o, N., Vagnoli, C., Brilli, L., 2020. Expected changes to alpine pastures in extent and composition under future climate conditions. Agronomy 10, 1–21. https://doi.org/10.3390/agronomy10070926.

Ding, L., Hu, C., Jiang, C., Zalmen, H., 2020. Improving the grassland management strategies of Qinghai-Tibetan plateau based on Israeli Noy-Meir's grazing-system dynamics model. Kexue Tongbao/Chinese. Sci. Bull. 65, 3867–3872. https://doi. org/10.1360/TB-2020-0238.

Ehrhardt, F., Soussana, J.F., Bellocchi, G., Grace, P., McAuliffe, R., Recous, S., S´andor, R., Smith, P., Snow, V., de Antoni Migliorati, M., Basso, B., Bhatia, A., Brilli, L., Doltra, J., Dorich, C.D., Doro, L., Fitton, N., Giacomini, S.J., Grant, B., Harrison, M. T., Jones, S.K., Kirschbaum, M.U.F., Klumpp, K., Laville, P., L´eonard, J., Liebig, M., Lieffering, M., Martin, R., Massad, R.S., Meier, E., Merbold, L., Moore, A.D., Myrgiotis, V., Newton, P., Pattey, E., Rolinski, S., Sharp, J., Smith, W.N., Wu, L., Zhang, Q., 2018. Assessing uncertainties in crop and pasture ensemble model simulations of productivity and N2O emissions. Glob. Chang. Biol. 24, e603–e616. https://doi.org/10.1111/gcb.13965.

Evangelista, A., Frate, L., Stinca, A., Carranza, M.L., Stanisci, A., 2016. VIOLA - the vegetation database of the central Apennines: structure, current status and usefulness for monitoring Annex i EU habitats (92/43/EEC). Plant Socio 53, 47–58. https://doi.org/10.7338/pls2016532/04. https://doi.org/10.7338/pls2016532/04.

Fan, L., Gao, Y., Brück, H., Bernhofer, C., 2009. Investigating the relationship between NDVI and LAI in semi-arid grassland in Inner Mongolia using in-situ measurements. Theor. Appl. Climatol. 95, 151–156. https://doi.org/10.1007/s00704-007-0369-2.

Fern´andez-Habas, J., Moreno, A.M.G., Hidalgo-Fern´andez, M.T., Leal-Murillo, J.R., Oar, B.A., G´omez-Gir´aldez, P.J., Gonz´alez-Dugo, M.P., Fern´andez-Rebollo, P., 2021. Investigating the potential of Sentinel-2 configuration to predict the quality of Mediterranean permanent grasslands in open woodlands. Sci. Total Environ., 148101 https://doi.org/10.1016/j.scitotenv.2021.148101.

Filippa, G., Cremonese, E., Galvagno, M., Migliavacca, M., Morra di Cella, U., Petey, M., Siniscalco, C., 2015. Five years of phenological monitoring in a mountain grassland: inter-

annual patterns and evaluation of the sampling protocol. Int. J. Biometeorol. 59, 1927–1937. https://doi.org/10.1007/s00484-015-0999-5.

Galvagno, M., Wohlfahrt, G., Cremonese, E., Filippa, G., Migliavacca, M., Mora di Cella, U., van Gorsel, E., 2017. Contribution of advection to nighttime ecosystem respiration at a mountain grassland in complex terrain. Agric. . Meteorol. 237–238, 270–281. https://doi.org/10.1016/j.agrformet.2017.02.018.

Galvagno, M., Wohlfahrt, G., Cremonese, E., Rossini, M., Colombo, R., Filippa, G., Julitta, T., Manca, G., Siniscalco, C., Morra Di Cella, U., Migliavacca, M., 2013. Phenology and carbon dioxide source/sink strength of a subalpine grassland in response to an exceptionally short snow season. Environ. Res. Lett. 8. https://doi. org/10.1088/1748-9326/8/2/025008.

Garioud, A., Valero, S., Giordano, S., Mallet, C., 2021. Recurrent-based regression of Sentinel time series for continuous vegetation monitoring. Remote Sens. Environ. 263. https://doi.org/10.1016/j.rse.2021.112419.

Graux, A., Gaurut, M., Agabriel, J., Baumont, R., Delagarde, R., Delaby, L., Soussana, J., 2011. Agriculture, ecosystems and environment development of the pasture simulation model for assessing livestock production under climate change. "Agric., Ecosyst. Environ. 144, 69–91. https://doi.org/10.1016/j.agee.2011.07.001.

Gurtz, J., Baltensweiler, A., Lang, H., 1999. Spatially distributed hydrotope-based modelling of evapotranspiration and runoff in mountainous basins. Hydrol. Process. 13, 2751–2768. https://doi.org/10.1002/(SICI)1099-1085(19991215)13:17<2751:: AID-HYP897>3.0.CO;2-O.

Hao, R., Yu, D., Liu, Yupeng, Liu, Yang, Qiao, J., Wang, X., Du, J., 2017. Impacts of changes in climate and landscape pattern on ecosystem services. Sci. Total Environ. 579, 718–728. https://doi.org/10.1016/j.scitotenv.2016.11.036.

Heinsch, F.A., Heinsch, F.A., Milesi, C., Jolly, W.M., Bowker, C.F., Kimball, J.S., Nemani, R.R., 2003. User ’ s Guide NASA MODIS Land Algorithm Joseph Glassy 4.

Holechek, J.L., Pieper, R.D., Carlton, H.H., 2011. Range Management: Principles and Practices, 6th edition. Inc,, New Jersey, NJ.

FAO, 2013. FAO Statistical Yearbook 2013. World food and Agriculture Food and Agriculture Organisation for the United Nations, Rome.

Holzworth, D.P., Huth, N.I., deVoil, P.G., Zurcher, E.J., Herrmann, N.I., McLean, G., Chenu, K., van Oosterom, E.J., Snow, V., Murphy, C., Moore, A.D., Brown, H., Whish, J.P.M., Verrall, S., Fainges, J., Bell, L.W., Peake, A.S., Poulton, P.L., Hochman, Z., Thorburn, P.J., Gaydon, D.S., Dalgliesh, N.P., Rodriguez, D., Cox, H., Chapman, S., Doherty, A., Teixeira, E., Sharp, J., Cichota, R., Vogeler, I., Li, F.Y., Wang, E., Hammer, G.L., Robertson, M.J., Dimes, J.P., Whitbread, A.M., Hunt, J., van Rees, H., McClelland, T., Carberry, P.S., Hargreaves, J.N.G., MacLeod, N., McDonald, C., Harsdorf, J., Wedgwood, S., Keating, B.A., 2014. APSIM - Evolution towards a new generation of agricultural systems simulation. Environ. Model. Softw 62, 327–350. https://doi.org/10.1016/j.envsoft.2014.07.009.

Insua, J.R., Utsumi, S.A., Basso, B., 2019. Assessing and modelling pasture growth under different nitrogen fertilizer and defoliation rates in argentina and the united states. Agron. J. 111, 702–713. https://doi.org/10.2134/agronj2018.07.0438.

Jin, X., Kumar, L., Li, Z., Feng, H., Xu, X., Yang, G., Wang, J., 2018. A review of data assimilation

of remote sensing and crop models. Eur. J. Agron. 92, 141–152. https:// doi.org/10.1016/j.eja.2017.11.002.

Jolly, W.M., Nemani, R., Running, S.W., 2005. A generalized, bioclimatic index to predict foliar phenology in response to climate. Glob. Chang. Biol. 11, 619–632. https://doi.org/10.1111/j.1365-2486.2005.00930.x.

Kirchner, J.W., Hooper, R.P., Kendall, C., Neal, C., Leavesley, G., 1996. Testing and validating environmental models. Sci. Total Environ. 183, 33–47. https://doi.org/ 10.1016/0048-9697(95)04971-1.

Knops, J.M.H., Reinhart, K., 2000. Specific leaf area along a nitrogen fertilization gradient. Am. Midl. Nat. 144, 265–272. https://doi.org/10.1674/0003-0031(2000) 144[0265:SLAAAN]2.0.CO;2.

Lemaire, G., Hodgson, S., Chabbi, A., 2011. Grassland Productivity and Ecosystems Services.

Leolini, L., Bregaglio, S., Moriondo, M., Ramos, M.C., Bindi, M., Ginaldi, F., 2018. A model library to simulate grapevine growth and development: software implementation, sensitivity analysis and field level application. Eur. J. Agron. 99, 92–105. https://doi.org/10.1016/j.eja.2018.06.006.

Li, Y., Dong, S., Gao, Q., Zhang, Y., Liu, S., Ganjurjav, H., Hu, G., Wang, X., Yan, Y., Wu, H., Gao, X., Li, S., Zhang, J., 2020. Rotational grazing promotes grassland aboveground plant biomass and its temporal stability under changing weather conditions on the Qinghai-Tibetan plateau. L. Degrad. Dev. 31, 2662–2671. https:// doi.org/10.1002/ldr.3596.

R Core Team, 2021. R: A language and environment for statistical computing. R Foundation for Statistical Computing, Vienna, Austria.

Liang, W., Yang, Y., Fan, D., Guan, H., Zhang, T., Long, D., Zhou, Y., Bai, D., 2015. Analysis of spatial and temporal patterns of net primary production and their climate controls in China from 1982 to 2010. Agric. Meteorol. 204, 22–36. https://doi.org/ 10.1016/j.agrformet.2015.01.015.

Liu, J., Pattey, E., J´ego, G., 2012. Assessment of vegetation indices for regional crop green LAI estimation from Landsat images over multiple growing seasons. Remote Sens. Sens. Environ. 123, 347–358. https://doi.org/10.1016/j.rse.2012.04.002.

Liu, Y., Xiao, J., Ju, W., Zhu, G., Wu, X., Fan, W., Li, D., Zhou, Y., 2018. Satellite-derived LAI products exhibit large discrepancies and can lead to substantial uncertainty in simulated carbon and water fluxes. Remote Sens. Environ. 206, 174–188. https:// doi.org/10.1016/j.rse.2017.12.024.

Liu, Z., Shao, Q., Liu, J., 2015. The performances of MODIS-GPP and -ET products in China and their sensitivity to input data (FPAR/LAI. Remote Sens. 7, 135–152. https://doi.org/10.3390/rs70100135.

Ma, L., Derner, J.D., Harmel, R.D., Tatarko, J., Moore, A.D., Rotz, C.A., Augustine, D.J., Boone, R.B., Coughenour, M.B., Beukes, P.C., van Wijk, M.T., Bellocchi, G., Cullen, B. R., Wilmer, H., 2019. Application of grazing land models in ecosystem management: current status and next frontiers. Adv. Agron. 158, 173–215. https://doi.org/ 10.1016/bs.agron.2019.07.003.

Maselli, F., Chiesi, M., Brilli, L., Moriondo, M., 2012. Simulation of olive fruit yield in Tuscany

through the integration of remote sensing and ground data. Ecol. Modell. 244, 1–12. https://doi.org/10.1016/j.ecolmodel.2012.06.028.

Maselli, F., Argenti, G., Chiesi, M., Angeli, L., Papale, D., 2013. Simulation of grassland productivity by the combination of ground and satellite data. Agric. Ecosyst. Environ. 165, 163–172. https://doi.org/10.1016/j.agee.2012.11.006.

Migliavacca, M., Galvagno, M., Cremonese, E., Rossini, M., Meroni, M., Sonnentag, O., Cogliati, S., Manca, G., Diotri, F., Busetto, L., Cescatti, A., Colombo, R., Fava, F., Morra di Cella, U., Pari, E., Siniscalco, C., Richardson, A.D., 2011. Using digital repeat photography and eddy covariance data to model grassland phenology and photosynthetic CO2 uptake. Agric. Meteorol. 151, 1325–1337. https://doi.org/ 10.1016/j.agrformet.2011.05.012.

Monteith, J.L., 1977. Climate and the efficiency of crop production in Britain. Philos. Trans. R. Soc. Biol. Sci. 281, 271–294.

Monteith, 1972. Solar Radiation and Productivity in Tropical Ecosystems Author (s): J. L. Monteith Source: Journal of Applied Ecology, Vol. 9, No. 3 (Dec., 1972), pp. 747–766 Published by: British Ecological Society Stable URL: 〈http://www.jstor. org/stable/〉. Society 9, 747–766. Moreno-Martínez, ´A., Izquierdo-Verdiguier, E., Maneta, M.P., Camps-Valls, G., Robinson, N., Mu˜noz-Marí, J., Sedano, F., Clinton, N., Running, S.W., 2020. Multispectral high resolution sensor fusion for smoothing and gap-filling in the cloud. Remote Sens. Environ. 247, 111901 https://doi.org/10.1016/j. rse.2020.111901.

Moriondo, M., Leolini, L., Brilli, L., Dibari, C., Tognetti, R., Giovannelli, A., Rapi, B., Battista, P., Caruso, G., Gucci, R., Argenti, G., Raschi, A., Centritto, M., Cantini, C., Bindi, M., 2019. A simple model simulating development and growth of an olive grove. Eur. J. Agron. 105, 129–145. https://doi.org/10.1016/j.eja.2019.02.002.

Movedi, E., Bellocchi, G., Argenti, G., Paleari, L., Vesely, F., Staglian`o, N., Dibari, C., Confalonieri, R., 2019. Development of generic crop models for simulation of multi- species plant communities in mown grasslands. Ecol. Modell. 401, 111–128. https:// doi.org/10.1016/j.ecolmodel.2019.03.001.

Oddi, L., Cremonese, E., Ascari, L., Filippa, G., Galvagno, M., Serafino, D., Di Cella, U.M., 2021. Using UAV imagery to detect and map woody species encroachment in a subalpine grassland: advantages and limits. Remote Sens. 13. https://doi.org/ 10.3390/rs13071239.

Palmer, A.R., Finca, A., Mantel, S.K., Gwate, O., Munch, Z., Gibson, L., 2017. Determining fPAR and leaf area index of several land cover classes in the Pot River and Tsitsa River catchments of the Eastern Cape. Afr. J. Range Forage Sci. 34, 33–37.

Parton, W.J., Ojima, D.S., Cole, C.V., Schimel, D.S., 1994. A general model for soil organic matter dynamics: sensitivity to litter chemistry, texture and management. Quant. Model. Soil Form. Process. Proc. Symp. Minneap. 1992, 147–167. https:// doi.org/10.2136/sssaspecpub39.c9.

Petriccione, B., Bricca, A., 2019. Thirty years of ecological research at the Gran Sasso d'Italia LTER site: Climate change in action. Nat. Conserv 34, 9–39. https://doi.org/ 10.3897/natureconservation.34.30218.

Pintaldi, E., D'Amico, M.E., Siniscalco, C., Cremonese, E., Celi, L., Filippa, G., Prati, M., Freppaz, M., 2016. Hummocks affect soil properties and soil-vegetation relationships in a subalpine grassland (North-Western Italian Alps). Catena 145, 214–226. https:// doi.org/10.1016/j.catena.2016.06.014.

Ponzetta, M.P., Cervasio, F., Crocetti, C., Messeri, A., Argenti, G., 2010. Habitat improvements with wildlife purposes in a grazed area on the Apennine Mountains. Ital. J. Agron. 5, 233–238. https://doi.org/10.4081/ija.2010.233.

Prieto-Blanco, A., North, P.R.J., Barnsley, M.J., Fox, N., 2009. Satellite-driven modelling of Net Primary Productivity (NPP): theoretical analysis. Remote Sens. Environ. 113, 137–147. https://doi.org/10.1016/j.rse.2008.09.002.

Riedo, M., Grub, A., Rosset, M., 1998. A pasture simulation model for dry matter production, and fluxes of carbon, nitrogen, water and energy 105, 141–183.

Rossini, M., Cogliati, S., Meroni, M., Migliavacca, M., Galvagno, M., Busetto, L., Cremonese, E., Julitta, T., Siniscalco, C., Morra Di Cella, U., Colombo, R., 2012. Remote sensing-based estimation of gross primary production in a subalpine grassland. Biogeosciences 9, 2565–2584. https://doi.org/10.5194/bg-9-2565-2012.

Rossini, M., Migliavacca, M., Galvagno, M., Meroni, M., Cogliati, S., Cremonese, E., Fava, F., Gitelson, A., Julitta, T., di Cella, U.M., Siniscalco, C., Colombo, R., 2014. Remote estimation of grassland gross primary production during extreme meteorological seasons. Int. J. Appl. Earth Obs. Geoinf. 29, 1–10. https://doi.org/ 10.1016/j.jag.2013.12.008.

Saxton, K.E., Rawls, W.J., Romberger, J.S., Papendick, R.I., 1986. Estimating generalized soil-water characteristics from texture. Soil Sci. Soc. Am. J. 50, 1031–1036.

Scocco, P., Piermarteri, K., Malfatti, A., Tardella, F.M., Catorci, A., 2016. Increase of drought stress negatively affects the sustainability of extensive sheep farming in sub- Mediterranean climate. J. Arid Environ. 128, 50–58. https://doi.org/10.1016/j. jaridenv.2016.01.006.

Simionesei, L., Ramos, T.B., Oliveira, A.R., Jongen, M., Darouich, H., Weber, K., Proença, Proença, V., Domingos, T., Neves, R., 2018. Modelling soilwater dynamics and pasture growth in the montado ecosystem using MOHID land. Water (Switzerland) 10, 1–19. https://doi.org/10.3390/w10040489.

Sinclair, T.R., 1986. Water and nitrogen limitations in soybean grain production I. Model development. F. Crop. Res. 15, 125–141.

Sinclair, T.R., 2006. A reminder of the limitations in using Beer's Law to estimate daily radiation interception by vegetation. Crop Sci. 46, 2343–2347. https://doi.org/ 10.2135/cropsci2006.01.0044.

Sinclair, T.R., Seligman, N., 2000. Criteria for publishing papers on crop modelling. F. Crop. Res. 68, 165–172. https://doi.org/10.1016/S0378-4290(00)00105-2.

Sinclair, T.R., Hammond, L.C., Harrison, J., 1998. Extractable soil water and transpiration rate of soybean on sandy soils. Agron. J. 90, 363–368. https://doi.org/ 10.2134/agronj1998.00021962009000030008x.

Snow, V.O., Rotz, C.A., Moore, A.D., Martin-Clouaire, R., Johnson, I.R., Hutchings, N.J., Eckard, R.J., 2014. The challenges - and some solutions - to process-based modelling of grazed agricultural systems. Environ. Model. Softw 62, 420–436. https://doi.org/ 10.1016/j.envsoft.2014.03.009.

Soltani, A., Sinclair, T.R., 2012a. Modelling physiology of crop development, growth and yield. Wallingford, Oxfordshire, UK.

Soltani, A., Sinclair, T.R., 2012b. Modelling Physiology of crop. St¨ockle, C.O., Donatelli, M., Nelson, R., 2003. CropSyst, a cropping systems simulation model. Eur. J. Agron. 18, 289–307. https://doi.org/10.1016/S1161-0301(02)00109- 0.

Swain, C.K., Bhattacharyya, P., Singh, N.R., Neogi, S., Sahoo, R.K., Nayak, A.K., Zhang, G., Leclerc, M.Y., 2016. Net ecosystem methane and carbon dioxide exchange in relation to heat and carbon balance in lowland tropical rice. Ecol. Eng. 95, 364–374. https://doi.org/10.1016/j.ecoleng.2016.06.053.

Tanner, C.B., Sinclair, T.R., 1983. Efficient water use in crop production: research or re- search? In: Taylor, H.M., Jordan, W.R., Sinclair, T.R. (Eds.), Limitations to Efficient Water Use in Crop Production. American Society of Agronomy, Crop Science Society of America, and Soil Science Society of America, Madison, Wisconsin, pp. 1–27.

Touhami, H.Ben, Lardy, R., Barra, V., Bellocchi, G., 2013. Screening parameters in the Pasture Simulation model using the Morris method. Ecol. Modell. 266, 42–57. https://doi.org/10.1016/j.ecolmodel.2013.07.005.

Tucker, C.J., 1979. Red and photographic infrared linear combinations for monitoring vegetation. Remote Sens. Environ. 8, 127–150.

Van Cleemput, E., Vanierschot, L., Fern´andez-Castilla, B., Honnay, O., Somers, B., 2018. The functional characterization of grass- and shrubland ecosystems using hyperspectral remote sensing: trends, accuracy and moderating variables. Remote Sens. Environ. 209, 747–763. https://doi.org/10.1016/j.rse.2018.02.030.

Verrelst, J., van der Tol, C., Magnani, F., Sabater, N., Rivera, J.P., Mohammed, G., Moreno, J., 2016. Evaluating the predictive power of sun-induced chlorophyll fluorescence to estimate net photosynthesis of vegetation canopies: a SCOPE modelling study. Remote Sens. Environ. 176, 139–151. https://doi.org/10.1016/j. rse.2016.01.018.

Vong, C.N., Zhou, J., Tooley, J.A., Naumann, H.D., Lory, J.A., 2019. Estimating forage dry matter and nutritive value using UAV- And ground-based sensors - a preliminary study. 2019 ASABE Annu. Int. Meet. 2–15. https://doi.org/10.13031/ aim.201900556.

Wakulin´ska, M., Marcinkowska-Ochtyra, A., 2020. Multi-temporal sentinel-2 data in classification of mountain vegetation. Remote Sens. 12. https://doi.org/10.3390/ RS12172696.

Wallach, D., Buis, S., Lecharpentier, P., Bourges, J., Clastre, P., Launay, M., Bergez, J.E., Guerif, M., Soudais, J., Justes, E., 2011. A package of parameter estimation methods and implementation for the STICS crop-soil model. Environ. Model. Softw. 26, 386–394. https://doi.org/10.1016/j.envsoft.2010.09.004.

Wang, G., Liu, S., Liu, T., Fu, Z., Yu, J., 2019. Modelling above-ground biomass based on vegetation indexes: a modified approach for biomass estimation in semi-arid grasslands. Int. J. Remote Sens. 40, 3835–3854. https://doi.org/10.1080/ 01431161.2018.1553319.

Wang, J., Xiao, X., Bajgain, R., Starks, P., Steiner, J., Doughty, R.B., Chang, Q., 2019. Estimating leaf area index and aboveground biomass of grazing pastures using Sentinel-1, Sentinel-2 and Landsat images. ISPRS J. Photogramm. Remote Sens. 154, 189–201. https://doi.org/10.1016/j.isprsjprs.2019.06.007.

Wang, W., Smith, J.A., Ramamurthy, P., Baeck, M.L., Bou-Zeid, E., Scanlon, T.M., 2016. On the correlation of water vapor and CO2: Application to fluxpartitioning of evapotranspiration.

Water Resour. Res. 52, 9452–9469.

Westoby, M., Baruch, Z., Bongers, F., Cavender-Bares, J., Chapin, T., Diemer, M., others, Wright, I.J., Reich, P.B., Ackerly, D.D., Cornelissen, J.H., 2004. The worldwide leaf economics spectrum. Nature 428, 821–827.

White, M.A., Thornton, P.E., Running, S.W., Nemani, R.R., 2000. Parameterization and sensitivity analysis of the BIOME–BGC terrestrial ecosystem model: net primary production controls. Earth Inter. 4, 1–85. https://doi.org/10.1175/1087-3562 (2000)004<0003:pasaot>2.0.co;2.

Wylie, B.K., Meyer, D.J., Tieszen, L.L., Mannel, S., 2002. Satellite mapping of surface biophysical parameters at the biome scale over the North American grasslands. a case Study Remote Sens. Environ. 79, 266–278. https://doi.org/10.1016/S0034- 4257(01)00278-4.

Xie, Q., Huang, W., Dash, J., Song, X., Huang, L., Zhao, J., Wang, R., 2015. Evaluating the potential of vegetation indices for winter wheat LAI estimation under different fertilization and water conditions. Adv. Sp. Res. 56, 2365–2373. https://doi.org/ 10.1016/j.asr.2015.09.022.

Xu, X., Sherry, R.A., Niu, S., Li, D., Luo, Y., 2013. Net primary productivity and rain-use efficiency as affected by warming, altered precipitation, and clipping in a mixed- grass prairie. Glob. Chang. Biol. 19, 2753–2764. https://doi.org/10.1111/ gcb.12248.

Yu, R., Evans, A.J., Malleson, N., 2018. Quantifying grazing patterns using a new growth function based on MODIS Leaf Area Index. Remote Sens. Environ. 209, 181–194. https://doi.org/10.1016/j.rse.2018.02.034.

Zhang, L., Hu, Z., Fan, J., Zhou, D., Tang, F., 2014. A meta-analysis of the canopy light extinction coefficient in terrestrial ecosystems. Front. Earth Sci. 8, 599–609. https:// doi.org/10.1007/s11707-014-0446-7.

Zhang, M., Lal, R., Zhao, Y., Jiang, W., Chen, Q., 2016. Estimating net primary production of natural grassland and its spatio-temporal distribution in China. Sci. Total Environ. 553, 184–195. https://doi.org/10.1016/j.scitotenv.2016.02.106.

Zhang, Y., Xu, M., Chen, H., Adams, J., 2009. Global pattern of NPP to GPP ratio derived from MODIS data: Effects of ecosystem type, geographical location and climate. Glob. Ecol. Biogeogr. 18, 280–290. https://doi.org/10.1111/j.1466- 8238.2008.00442.x.

Chapter 4.

Impacts of Climate Change on European Grassland Phenology: A 20-Year Analysis of MODIS Satellite Data

Chapter 4 has been based on the study:
Bellini, E., Moriondo M., Dibari C., Leolini L., Staglianò N., Stendardi L., Filippa G., Galvagno M. and Argenti G. 2023. Impacts of Climate Change on European Grassland Phenology: A 20-Year Analysis of MODIS Satellite Data. (*Published*) *Remote Sensing*, 15, 218. https://doi.org/ 10.3390/rs15010218.

PhD candidate's contribution:

Edoardo Bellini produced the results and wrote the sections of the chapter under the supervision of the other co-authors.

4. Impacts of Climate Change on European Grassland Phenology: A 20-Year Analysis of MODIS Satellite Data

Edoardo Bellini [1], Marco Moriondo [2,*], Camilla Dibari [1], Luisa Leolini [1], Nicolina Staglianò [1], Laura Stendardi [1], Gianluca Filippa [3], Marta Galvagno [3] and Giovanni Argenti [1]

[1] Department of Agriculture, Food, Environment and Forestry (DAGRI), University of Florence, 50144 Florence, Italy. edoardo.bellini@unifi.it (E.B.); camilla.dibari@unifi.it (C.D.); luisa.leolini@unifi.it (L.L.); nicolina.stagliano@unifi.it (N.S.); laura.stendardi@unifi.it (L.S.); giovanni.argenti@unifi.it (G.A.)
[2] Institute of BioEconomy, Italian National Research Council (IBE-CNR), 50019 Sesto Fiorentino, Italy.
[3] Environmental Protection Agency of Aosta Valley-Climate Change Unit, Saint-Christophe, 11100 Aosta, Italy. g.filippa@arpa.vda.it (G.F.); m.galvagno@arpa.vda.it (M.G.)
[*] Correspondence: marco.moriondo@cnr.it; Tel.: +39-0552755747

Abstract: The use of very long spatial datasets from satellites has opened up numerous opportunities, including the monitoring of vegetation phenology over the course of time. Considering the importance of grassland systems and the influence of climate change on their phenology, the specific objectives of this study are: (a) to identify a methodology for a reliable estimation of grassland phenological dates from a satellite vegetation index (i.e., kernel normalized difference vegetation index, kNDVI) and (b) to quantify the changes that have occurred over the period 2001–2021 in a representative dataset of European grasslands and assess the extent of climate change impacts. In order to identify the best methodological approach for estimating the start (SOS), peak (POS) and end (EOS) of the growing season from the satellite, we compared dates extracted from the MODIS-kNDVI annual trajectories with different combinations of fitting models (FMs) and extraction methods (EM), with those extracted from the gross primary productivity (GPP) measured from eddy covariance flux towers in specific grasslands. SOS and POS were effectively identified with various FM×EM approaches, whereas satellite-EOS did not obtain sufficiently reliable estimates and was excluded from the trend analysis. The methodological indications (i.e., FM×EM selection) were then used to calculate the SOS and POS for 31 grassland sites in Europe from MODIS-kNDVI during the period 2001–2021. SOS tended towards an anticipation at the majority of sites (83.9%), with an average advance at significant sites of 0.76 days year^{-1}. For POS, the trend was also towards advancement, although the results are less homogeneous (67.7% of sites with advancement), and with a less marked advance at significant sites (0.56 days year^{-1}). From the analyses carried out, the SOS and POS of several sites were influenced by the winter and spring temperatures, which recorded rises during the period 2001–2021. Contrasting results were recorded for the SOS-POS duration, which did not show a clear trend towards lengthening or shortening. Considering latitude and altitude, the

results highlighted that the greatest changes in terms of SOS and POS anticipation were recorded for sites at higher latitudes and lower altitudes.
Keywords: start of season (SOS); peak of season (POS); end of season (EOS); vegetation index; GPP; kNDVI

1. Introduction

Phenology is defined as the "study of the timing of recurring biological events, the causes of their timing with regard to biotic and abiotic forces, and the interrelation among phases of the same or different species" (Lieth, 1974). Vegetation phenology specifically addresses processes linked to the plant cycle, such as leaf emergence, flowering, leaf colouration and fall (Richardson et al., 2013). These are controlled by molecular mechanisms inside the organism and driven by factors such as temperature and photoperiod (Singh et al., 2017).

The study of plant phenology through on-field observations, although a reliable approach (Templ et al., 2018), is time-consuming and costly when applied at large spatial scales or over long time series. Moreover, observed phenological data are site specific, often sparsely distributed and measured for a few plant species only and at discrete phenophases (Cui et al., 2019).

To overcome these issues, the collection of data and information on phenology through remote sensing devices and methodologies has become of great importance over the years as a result of scientific advances in this field of study. Within remote sensing, different types of technologies can be considered for phenological analysis, such as satellites equipped with specific sensors (Dixon et al., 2021; Liu et al., 2017; Peng et al., 2021) or Phenocam digital cameras (Julitta et al., 2014; Migliavacca et al., 2011; Watson et al., 2019; Zhang et al., 2018). Taking into account satellite images and the different vegetation indices derived from them (Sonobe et al., 2018), the use of these data has been widely experimented in the literature in different environments, such as evergreen forests, deciduous forests, croplands and grasslands (Gonsamo et al., 2012; Tian et al., 2021), to assess the vegetation cycles through the extraction of phenological dates of the start, peak or end of the growing season. Approaches to retrieving these relevant phenological dates from vegetation indices have been previously investigated with regard to the smoothing and filtering functions of raw satellite data (Lara and Gandini, 2016) and date extraction techniques (Tian et al., 2021). Furthermore, there has been the development of specific software, such as Phenopix (Filippa et al., 2016), that simplified and automated data processing techniques for phenological studies.

In addition to data collected from on-field and remote sensing observations, another important source of information for studying phenology is the gross primary productivity (GPP), i.e., the total amount of CO_2 fixed by plants through vegetation photosynthesis (Gitelson et al., 2006; Running et al., 2004;

Wang et al., 2018), elaborated from eddy covariance measurements at flux tower sites. Since phenology is one of the most important controls of the interannual variability of GPP (Fu et al., 2014; Q. Zhang et al., 2014), these measurements have been used in a number of studies as a proxy for vegetation phenology (Peng et al., 2017; Tian et al., 2021). Unlike phenological on-field observations that are based on the human eye, GPP is focused on photosynthetic phenology, which is a result of both plant canopy development and light use efficiency (Medlyn, 1998). By measuring the photosynthetic carbon uptake of the vegetation canopy, dates of start and end of season elaborated from GPP measurements provide indications of when ecosystems switch from a source to a sink of C, and vice versa (Galvagno et al., 2013). Given the importance of these data, GPP measurements are also used to evaluate the efficiency of remote sensing data in estimating ecosystem phenological dates (Jin et al., 2017; Jin and Eklundh, 2014).

In the last decades, the study of phenological events in plant communities has become increasingly important to assess the impacts of climate warming on vegetation cycles, with consequences on agricultural, forest and grassland systems (IPCC, 2014; Sparks and Menzel, 2013). With a specific focus on the latter, monitoring grassland ecosystems, which cover ca. 70% of the total world agricultural area (FAO, 2013), has gained interest due to the large amount of ecosystem services they provide, e.g., erosion protection, water regulation, carbon storage, biodiversity, food for animal production systems and wildlife, aesthetic and recreational functions (Bengtsson et al., 2019; Hao et al., 2017; Ni, 2002; Ponzetta et al., 2010). Given the huge spatial extent of these environments and the large number of functions they perform, understanding trends and potential climate-induced shifts in grassland phenology is impelling (Dibari et al., 2020). Studies of different environments in Europe have already shown changes in phenological phases over the period 1951–2018 in a limited number of countries for which long series of observed data were available (Menzel et al., 2020).

In this regard, long time series of vegetation indices, such as those elaborated from MODIS satellite images, allow the study of phenology over a relatively long period of time, providing information at 250 m spatial resolution and 16-day temporal resolution. This involves assessing changes in phenological dates over the past decades and quantifying the extent of the impacts of climate change on the plant life cycle that are already visible in grassland systems (Gong et al., 2015). Analyses of satellite-derived phenology over the period 1982–2001 also showed a general advance driven by climate change (Stöckli and Vidale, 2004). However, a comprehensive phenological analysis specific to European grasslands in recent decades is still lacking, as is the evaluation of the impact of rising temperatures on these changes.

Building on these premises, the objectives of this research were, therefore, twofold:

(*i*) Identification of a reliable approach to determine the start (SOS), peak (POS) and end of the growing season (EOS) through the use of specific vegetation indices (i.e., kernel normalized difference vegetation index, kNDVI) processed from MODIS satellite imagery, relying on observed GPP data from grassland sites as comparison;

(*ii*) Analysis of phenological trends of different European grasslands in the period 2001–2021 using the methodology identified in point (*i*) in order to highlight possible changes in the dates of SOS, POS and EOS and the relevant climatic drivers.

2. Materials and Methods

2.1. Preliminary Analysis and Optimisation of the Extraction Method

In order to analyse the trend of phenological dates of a representative dataset of European grasslands over the last 20 years, it was necessary to identify the best strategy for extracting key grassland phenological phases (i.e., SOS, POS and EOS) from satellite images (Figure 1). The effectiveness of the use of satellite-derived vegetation indices (i.e., kNDVI) in the assessment of grassland phenological stages was evaluated using as a benchmark observed seasonal trend of grasslands' gross primary production (GPP) as fitted by different models (FM) and extraction methods (EM). The complete procedure is given below.

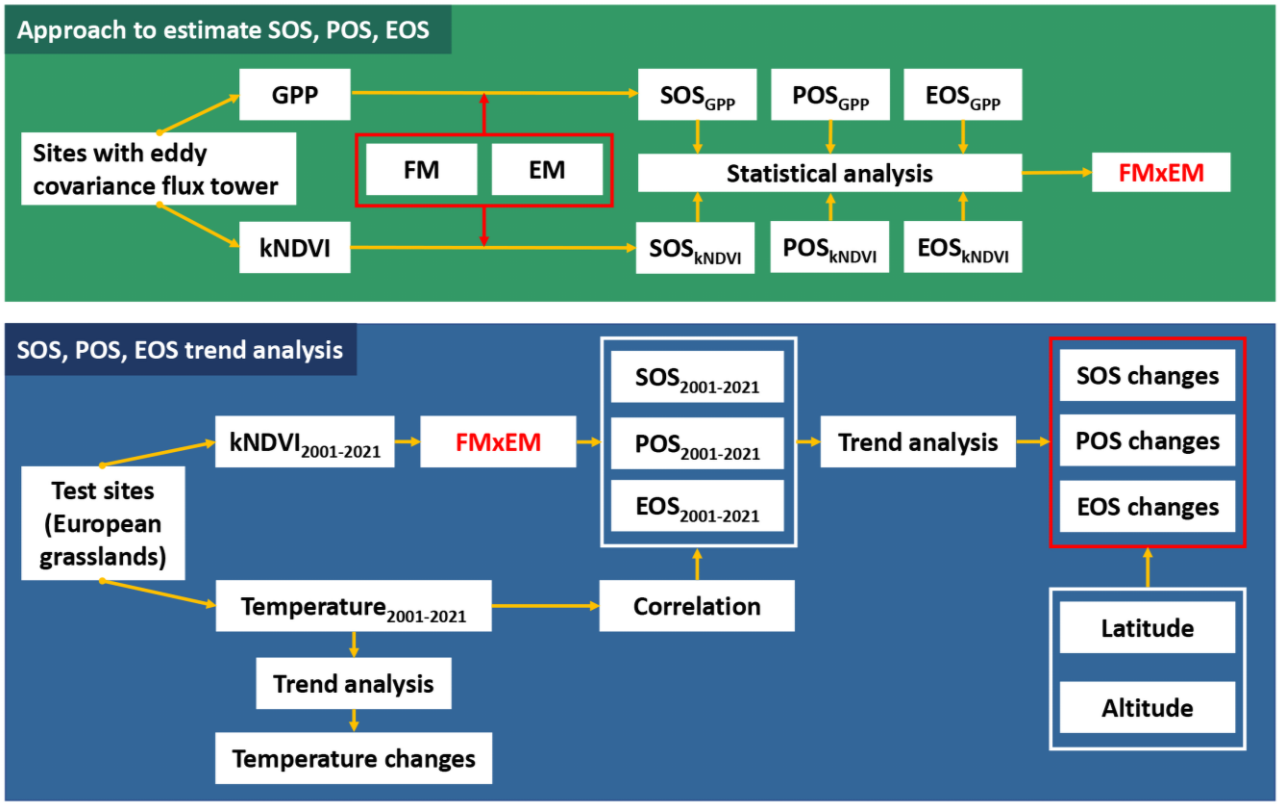

Figure 1. Workflow of the methodology, divided into "Approach to estimate SOS, POS, EOS" (2.1) and "SOS, POS, EOS trend analysis" (2.2).

2.1.1. GPP Data and Study Areas

Daily GPP data (g C m^{-2} d^{-1}), used as observed values of grassland growing seasons, were collected at study sites of the FLUXNET (https://fluxnet.org/, accessed 5 July 2022, Pastorello et al., 2020) and European Fluxes Database Cluster (http://www.europe-fluxdata.eu/, accessed on 7 July 2022) networks. At these sites, CO_2 flux of grasslands is regularly measured from in situ towers by means of the eddy covariance method, and then further partitioned into ecosystem respiration and GPP (Liang and Wang, 2020). From these two networks, 9 study areas in Europe with different altitudinal and botanical conditions were selected in order to obtain a representative European dataset. The list of study areas with the relative information is reported in Table 1. From the GPP patterns elaborated from this dataset, SOS, POS and EOS were extracted with the different approaches that are explained in Section 2.1.3.

Table 1. List of grassland sites used to obtain daily GPP data. Mamsl represents meters above mean sea level (m), while EFDC represents the European Fluxes Database Cluster.

ID	Site	Country	Network	Lat	Lon	Mamsl	Years
AT-Neu	Neustift (Wohlfahrt et al., 2008)	Austria	FLUXNET	47.1167	11.3175	970	2002–2012
CH-Cha	Chamau (Merbold et al., 2014)	Switzerland	FLUXNET	47.2102	8.4104	393	2002–2008
CH-Fru	Früebüel (Imer et al., 2013)	Switzerland	FLUXNET	47.1158	8.5378	982	2005–2014
CZ-BK2	Bily Kriz	Czech Republic	FLUXNET	49.4944	18.5429	855	2006–2012
DE-Gri	Grillenburg (Prescher et al., 2010)	Germany	FLUXNET	50.9500	13.5126	385	2004–2018
DE-Rur	Rollesbroich (Post et al., 2015)	Germany	FLUXNET	50.6219	6.3041	514	2011–2018
IT-Mal	Malga Arpaco	Italy	EFDC	46.1140	11.70334	1662	2003–2004
IT-Mbo	Monte Bondone (Marcolla et al., 2011)	Italy	FLUXNET	46.0147	11.0458	1550	2004–2013
IT-Tor	Torgnon (Galvagno et al., 2013)	Italy	FLUXNET	45.8444	7.5781	2160	2009–2018

2.1.2. Satellite Data

For the purpose of the study, we selected the Moderate Resolution Imaging Spectroradiometer (MODIS) imagery to retrieve the vegetation index from which to extract SOS, POS and EOS, corresponding to what was assessed for GPP data. Despite its lower spatial resolution compared to

other more recent satellites (e.g., Sentinel-2), MODIS provides a long-time series of data allowing the analysis of phenological trends in European grasslands over the last decades.

The vegetation index used to reproduce the growing season of grasslands was the kernel NDVI (kNDVI), a specific vegetation index used to reconstruct GPP patterns in different environments, including grasslands (Camps-Valls et al., 2021). The kNDVI is calculated as follows:

$$\text{kNDVI} = \frac{1-k(n,r)}{1+k(n,r)} \quad (1)$$

where *n* and *r* refer to the reflectance in the near-infrared (NIR) and red bands (RED), respectively, BAND 2 and BAND 1 in MODIS at 250 m spatial resolution and 8 days of temporal resolution (product: MODIS/006/MOD09Q1), while the kernel function *k* measures the similarity between these two bands. We used the RBF kernel proposed by the same authors (Camps-Valls et al., 2021):

$$k(a,b) = exp\ \frac{(-(a-b)^2)}{((2\sigma)^2)} \quad (2)$$

where the σ parameter controls the notion of the distance between the NIR and RED bands, elaborated as the mean distance between these two bands:

$$\sigma = 0.5(n+r) \quad (3)$$

For each site, kNDVI values were then processed from the MODIS RED and NIR bands according to the previous formulas, using the specific coordinates of the grassland sites with eddy covariance stations.

2.1.3. Fitting Models and Extraction Methods

In order to perform an accurate satellite analysis of phenological date trends over the period 2001–2021, different fitting models (FMs) and date extraction methods (EMs) were applied both to raw data of GPP and kNDVI to find the most performing FM×EM approach. The methodology was then chosen taking into account the results of the comparison between SOS, POS and EOS extracted from GPP and kNDVI annual patterns.

Consequently, raw data of GPP and kNDVI underwent a process for retrieving the phenological dates of SOS, POS and EOS. Specifically, using a work package for phenological analysis within the R work environment *(phenopix*, Filippa et al., 2016), the annual patterns of GPP and kNDVI were subjected to the fitting operation and, subsequently, to SOS, POS and EOS extraction.

The FM used in this comparison were 4: Elmore et al. (2012) (ELM), Gu et al., (2009) (GU), Beck et al. (2006) (BEC) and Klosterman et al. (2014) (KLS). These methods fitted different double logistic

curves to the raw data of GPP and kNDVI according to the aforementioned studies. Equations of ELM, GU, BEC and KLS (Filippa et al., 2016) are shown below:

$$f(t) = mn + (mx - mn) \cdot \left(\frac{1}{1+e^{(m_3'-t)/m_4'}} - \frac{1}{1+e^{(m_5'-t)/m_6'}}\right) \quad (4)$$

$$f(t) = y_0 + \frac{a_1}{[1+e^{-(t-t_{01})/b_1}]c_1} - \frac{a_2}{[1+e^{-(t-t_{02})/b_2}]c_2} \quad (5)$$

$$f(t) = mn + (mx - mn) \cdot \left(\frac{1}{1+e^{(-rsp\cdot(t-sos))}} + \frac{1}{1+e^{(-rau\cdot(t-eos))}}\right) \quad (6)$$

$$f(t) = mn + (mx - mn) \cdot \left(\frac{1}{1+e^{(-rsp\cdot(t-sos))}} + \frac{1}{1+e^{(-rau\cdot(t-eos))}}\right) \quad (7)$$

The selected FMs optimise a different number of parameters and hence present diverse flexibility in fitting raw data. For a more comprehensive understanding of the methods and curve parameters, see the corresponding publications.

The GPP and kNDVI curves obtained after FM application were then used to extract SOS, POS and EOS with four extraction methods (Filippa et al., 2016): three working on inflection points of the derivatives (*Klosterman*, *Gu*, *Derivatives*), and one that identifies the dates when a fixed threshold of the seasonal amplitude is reached (*Thresholds*). Specifically, *Klosterman* is based on local extremes in the rate of change of curvature k (Kline, 1998), *Derivatives* on local extremes in the first derivative, and *Gu* on a combination of local maxima in the first derivative (Gu et al., 2009). Regarding the *Thresholds* method, in this trial we tested different values for the fixed threshold: 10 ($TRS_{0.1}$), 20 ($TRS_{0.2}$), 30 ($TRS_{0.3}$), 40 ($TRS_{0.4}$) and 50% ($TRS_{0.5}$) of the seasonal amplitude.

2.1.4. Evaluation Criteria

The statistical analysis performed to evaluate the FMxEM methodology that provides the best match between SOS, POS and EOS from observed values (i.e., GPP) and satellite-derived values (i.e., kNDVI) was conducted using four statistical indicators: the coefficient of determination (R^2), the mean absolute error (MAE), Akaike's information criterion (AIC) and root-mean-square error (RMSE).

The four indices are calculated as follows:

$$R^2 = \frac{\sum_{i=1}^{n}(y_i - \underline{y}_i)^2}{\sum_{i=1}^{n}(y_i - \hat{y}_i)^2} \quad (8)$$

$$MAE = \frac{\sum_{i=1}^{n}|y_i - \hat{y}_i|}{n} \quad (9)$$

$$AIC = 2k - 2\ln\ln(\hat{L}) \quad (10)$$

$$RMSE = \sqrt{\frac{1}{n}\sum_{i}^{n}(y_i - \hat{y}_i)^2} \quad (11)$$

where n represents the number of observations, y_i the observed value, $\underline{y_i}$ the mean observed value, $\hat{y}_i$ the simulated value, k the number of estimated parameter and $\hat{L}$ the maximum value of the likelihood function. In order to exclude outlier points, FM×EM approaches were evaluated by excluding years in which the difference between observed and simulated phenological dates was higher than 70 days. The percentage of points used out of the total was reported as *pp* (point percentage).

2.2. SOS, POS, EOS Analysis in the 2001–2021 Period

The approach to extract SOS, POS and EOS from MODIS satellite imagery was selected after the comparison between phenological dates extracted from kNDVI and observed GPP and then applied to different grassland systems in Europe over the period 2001–2021. Subsequently, the influence of seasonal mean temperatures was evaluated to understand the impact of climate change (Figure 1).

2.2.1. Study Areas and Meteorological Time Series

The analysis of the period 2001–2021 was performed across different grassland sites in Europe. Study areas were identified from WEkEO (https://www.wekeo.eu/services accessed on 27 July 2022), the EU Copernicus DIAS reference service for environmental data, virtual processing environments and skilled user support. From the specific layer that identifies the category "grasslands", we selected 31 different sites (Figure 2) from which the MODIS-kNDVI annual patterns to retrieve SOS, POS and EOS were elaborated and extracted. Sites were selected to include areas with different altitudinal and latitudinal conditions to increase the representativeness of the dataset (Table 2).

Meteorological data were extracted from the National Centers for Environmental Information (NCEI) stations of the National Oceanic and Atmospheric Administration (NOAA) dataset (https://www.ncei.noaa.gov/maps/daily/ accessed on 29 July 2022). Wherever possible, mean daily

temperatures were collected from stations located in the closest proximity to the grassland site coordinates.

Figure 2. Distribution of study areas across Europe.

Table 2. European grassland sites selected for phenological analysis during the period 2001–2021.

Site ID	Country	Latitude	Longitude	Altitude	Meteo Station	Meteo Years
AUS1	Austria	46.7782 N	14.9746 E	1740	Feistritz Ob Bleiburg	2008–2021
AUS2	Austria	47.0373 N	11.2085 E	1931	Obergurgl	2002–2021
BOS	Bosnia	44.2219 N	16.5075 E	1092	Livno	2001–2021
BUL	Bulgaria	42.1875 N	23.2977 E	2434	Mussala Top Sommet	2001–2021
CZE	Czech Republic	48.5850 N	14.3765 E	642	Budejovice Roznov	2001–2021
DEN	Denmark	56.1995 N	10.5378 E	40	Aarhus	2001–2021
FRA1	France	45.5949 N	6.6931 E	1812	Bourg St Maurice	2001–2021
FRA2	France	45.1842 N	2.7997 E	1169	Aurillac	2001–2021
FRA3	France	42.2984 N	9.0294 E	1125	Ile Rousse	2001–2021

GEO	Georgia	42.6512 N	44.601 E	2258	Pasanauri	2004–2016
GER1	Germany	50.7660 N	10.7831 E	518	Erfurt	2005–2021
GER2	Germany	51.7090 N	10.5377 E	697	Fritzlar	2001–2021
HUN	Hungary	47.4892 N	20.9926 E	276	Debrecen	2001–2021
ITA1	Italy	45.1806 N	7.2695 E	1975	Bousson	2006–2021
ITA2	Italy	45.6908 N	11.0631 E	1576	Paganella Mountain	2001–2021
ITA3	Italy	42.4005 N	13.6756 E	1623	No station	
ITA4	Italy	40.0129 N	9.3181 E	1464	Perdasdefogu	2006–2021
LAT	Latvia	57.5046 N	27.3139 E	581	Aluksne	2004–2020
POL	Poland	50.4299 N	16.3272 E	630	Klodzko	2001–2021
ROM	Romania	46.8456 N	25.1027 E	1192	Batos	2014–2021
RUS1	Russia	53.6425 N	35.5488 E	165	Bryansk	2001–2021
RUS2	Russia	43.2756 N	41.6877 E	2544	Teberda	2013–2020
SCO	Scotland	56.5194 N	4.2276 W	559	Glen Ogle	2001–2021
SLK	Slovakia	49.1370 N	20.2007 E	1357	No station	
SLV	Slovenia	46.4887 N	14.0553 E	1238	Ratece	2013–2021
SPA1	Spain	43.0329 N	1.147 W	992	Pamplona	2001–2021
SPA2	Spain	42.5973 N	0.0713 E	1759	No station	
SWE	Sweden	64.9977 N	14.5455 E	854	Stekenjokk	2002–2021
SWI1	Switzerland	46.9242 N	6.7304 E	1219	Bullet La Fretaz	2002–2021
SWI2	Switzerland	46.9014 N	8.9249 E	1749	Disentis Sedrun	2001–2021
TUR	Turkey	41.2610 N	42.5550 E	2524	Ardahan	2009–2021

Coordinates were reported in WGS84.

2.2.2. Procedure and Trend Analysis

In order to proceed with the extraction of phenological dates (i.e., SOS, POS and EOS), an area of 250 × 250 m cleared of any interference (bare soil, rocks, shrubs, trees) was identified within each

grassland site on the WEkEO portal. From the centroid of this area, coordinates were subsequently extracted and used to identify the MODIS pixel for the processing of the kNDVI vegetation index. For each pixel, annual patterns of kNDVI for the period 2001–2021 were then recreated. From these trends, dates of SOS, POS and EOS were extracted according to the results obtained by the different approaches tested during the preliminary analysis. Specifically, the choice of methods took into account the need to use a single fitting model in order to extract SOS, POS and EOS from the same curve. Instead, the extraction methods were selected in accordance with the best results obtained in the preliminary analysis for each phenological date (i.e., SOS, POS and EOS) in order to achieve better accuracy. The selected FM×EM approaches (same FM, different EM for phenological date) were then applied to all sites and years to estimate SOS, POS and EOS.

For each site, values of SOS, POS and EOS depicting a difference with the mean value higher than twice the value of deviance were discarded so as to exclude outliers from the analysis. Furthermore, in order to smooth out short-term fluctuations, a moving average with a three-year window was applied on phenological dates during the time period considered.

After extracting and filtering SOS, POS and EOS, advances or delays in the cycle of grassland vegetation during the time period considered (2001–2021) were analysed.

The results were then correlated with the processed weather data extracted from stations located in proximity to the study areas. Specifically, daily data of temperatures at each site were aggregated seasonally: winter (January, February and March), spring (April, May and June), summer (July, August and September) and autumn (October, November and December). Then, as well as for phenological dates, a moving average with a three-year window was performed on average seasonal values of mean temperature to smooth fluctuations and highlight temporal trends. Data were elaborated with a linear regression analysis in order to evaluate possible changes in mean seasonal temperatures over the period 2001–2021.

Finally, mean temperature data were compared through a correlation analysis to phenological dates extracted from kNDVI patterns to investigate the potential impact of this factor on advances or delays in the grassland growing season. As in Stöckli and Vidale (2004), analysis of phenological trends considered 3 different levels of significance (statistical analysis F-test): 1, 5 and 10%.

3. Results

3.1. Optimisation of the Extraction Method

The analysis conducted by comparing SOS, POS and EOS extracted from GPP with those extracted from the kNDVI index course (Figure 3) allowed the identification of reliable methodologies to assess phenological dates.

Regarding SOS, the FM×EM methodologies providing the best match between observed (i.e., GPP) and estimated data (i.e., kNDVI) were: ELM×$TRS_{0.3}$, GU×$TRS_{0.3}$ and BEC×$TRS_{0.4}$.

In the case of the peak of the season (POS), the use of the TRS extraction method was limited to one result, as this date was extracted from the maximum value reached by the curve (TRS = 1). As shown in Table 3, the best results in POS calculation were obtained with ELM×GU and BEC×GU.

The identification of EOS dates via remote sensing, on the other hand, was more problematic, with sub-optimal statistical values (R^2, MAE, AIC, RMSE) and a generally lower number of usable points after filtering with respect to SOS and POS (Table 3). Due to the low performance in determining EOS through the kNDVI index, the end of the season was not considered in the analysis over the 2001–2021 period.

Among the methodologies that performed best in predicting SOS and POS, those chosen for the analysis of the period 2001–2021 were ELM×$TRS_{0.3}$ and ELM×GU, respectively. The choice fell on these two specific methodologies since for the extraction of start and peak dates, it was relevant to maintain the same type of fitting model (i.e., ELM), even if the extraction methods that worked better for SOS and POS were different ($TRS_{0.3}$ and GU for SOS and POS, respectively).

Table 3. Goodness of fit indicators between phenological dates extracted from GPP and kNDVI patterns with different FM×EM approaches. The results underlined and in bold are those relating to the approach chosen for the start (SOS) and peak (POS) of the season, respectively.

		SOS				**POS**				**EOS**			
		ELM	**GU**	**BEC**	**KLS**	**ELM**	**GU**	**BEC**	**KLS**	**ELM**	**GU**	**BEC**	**KLS**
GU	MAE	15.2	17.1	15.2	17.4	**13.4**	14.4	13.9	12.5	19.2	21.6	25.3	24.7
	R^2	0.76	0.74	0.75	0.83	**0.66**	0.62	0.54	0.56	0.08	0.06	0.00	0.05
	AIC	627	671	647	577	**647**	652	651	614	533	595	527	496
	RMSE	19.2	21.5	20.0	20.7	**18.5**	19.3	19.3	18.0	26.0	26.3	29.2	29.7
	pp	93	96	94	88	**91**	93	93	88	77	83	73	72
DER	MAE	15.0	16.9	14.2	12.6	16.2	28.6	23.8	16.8	18.8	35.8	39.5	36.3
	R^2	0.63	0.69	0.73	0.77	0.55	0.49	0.30	0.61	0.09	0.05	0.12	0.16
	AIC	682	668	674	568	512	480	530	416	557	498	560	479
	RMSE	21.1	21.9	17.8	16.3	21.1	34.6	30.2	23.7	25.4	40.6	43.1	40.1
	pp	95	95	99	86	73	64	69	56	79	69	80	72
KLS	MAE	17.4	15.0	13.9	19.5	10.3	15.8	13.9	13.6	22.6	23.3	24.1	27.1
	R^2	0.85	0.73	0.57	0.6	0.89	0.57	0.57	0.71	0.00	0.00	0.02	0.17
	AIC	116	300	582	505	110	345	582	431	104	222	458	351

	RMSE	21.5	18.2	19.0	24.0	13.1	22.2	19.0	19.3	33.1	29.5	28.65	32.7
	pp	17	46	83	69	16	47	83	60	16	30	64	47
$TRS_{0.1}$	MAE	15.4	19.4	21.0	19.2	16.2	28.5	23.8	16.8	21.1	21.5	22.9	24.4
	R^2	0.35	0.57	0.56	0.51	0.55	0.49	0.30	0.61	0.06	0.06	0.00	0.00
	AIC	635	612	651	598	512	480	530	416	589	302	325	235
	RMSE	19.3	24.1	25.7	24.3	21.06	34.6	30.2	23.7	26.5	26.0	28.0	30.0
	pp	91	83	94	81	73	64	69	56	84	46	48	33
$TRS_{0.2}$	MAE	14.0	14.8	13.6	15.8	-	-	-	-	22.8	21.9	24.9	25.9
	R^2	0.78	0.79	0.79	0.91	-	-	-	-	0.14	0.14	0.01	0.09
	AIC	609	611	625	497	-	-	-	-	588	498	583	459
	RMSE	17.7	19.7	17.6	19.5					28.3	27.0	30.4	30.2
	pp	91	89	94	75	-	-	-	-	85	72	80	68
$TRS_{0.3}$	MAE	**13.6**	15.0	12.9	14.6	-	-	-	-	27.5	29.4	28.9	31.6
	R^2	**0.82**	0.85	0.80	0.86	-	-	-	-	0.12	0.16	0.07	0.15
	AIC	**599**	593	627	553	-	-	-	-	588	547	548	529
	RMSE	**16.9**	19.0	16.2	17.9					32.0	33.8	33.9	35.8
	pp	**91**	90	95	86	-	-	-	-	85	79	78	78
$TRS_{0.4}$	MAE	13.7	14.9	12.8	13.3	-	-	-	-	34.2	36.1	35.5	36.6
	R^2	0.80	0.81	0.79	0.80	-	-	-	-	0.10	0.22	0.14	0.22
	AIC	629	624	626	580	-	-	-	-	569	574	545	522
	RMSE	18.1	19.3	15.9	16.7					38.4	39.4	39.1	39.8
	pp	94	93	95	88	-	-	-	-	83	83	79	78
$TRS_{0.5}$	MAE	13.7	15.7	13.3	12.6	-	-	-	-	39.8	42.0	40.3	40.3
	R^2	0.73	0.69	0.76	0.76	-	-	-	-	0.12	0.21	0.21	0.19
	AIC	652	674	648	566	-	-	-	-	523	567	527	505
	RMSE	18.6	20.5	17.1	16.7					43.5	45.0	43.1	43.6
	pp	94	95	96	84	-	-	-	-	75	81	78	74

The FMs reported are Elmore (ELM), Gu (GU), Beck (BEC) and Klosterman (KLS), the EMs Gu (GU), Derivatives (DER), Klosterman (KLS) and Threshold (TRS). Pp represents the percentage of points used for the evaluation (difference between dates extracted from GPP and kNDVI < 70 days).

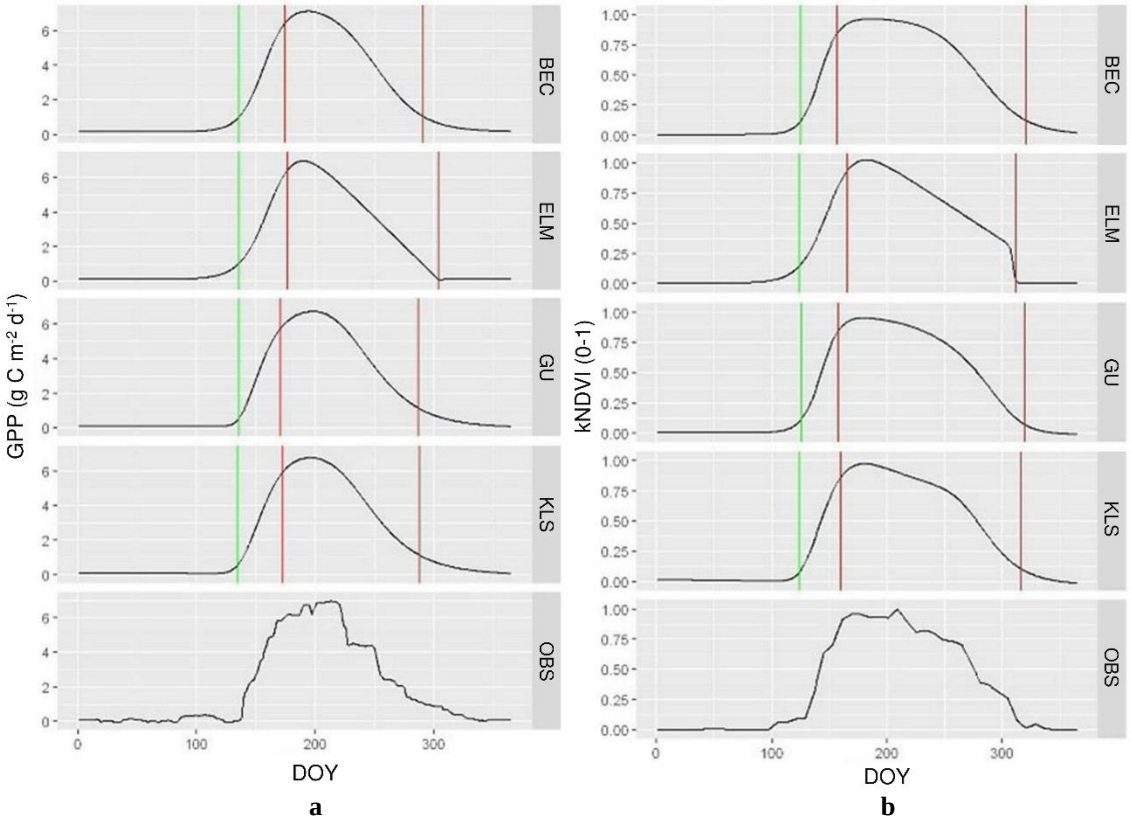

Figure 3. Example of SOS, POS and EOS extraction from GPP (**a**) and kNDVI (**b**) patterns of the Torgnon site (year 2017), with different fitting models: Becker (BEC), Elmore (ELM), Gu (GU), Klosterman (KLS)) and GU extraction. OBS represents the raw values of GPP and kNDVI. Vertical bars represent estimated SOS (green), POS (red) and EOS (dark red).

3.2. SOS and POS Trend Analysis (2001–2021)

The procedures selected during the methodological analysis (ELM×$TRS_{0.3}$ and ELM×GU, respectively, for SOS and POS) were used to investigate possible changes in the phenological timing of European grasslands. Given that from the results obtained in 3.1 (Table 3), the end of the season (EOS) was not well identified by MODIS-kNDVI when compared to EOS extracted from GPP, the analysis considered exclusively the start (SOS) and peak (POS) dates of the growing season.

Satellite-derived SOS showed a clear trend over the time span considered. As depicted in Table 4 and Figure 4, 26 sites (out of 31, i.e., 83.9% of the total) evidenced a negative correlation between SOS and years, indicating a progressive advance in the start of the growing season from 2001 onwards. From the SOS-years regression analysis, 17 grasslands sites showed a level of significance (F) < *0.1* in SOS anticipation. Specifically, 3 sites reported F values between 0.05 and 0.1 (AUS1, POL,

RUS1), 5 between 0.01 and 0.05 (GEO, GER2, RUS2, SLV, TUR) and 9 < 0.01 (AUS2, BOS, CZE, DEN, FRA2, ITA3, HUN, SLK, SWI1).

The advance in SOS was subsequently quantified (Figure 4) by applying the equation identified from the specific SOS-years linear regression. From 2001 to 2021, the average advance of the growing season at significant sites ($F \leq 0.1$) was 15.92 days (0.76 days year^{-1}). However, it should be noted that the significant sites analysed showed different levels of SOS earliness, ranging for example from the 5.6-day advance of the RUS1 site to the 42.0-day advance of the DEN site.

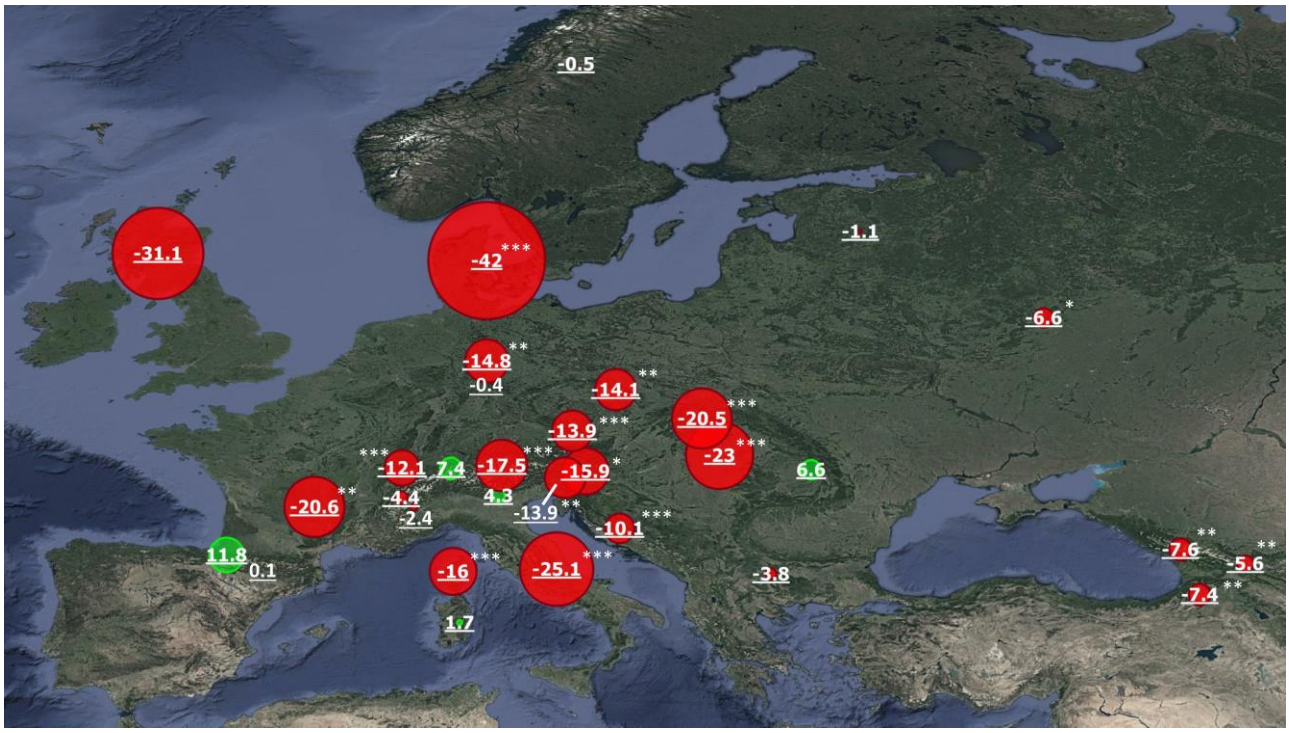

Figure 4. Changes (days) in SOS during the period 2001–2021. SOS advance is highlighted with red circles, whereas delay is highlighted with green circles. Sites that display a significant SOS-year correlation are marked with * ($0.05 < F \leq 0.1$), ** ($0.01 < F \leq 0.05$) and *** ($F \leq 0.01$).

As with SOS, the POS dates in the period 2001–2021 showed a trend towards an earlier peak of the grassland growing season. In fact, although in a smaller percentage than in SOS, 21 sites (67.7% of the total) evidenced an advance in POS dates (Table 4 and Figure 5).

From POS-years regression analysis, 13 grassland sites showed a level of significance (*F*) of < 0.1 in POS advance during the period 2001–2021. Specifically, 6 sites reported F values between 0.05 and 0.1 (BOS, DEN, FRA2), 3 between 0.01 and 0.05 (AUS2, CZE, SWE) and 4 < 0.01 (GER2, LAT, RUS2, TUR). In the case of POS, in addition to sites that showed a significant advance in the beginning of the season, two sites highlighted contrasting trends (FRA1 and ITA2), showing a clear delay in the peak of the season (0.01 < F < 0.05). As for SOS, changes in phenological dates during the period 2001–2021 were quantified for each site (Figure 5). Considering all the significant sites (F ≤ 0.1), including those that showed a delay, the average advance in the peak of the growing season was 11.66 days (0.56 days year^{-1}).

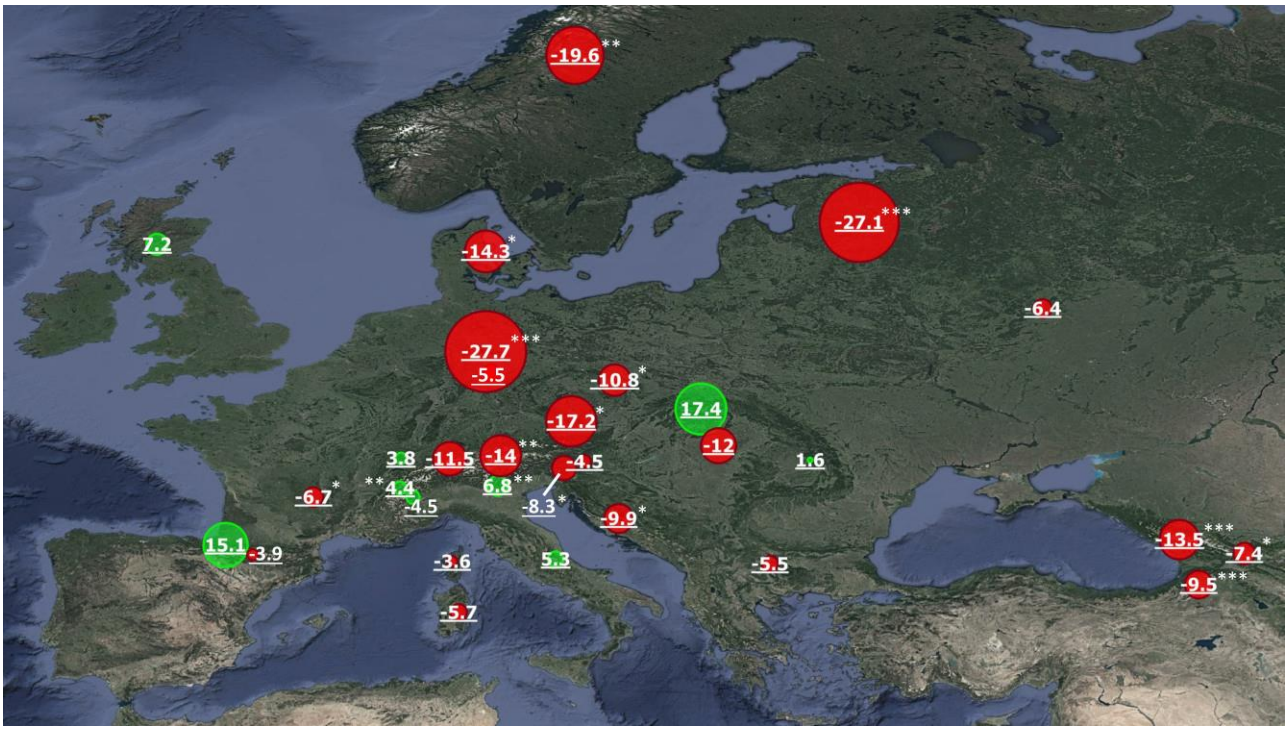

Figure 5. Changes (days) in POS during the period 2001–2021. SOS advance is highlighted with red circles, whereas delay is highlighted with green circles. Sites that display a significant POS-year correlation are marked with * (0.05 < F ≤ 0.1), ** (0.01 < F ≤ 0.05) and *** (F ≤ 0.01).

Table 4. Results of SOS and POS analysis over the period 2001–2021. *Mean* represents the mean value of SOS and POS during the period 2001–2021, reported to give general information about each site (data not included in the analysis). *R* columns show the correlation coefficient (R) between phenological dates (i.e., SOS and POS) and years, *Sign*. the significance (*F*) of the SOS and POS-years regression, and *Days* the difference between SOS and POS in the years 2001 and 2021 according to the equation found with the linear regression.

	SOS					POS				
ID	**Mean**	**R**	**Days**	**Sign.**	**Pp**	**Mean**	**R**	**Days**	**Sign.**	**Pp**
AUS1	139.32	−0.43	**−15.89**	**0.06**	0.9	169.35	−0.25	−4.54	0.3	0.95

AUS2	159.3	−0.66	**−17.51**	**<0.01**	0.95	187.16	−0.52	**−14.02**	**0.03**	0.9
BOS	116.05	−0.68	**−10.08**	**<0.01**	0.9	157.52	−0.4	**−9.93**	**0.09**	1
BUL	172.7	−0.17	−3.77	0.48	0.95	197.9	−0.11	−5.53	0.65	0.95
CZE	85.16	−0.66	**−13.88**	**<0.01**	0.9	129.68	−0.52	**−17.2**	**0.02**	0.9
DEN	91.63	−0.74	**−42**	**<0.01**	0.86	124.18	−0.44	**−14.31**	**0.06**	0.81
FRA1	124.3	−0.34	−4.42	0.15	0.95	154.19	0.5	**4.44**	**0.03**	0.95
FRA2	94.47	−0.61	**−20.6**	**<0.01**	0.9	140.42	−0.4	**−6.66**	**0.09**	0.9
FRA3	97.5	−0.61	**−15.99**	**<0.01**	0.95	130.85	−0.12	−3.57	0.64	0.95
GEO	148.95	−0.47	**−5.55**	**0.04**	0.95	177.65	−0.4	**−7.42**	**0.1**	0.95
GER1	84.75	−0.01	−0.42	0.96	0.76	117.67	−0.15	−5.47	0.53	0.86
GER2	99.05	−0.48	**−14.76**	**0.04**	0.9	131.48	−0.62	**−27.73**	**<0.01**	1
HUN	69.23	−0.65	**−22.95**	**<0.01**	0.65	154.11	0	−12.02	0.74	0.95
ITA1	138.84	−0.07	−2.42	0.77	0.9	167.9	0.17	4.51	0.49	0.95
ITA2	136.95	0.22	4.3	0.36	0.95	165.65	0.5	**6.8**	**0.03**	0.95
ITA3	11.56	−0.77	**−25.14**	**<0.01**	0.86	143	0.22	5.28	0.36	0.95
ITA4	107.35	0.08	1.71	0.73	0.81	128.05	−0.2	−5.74	0.41	1
LAT	113.11	−0.11	−1.12	0.65	0.9	146.35	−0.89	**−27.1**	**<0.01**	0.95
POL	102.58	−0.43	**−14.06**	**0.07**	0.9	138.8	−0.4	**−10.82**	**0.09**	0.95
ROM	128	0.22	6.64	0.38	0.95	166.85	0.07	1.58	0.78	0.95
RUS1	119.26	−0.39	**−6.56**	**0.1**	0.9	149.94	−0.24	−6.37	0.33	0.81
RUS2	148	−0.52	**−7.59**	**0.02**	0.95	181.76	−0.64	**−13.49**	**<0.01**	1
SCO	125.2	−0.34	−31.05	0.16	0.95	161.39	0.13	7.21	0.61	0.86
SLK	122.76	−0.66	**−20.52**	**<0.01**	0.81	157.82	0.37	17.35	0.18	0.81
SLV	130	−0.54	**−13.89**	**0.02**	0.86	164.25	−0.4	**−8.3**	**0.09**	0.9
SPA1	88.28	0.32	11.75	0.18	0.9	155.21	0.37	15.1	0.12	0.9
SPA2	125.67	0	−0.05	0.99	1	154.89	−0.24	−3.86	0.32	0.9
SWE	172.21	−0.02	−0.5	0.94	0.9	191.53	−0.55	**−19.62**	**0.02**	0.9
SWI1	110.35	−0.7	**−12.11**	**<0.01**	0.95	135.04	0.19	3.78	0.44	0.95
SWI2	124.6	0.32	7.37	0.17	0.95	152.86	−0.33	−11.51	0.17	1
TUR	151.8	−0.55	**−7.4**	**0.02**	0.95	185.9	−0.55	**−9.54**	**<0.01**	0.95

Pp is the percentage of points used out of the total after the filtering procedure. Results with significance <0.1 are shown in bold.

In order to carry out an assessment of temperature influence in determining the phenological dates of European grasslands over the 2001–2021 period, statistical analyses were performed to assess the temperature trend over the years considered and the impacts of thermal factors on SOS and POS. From the results of the linear regressions performed between temperatures and years (Table 5), the mean winter temperatures showed an increasing trend in 21 of the 23 sites (sites with no or little weather data were excluded), corresponding to 91.30% of the total. Of these, 16 (69.57%) showed a significant change ($F < 0.1$) over the time period analysed. On the other hand, the average spring temperatures showed a less homogenous trend, with a lower tendency of temperature increase (65.21%) and fewer sites (6) with significant change (26.08%).

The results on the influence of winter and spring temperatures on SOS, showed a negative correlation between SOS and temperatures, significant in 7 sites ($F < 0.1$, AUS1, BOS, CZE, DEN, FRA2, LAT, SWI1) with winter temperature and in 6 (BOS, FRA1, LAT, POL, SWE, SWI1) with spring temperature as the main driver.

Since POS always occurred several weeks after winter's end, in the analysis we considered only the effect of spring temperatures. Here, too, the relationship highlighted a negative correlation between phenological dates (i.e., POS) and temperature. In particular, 10 sites (AUS2, BOS, DEN, FRA3, ITA4, LAT, POL, RUS1, SCO, SPA1) showed a significance *F* in the POS-spring temperature relationship of less than 0.1.

Table 5. Results of the statistical analysis conducted on weather data from 2001 to 2021. *R years* highlights temperature trends over the 2001–2021 period by reporting the values of the correlation coefficients found by correlating the average winter and spring temperatures with the reference years, while *R SOS* and *R POS* report the values found by comparing the extracted SOS and POS with the average winter and spring temperatures of the respective years. For each comparison, the level of significance F is reported (*Sign.*). *T mean* values represent the mean temperatures of the winter and spring seasons, reported to give general information about each site (data not included in the analysis).

	Winter					**Spring**					
ID	**T Mean**	**R Years**	**Sign.**	**R SOS**	**Sign.**	**T Mean**	**R Years**	**Sign.**	**R SOS**	**Sign.**	**R POS**	**Sign.**
AUS1	1.12	0.78	**<0.01**	−0.51	**0.09**	13.93	−0.11	0.74	−0.41	0.19	−0.22	0.5
AUS2	−4.15	0.72	**<0.01**	−0.36	0.16	5.9	0	0.99	−0.03	0.91	−0.52	**0.03**
BOS	3.73	0.74	**<0.01**	−0.63	**0.01**	16.1	0.62	**0.01**	−0.61	**0.01**	−0.64	**0.01**
BUL	−9.07	0.68	**<0.01**	−0.28	0.25	−0.22	0.47	**0.04**	−0.16	0.51	0.18	0.45
CZE	1.73	0.66	**<0.01**	−0.55	**0.02**	13.82	0.33	0.18	-	-	−0.3	0.23
DEN	2.16	0.72	**<0.01**	−0.64	**<0.01**	11.44	0.76	**<0.01**	−0.29	0.24	−0.62	**<0.01**
FRA1	2.33	0.56	**0.01**	−0.27	0.27	13.79	0.05	0.84	−0.57	**0.01**	−0.06	0.82

FRA2	4	0.36	0.13	−0.67	**<0.01**	12.93	−0.24	0.32	−0.17	0.48	0.09	0.72
FRA3	10.82	0.65	**<0.01**	−0.08	0.75	18.07	0.11	0.65	0.09	0.71	−0.49	**0.03**
GEO	0.06	0.25	0.43	0.02	0.95	13.22	−0.01	0.97	−0.29	0.34	0.15	0.62
GER1	1.91	0.46	**0.08**	−0.03	0.91	12.92	0.24	0.39	-	-	−0.41	0.13
GER2	2.77	0.3	0.21	0	1	13.15	0.12	0.63	−0.32	0.18	0	0.99
HUN	2.26	0.61	**0.01**	−0.31	0.27	16.45	0.36	0.13	-	-	0.04	0.87
ITA1 [a]	−0.24	-	-	-	-	9.46	-	-	-	-	-	-
ITA2	−3.83	0.1	0.67	0.02	0.93	4.94	−0.36	0.13	−0.04	0.88	−0.16	0.52
ITA3 [b]	-	-	-	-	-	-	-	-	-	-	-	-
ITA4	8.17	0.67	**0.01**	0.32	0.27	17.48	−0.07	0.82	−0.35	0.22	−0.56	**0.04**
LAT	−3.92	0.53	**0.04**	−0.52	**0.05**	10.8	0.51	**0.05**	−0.53	**0.04**	−0.55	**0.03**
POL	−0.32	0.53	**0.02**	−0.32	0.18	12.32	0.23	0.34	−0.57	**0.01**	−0.55	**0.02**
ROM [a]	1.88	-	-	-	-	15.02	-	-	-	-	-	-
RUS1	−3.57	0.48	**0.04**	−0.33	0.17	14.09	0.44	**0.06**	−0.28	0.25	−0.74	**<0.01**
RUS2 [a]	1.24	-	-	-	-	11.53	-	-	-	-	-	-
SCO	1.22	−0.37	0.12	−0.18	0.47	6.71	0.24	−0.31	−0.14	0.56	−0.47	**0.05**
SLK [b]	-	-	-	-	-	-	-	-	-	-	-	-
SLV [a]	−0.25	-	-	-	-	11.69	-	-	-	-	-	-
SPA1	7.08	−0.11	0.66	0.08	0.74	15.48	−0.87	**<0.001**	-	-	−0.45	**0.05**
SPA2 [b]	-	-	-	-	-	-	-	-	-	-	-	-
SWE	−8.69	0.03	0.89	0.24	0.34	1	−0.34	0.17	−0.69	**<0.00**	−0.2	0.43
SWI1	−0.1	0.63	**<0.001**	−0.56	**0.02**	9.37	0.17	0.51	−0.46	**0.06**	−0.15	0.55
SWI2	0.15	0.52	**0.02**	0.01	0.97	10.51	0.03	0.92	−0.16	0.51	−0.02	0.92
TUR [a]	−3.43	-	-	-	-	13.17	-	-	-	-	-	-

Site names with [a] and [b] represent the sites with insufficient ([a]) or no ([b]) weather data to conduct the analysis. Results with significance <0.1 are shown in bold.

Taking into account the grasslands where the change was significant at both the SOS and POS dates (11 sites), we investigated the influence of two other potential phenological season variables: the latitude and altitude of the test sites. As can be seen in Figure 6, the change in advance during the period 2001–2021 is greater with increasing latitude for both SOS and POS, with the former showing a higher correlation (R = −0.81) than the latter (R = −0.55). Observing the correlations between changes in phenological dates and altitude, sites at higher altitudes show less advance in SOS and

POS than those at lower altitudes. As in the case of the SOS and POS-latitude correlation, the absolute values of R are greater for the change in SOS dates (R = 0.69) than for POS (R = 0.36).

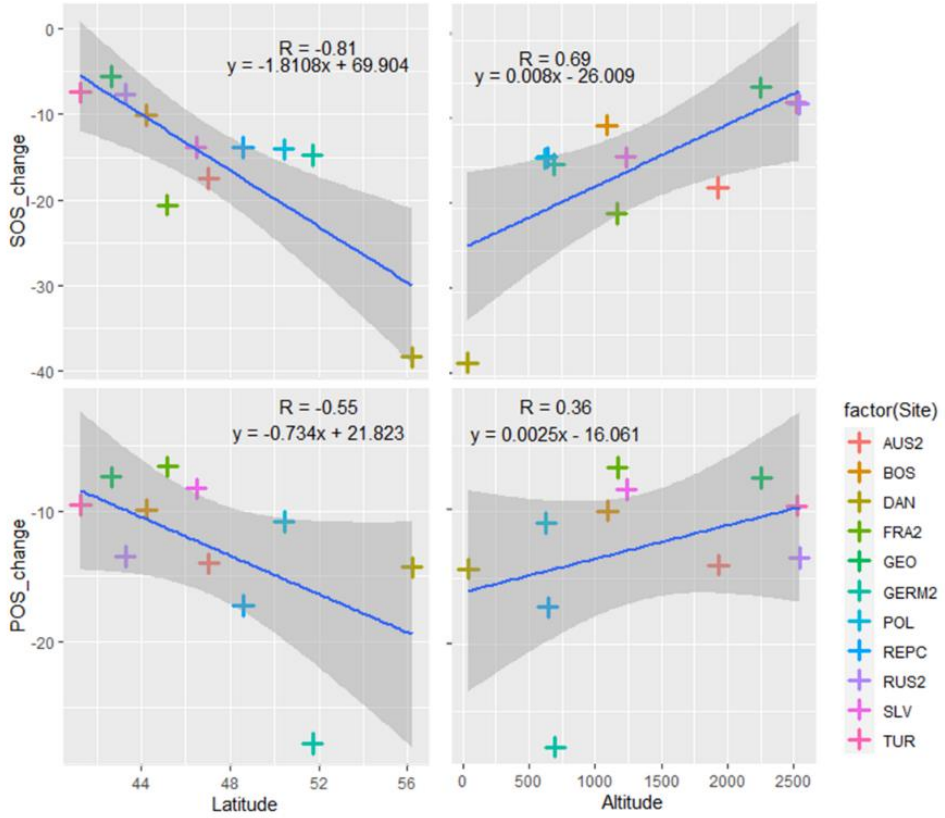

Figure 6. SOS and POS changes during the period 2001–2021 compared with the latitude and altitude of the sites where changes are significant in both SOS and POS.

In addition to the analysis of the changes that occurred in SOS and POS over the reference period, changes in the duration of the timeframe between SOS and POS (i.e., SOS-POS duration) were also analysed (Figure 7).

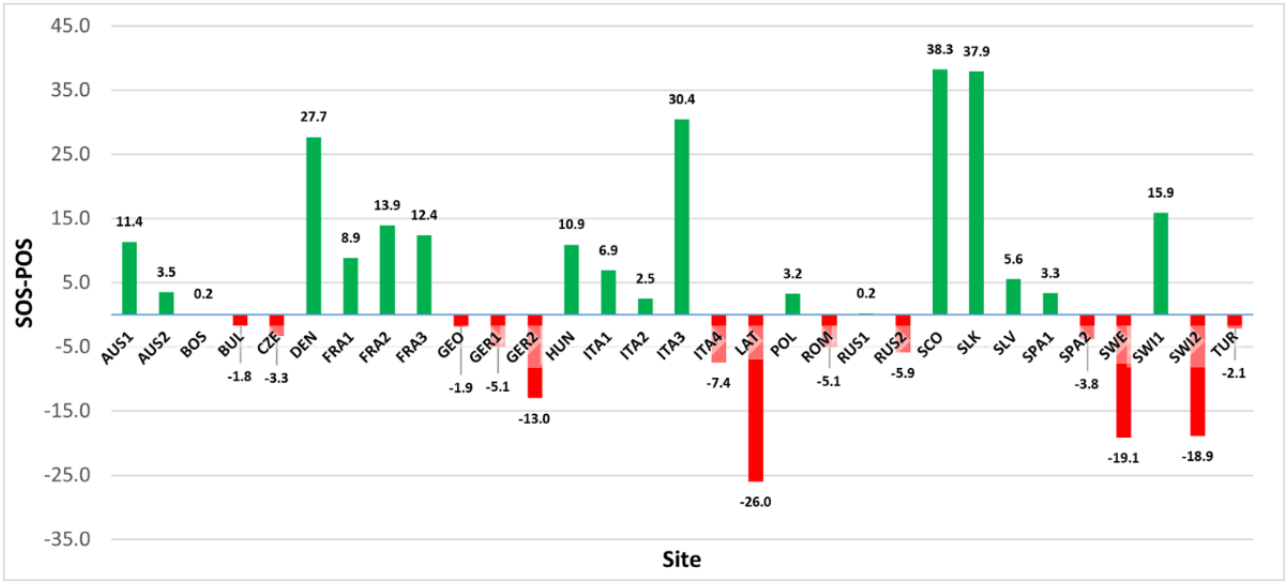

Figure 7. Changes in SOS-POS (number of days) interval during the period 2001–2021 for all test sites.

The data did not show any common trend within the framework of the European grasslands analysed. Indeed, within the dataset considered, some sites showed an increase in the SOS-POS duration (56.67%), while others showed a decrease (43.33%). The lengthening of the SOS-POS duration between 2001 and 2021 was determined by a less marked anticipation of the POS with respect to the SOS (e.g., DEN) or the postponement of the former (e.g., FRA1). The reduction in the SOS-POS duration, on the other hand, was generally caused by a higher advance in POS than in SOS (e.g., GER2).

The change in the time duration of the SOS-POS interval was also analysed in the light of the individual changes in SOS dates. Figure 8 depicts the change in the SOS-POS interval, showing an increase in the number of days as the magnitude of the SOS advance grows and highlighting the influence of an advanced SOS on the lengthening of SOS-POS duration. The analysis was also conducted considering three different levels of altitudinal and latitudinal ranges, but no clear trends emerged.

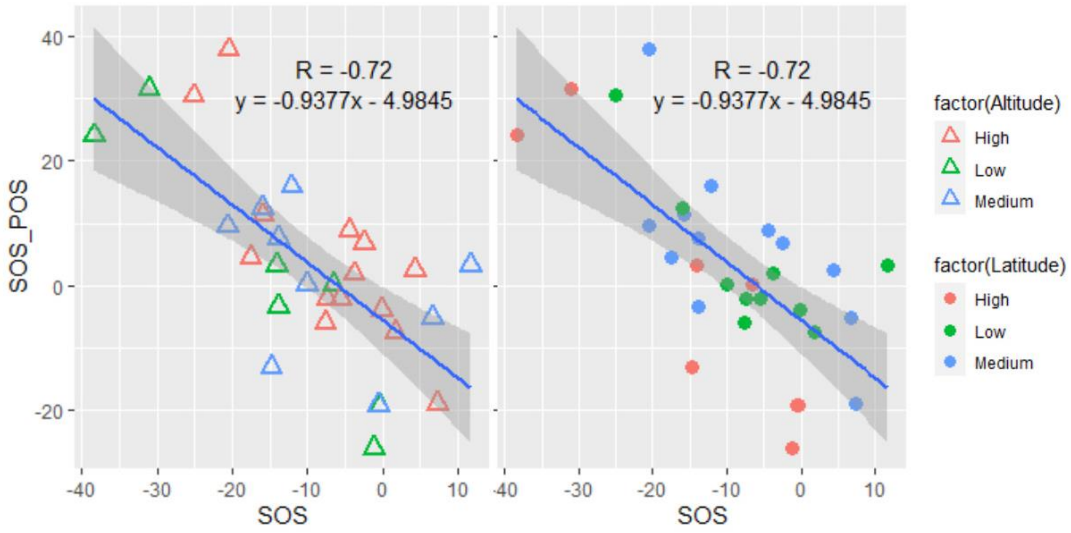

Figure 8. Relationships between changes in SOS-POS duration and changes in SOS during the period 2001–2021. Figures represent the same equation, highlighting sites graphically according to altitude (left) or latitude (right). Sites are divided into 3 different classes of altitude (low, 0–650 m; medium, 650–1300 m; high +1300 m) and latitude (low, 40–45°; medium, 45–50°; high +50°).

Figure 9 shows an example of the trend in average temperatures for the 30 days following the SOS at the DEN site, highlighting how an earlier SOS date results in a generally colder initial growing season, which can lead to a delay in the POS date and a lengthening of the SOS-POS duration (e.g., DEN). Although colder average temperatures are generally present when the start of the season occurs early, the lengthening of the SOS-POS duration, visible for example at the DEN site, was not always visible at all test sites (e.g., Figure 7), likely due to different grass species.

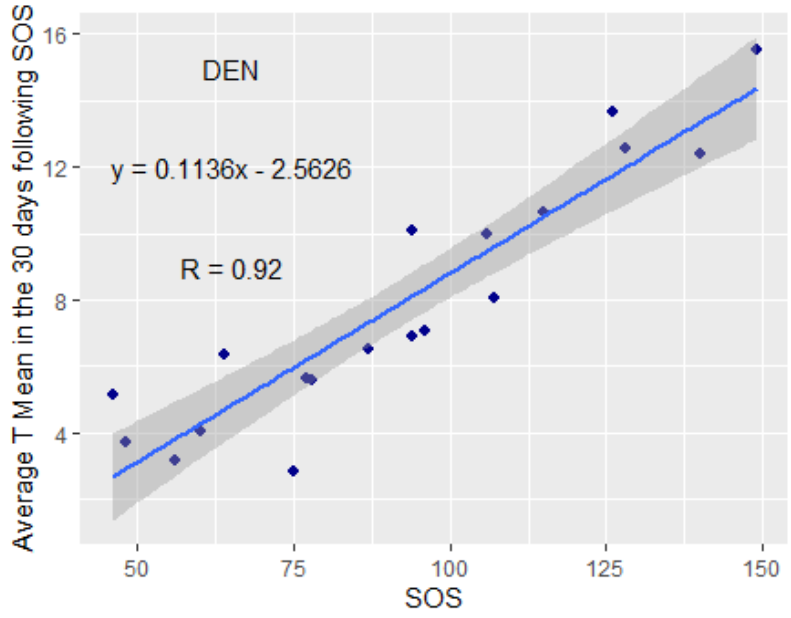

Figure 9. Example of relationships between SOS and the mean temperature of the 30 days after SOS at the DEN site.

4. Discussion

This study aimed to identify the best methodology for the estimation of phenological dates through satellite-processed vegetation indices. As in other studies (Jin et al., 2017; Jin and Eklundh, 2014), GPP measurements were used to extract SOS, POS and EOS as observed data to be compared with those elaborated from kNDVI patterns. Due to the valuable relationship between kNDVI and GPP found for grasslands in (Camps-Valls et al., 2021), the use of this index enabled phenological dates (i.e., SOS and POS) to be estimated in agreement with those extracted by GPP patterns at sites endowed with eddy covariance flux towers. Various fitting models and extraction methods were tested and evaluated in our study, providing different results for SOS, POS and EOS detection. For consistency, a trend analysis was performed by deploying only one fitting model (i.e., ELM) among those selected. Then, we identified the best extraction method for each specific phenological date (i.e., $TRS_{0.3}$ and GU for SOS and POS, respectively). It is important to underline that the fitting model (i.e., the curve that fits kNDVI points and from which dates are extracted) is the same in all trend analyses (i.e., SOS and POS) and for all sites and years. The choice to use different extraction methods on the same curve for SOS and POS derived from the results obtained in Section 3.1. Although it was more coherent to select only one method, we decided to select the most robust extraction methods for each phenological date (i.e., SOS and POS) in order to achieve more precision in SOS and POS estimation during the analysis of the 2001–2021 period. In fact, using the same extraction method could determine greater errors, since, for example, one method can be optimal for SOS but sub-optimal for POS estimation. SOS and POS dates extracted from kNDVI were in line with those estimated from GPP, even if some uncertainties were still present, as seen from MAE (13.6 and 13.4 days, respectively for SOS and POS) and RMSE values (16.9 and 18.5 days, respectively for SOS and POS). EOS, conversely, proved to be more difficult to detect than SOS and POS. This is confirmed by Tian et al. (2021), who achieved lower levels of accuracy in estimating EOS in different environments, and by Zheng and Zhu (2017), who observed large differences and poor correlation between EOS extracted from satellite vegetation indices and ground-observed EOS in a specific study on grasslands. Differently from Tian et al. (2021) and Gonsamo et al. (2012) for forests and croplands, in this study the estimation of EOS from satellites did not reach a level of accuracy that can provide a reliable analysis for EOS trends over the period 2001–2021. However, it should also be noted that the extraction of SOS and EOS dates in grasslands is subject to greater uncertainties than in other environments, such as deciduous-broadleaf and mixed forests (Xu et al., 2020). Leaf senescence responses in herbaceous species are influenced by several meteorological variables, with a complex dependence on species, functional types and geographical gradients (Ren et al., 2022). Differences in scale and content (spectral response and phenological event) between satellite-derived and ground-

observed phenology can result in discrepancies between satellite-derived phenological dates and changes in leaf colouring, although these measurements are related (e.g., EOS and the beginning of leaf colouring) (Badeck et al., 2004; White et al., 2009; Xu et al., 2014). This is especially noticeable for EOS. In fact, the change in canopy greenness is slower and longer in autumn with respect to spring (Gallinat et al., 2015; Wu et al., 2017), thus causing a reduced variability in EOS compared to SOS and a greater difficulty in detecting the end of season from satellite (Tian et al., 2021; Zheng and Zhu, 2017).

From our trend analysis, the European grasslands analysed showed a general advance in the start (SOS) and peak of the season (POS) over the 2001–2021 time period. This anticipation is in agreement with what was observed in different time frames in both grassland (Adu et al., 2021; Gong et al., 2015; Hou et al., 2014; Li et al., 2021; Ren et al., 2020) and non-grassland biomes in Europe (Menzel et al., 2020; Stöckli and Vidale, 2004). Specifically, in our study, SOS and POS advance in significant sites (Table 4) was 0.76 days year^{-1} and 0.56 days year^{-1}, respectively for the 2001–2021 period. In some cases, however, an opposite trend was observed, i.e., a slight tendency to delay in the SOS and/or POS dates. This could be partially explained for SOS and, consequently POS, by an insufficient cooling effect due to warming conditions in late autumn or winter (Adu et al., 2021). On the other hand, as regards the POS only, the anticipation of SOS in response to increasing temperatures may shift the following SOS-POS duration to colder environmental conditions (e.g., Figure 9), which in turn may lead in some cases to a progressive lengthening of SOS-POS durations. This is in agreement with the modelling exercise of Sadras and Monzon (2006), who suggested that an earlier flowering in wheat due to temperature increase during the period 1971–2000 may have determined shifts in post-flowering development at lower temperatures, neutralising the trend of increasing temperatures and leaving post-flowering phase duration unchanged. The same was observed in the field of grapevine (Sadras and Moran, 2013). This could explain part of our results regarding SOS-POS duration, particularly for those sites showing a lengthening. However, the trend is not evident in all the grassland sites analysed in this study, as a certain number of sites (i.e., 13) showed a shortening of the SOS-POS length. These outcomes result from a not too marked SOS anticipation (e.g., LAT, SWE, SWI2) and a consequent relapse of SOS into a time range (i.e., DOY) similar to the ones observed at the turn of the year 2001. In addition, the generally higher temperatures (i.e., global warming) and, probably, less water availability occurring after each specific SOS probably caused an advance in the vegetation peak (Cleland et al., 2006; Hua et al., 2021), inducing a shortening in SOS-POS duration, as the SOS remains unchanged and the POS is advanced. The presence of a spurious bias in SOS-POS length deriving from the different extraction methods for SOS and POS in estimating SOS-POS length is possible. However, investigating SOS-POS length

per se was not our final goal, since our attention was mainly focused on trends. In fact, if a bias was present, this error did not influence the trend analysis, as it was present in the same way in all years from which SOS and POS were extracted.

The study of seasonal average temperatures (i.e., winter and spring) showed a general rise in temperatures across Europe for the period 2001–2021, resulting in a negative correlation, significant in some cases (Table 5), with SOS and POS dates. Summer and autumn temperatures were not considered since EOS, the phenological date that occurs after these seasons, was excluded from the trend analysis since satellite estimations were not sufficiently reliable.

The effect of temperature was found to be a decisive factor in the change of phenological dates of SOS and POS, in agreement with Ganjurjav et al. (2018) and Ren et al. (2020), also influencing phenology spatially (Vitasse et al., 2021). Consequently, the rise in temperatures recorded in the 2001–2021 time frame could also have had an indirect effect on the advancement of the SOS date by causing an advancement in the snowmelt dates recorded in recent years (Hock et al., 2019), without the risk of increasing frost exposure (Klein, 2018). Snow melt and snow cover are indeed decisive in determining the length of the growing season and the phenological development of high-altitude and high-latitude grassland (Körner, 2021; Vorkauf et al., 2021), also influencing water availability or thermal conditions by soil insulation (Grippa et al., 2005). However, according to Xie et al. (Xie et al., 2021), in a specific study on the European Alps, spring temperature was the predominant factor in SOS advancement, while snow cover and snow melt, although important, played a secondary role. Temperature is therefore an important factor, but our results often do not show a significant relationship between this parameter and SOS and POS (Table 5). This can be explained by the fact that, in addition to temperature, there are other factors that may influence phenological dates, such as CO_2 concentration, the presence of nitrogen in soil, solar radiation, wind speed, atmospheric pressure, snow cover or precipitation (Cleland et al., 2006; Hua et al., 2021). Snow cover for instance, as reported in Jerome et al. (2021), can act through temperature accumulation but also independently as a driver of plant phenology. Regarding precipitation, Xu et al. (2021) observed an earlier onset of the grassland growing season due to higher temperatures only when water was not a limiting factor, with a non-linear response. In contrast, Hua et al. (2021) pointed out that high precipitation can have a delaying effect on the peak season (POS) as a result of the high correlation between this phenological stage and rainfall.

Our study highlighted the influence of altitudinal and latitudinal conditions on the phenological stages of grassland with significant changes ($F \leq 0.1$) in SOS and POS during 2001–2021. Correlations between the magnitude of change in SOS and altitude and latitude indicated higher absolute values than the respective correlations with POS. The sites that showed higher changes in the dates of SOS

and, to a lesser extent, POS were those located at higher latitudes and lower altitudes (e.g., DEN, 56.1995 N, 40 m a.s.l.), while at low latitudes and high altitudes (e.g., TUR, 41.2610 N, 2524 m a.s.l.) showed smaller phenological changes.

The contrasting behaviour of changes (i.e., advances and/or postponement) in SOS and POS dates can also be explained by the variability in botanical composition as a result of the different environments in which the study sites are located. This is confirmed by several studies (Castillioni et al., 2022; Mutanga and Shoko, 2018; Ren et al., 2022; Weil et al., 2017; Weisberg et al., 2021) that highlight the importance of species or functional types on the phenological stages of plants. In addition, as observed by Cleland et al. (2006), diverse plant functional types have different phenological changes in response to multiple environmental factors (e.g., CO_2 concentration or soil resources). Moreover, the changes in temperatures recorded over the last few decades, beyond having a direct effect on the early or late season, may have influenced the change in the composition of functional groups (Dibari et al., 2021), which in turn may alter the grassland phenological stages. Nevertheless, the main aim of our work was to highlight general trends in phenology, without a particular focus on the species present in the test areas. Given the spatial-temporal extent of the trend analysis, reliable and timely information on the specific botanical composition at the 31 study sites over the years of investigation was, moreover, difficult to obtain. Indications regarding phenological responses of different species can, however, also be gathered indirectly from observing the results in Figure 6, which analyses the phenological changes observed at different altitudinal and latitudinal gradients, conditions that reflect the type of vegetation that may be present in those environments.

Although investigating the phenology of different species was not our main objective, knowing the type of species or functional groups present would have provided useful information to increase understanding of the results. In fact, as explained above, this information may clarify the contrasting results obtained for some study sites. Nevertheless, the results showed a clear general tendency of grassland phenology to advance, especially the SOS date.

Overall, our results confirmed what was already observed in a sparse and limited number of EU countries (Menzel et al., 2020) and under a different time span in Europe (Stöckli and Vidale, 2004), while remaining in line with other studies in other areas of the world (Adu et al., 2021; Hua et al., 2021). The analysis conducted with an exclusive focus on the grassland environment provides important indications of both the extent of these phenological changes and their distribution within the European continent, as well as the influence of increasing temperatures.

The phenological estimates obtained from MODIS satellite data over the time period 2001–2021 represent key information for understanding the evolution of grassland phenology that has occurred

in recent years and the trend towards which it is heading, providing policy makers and stakeholders with useful indications for the identification of possible adaptation and mitigation strategies.

Despite the uncertainties, the methodology presented in this paper can represent a first step in a European-wide assessment of grassland phenology, opening up the possibility of investigating phenological trends over large and numerous grassland areas of the continent. Concerning future perspectives, a specific end-of-season study could be important to reduce uncertainties in EOS detection from satellites and refine the methodology. In addition, the analysis performed can be extended by focusing on the differences that may occur in grasslands characterised by the presence of different dominant species and groups. The analysis of the factors driving the phenological changes can also be extended to water conditions (i.e., precipitation and snowmelt date) in the case of high-quality data over an extended period of time.

5. Conclusions

This study provided important information on the phenology of European grasslands. kNDVI resulted in being a reliable vegetation index for estimating the phenological dates of SOS and POS, but the same effectiveness cannot be applied to EOS. The analysis of MODIS satellite data from 2001 to 2021 showed a clear trend towards an earlier start to the growing season (SOS) across Europe. An advance in the date of the peak season (POS) is also evident, although generally less marked and, in some cases, even delayed than at the beginning of the reference period of analysis. The seasonal average temperature (i.e., winter and spring) was generally found to be increasing at all sites, often proving to be a significant driver of the advancement of grassland phenological dates over the European domain. Analyses conducted with a specific focus on grasslands have provided very important insights into the status of these systems throughout Europe and the evolution, in phenological terms, that they have been undergoing in recent decades.

Author Contributions: Conceptualization, E.B. and M.M.; methodology, M.G., G.F., E.B. and M.M.; software, G.F.; validation, E.B., L.L. and L.S.; formal analysis, E.B., C.D., L.S. and L.L.; investigation, E.B. and G.A.; resources, C.D. and G.A.; Data Curation, E.B., N.S. and L.S.; Writing–Original Draft Preparation, E.B.; writing–review and editing, M.M., G.A., C.D., M.G., G.F., N.S., L.S. and L.L; visualization, E.B. and M.M.; supervision, M.M. and G.A.; project administration, C.D.; funding acquisition, C.D. All authors have read and agreed to the published version of the manuscript.

Funding: This research received no external funding.

Data Availability Statement: Not applicable.

Acknowledgments: Research partially supported by the project “Unraveling interactions between WATER and carbon cycles during drought and their impact on water resources and forest and grassland ecosySTEMs in the Mediterranean climate (WATERSTEM)”, financed by the Italian Ministry of University and Research.

Conflicts of Interest: The authors declare no conflict of interest.

References

Adu, B., Qin, G., Li, C., Wu, J., 2021. Grassland phenology’s sensitivity to extreme climate indices in the Sichuan Province, Western China. Atmosphere (Basel). 12. https://doi.org/10.3390/atmos12121650

Badeck, F.W., Bondeau, A., Böttcher, K., Doktor, D., Lucht, W., Schaber, J., Sitch, S., 2004. Responses of spring phenology to climate change. New Phytol. 162, 295–309. https://doi.org/10.1111/j.1469-8137.2004.01059.x

Beck, P.S.A., Atzberger, C., Høgda, K.A., Johansen, B., Skidmore, A.K., 2006. Improved monitoring of vegetation dynamics at very high latitudes: A new method using MODIS NDVI. Remote Sens. Environ. 100, 321–334. https://doi.org/10.1016/j.rse.2005.10.021

Bengtsson, J., Bullock, J.M., Egoh, B., Everson, C., Everson, T., O’Connor, T., O’Farrell, P.J., Smith, H.G., Lindborg, R., 2019. Grasslands—more important for ecosystem services than you might think. Ecosphere 10, 1–20. https://doi.org/10.1002/ecs2.2582

Camps-Valls, G., Campos-Taberner, M., Moreno-Martínez, Á., Walther, S., Duveiller, G., Cescatti, A., Mahecha, M.D., Muñoz-Marí, J., García-Haro, F.J., Guanter, L., Jung, M., Gamon, J.A., Reichstein, M., Running, S.W., 2021. A unified vegetation index for quantifying the terrestrial biosphere. Sci. Adv. 7, 1–10. https://doi.org/10.1126/sciadv.abc7447

Castillioni, K., Newman, G.S., Souza, L., Iler, A.M., 2022. Effects of drought on grassland phenology depend on functional types. New Phytol. 236, 1558–1571. https://doi.org/10.1111/nph.18462

Cleland, E.E., Chiariello, N.R., Loarie, S.R., Mooney, H.A., Field, C.B., 2006. Diverse responses of phenology to global changes in a grassland ecosystem. Proc. Natl. Acad. Sci. U. S. A. 103, 13740–13744. https://doi.org/10.1073/pnas.0600815103

Cui, T., Martz, L., Lamb, E.G., Zhao, L., Guo, X., 2019. Comparison of Grassland Phenology Derived from MODIS Satellite and PhenoCam Near-Surface Remote Sensing in North America. Can. J. Remote Sens. 45, 707–722. https://doi.org/10.1080/07038992.2019.1674643

Dibari, C., Costafreda-Aumedes, S., Argenti, G., Bindi, M., Carotenuto, F., Moriondo, M., Padovan, G., Pardini, A., Staglianò, N., Vagnoli, C., Brilli, L., 2020. Expected changes to alpine pastures in extent and composition under future climate conditions. Agronomy 10, 1–21. https://doi.org/10.3390/agronomy10070926

Dibari, C., Pulina, A., Argenti, G., Aglietti, C., Bindi, M., Moriondo, M., Mula, L., Pasqui, M., Seddaiu, G., Roggero, P.P., 2021. Climate change impacts on the alpine, continental and mediterranean grassland systems of italy: A review. Ital. J. Agron. 16, 1843.

Dixon, D.J., Callow, J.N., Duncan, J.M.A., Setterfield, S.A., Pauli, N., 2021. Satellite prediction of forest flowering phenology. Remote Sens. Environ. 255, 112197. https://doi.org/10.1016/j.rse.2020.112197

Elmore, A.J., Guinn, S.M., Minsley, B.J., Richardson, A.D., 2012. Landscape controls on the timing of spring, autumn, and growing season length in mid-Atlantic forests. Glob. Chang. Biol. 18, 656–674. https://doi.org/10.1111/j.1365-2486.2011.02521.x

FAO, 2013. FAO Statistical Yearbook 2013. World food and Agriculture Food and Agriculture Organisation for the United Nations, Rome.

Filippa, G., Cremonese, E., Migliavacca, M., Galvagno, M., Forkel, M., Wingate, L., Tomelleri, E., Morra di Cella, U., Richardson, A.D., 2016. Phenopix: A R package for image-based vegetation phenology. Agric. For. Meteorol. 220, 141–150. https://doi.org/10.1016/j.agrformet.2016.01.006

Fu, Y.S.H., Campioli, M., Vitasse, Y., De Boeck, H.J., Van Den Berge, J., AbdElgawad, H., Asard, H., Piao, S., Deckmyn, G., Janssens, I.A., 2014. Variation in leaf flushing date influences autumnal senescence and next year's flushing date in two temperate tree species. Proc. Natl. Acad. Sci. U. S. A. 111, 7355–7360. https://doi.org/10.1073/pnas.1321727111

Gallinat, A.S., Primack, R.B., Wagner, D.L., 2015. Autumn, the neglected season in climate change research. Trends Ecol. Evol. 30, 169–176. https://doi.org/10.1016/j.tree.2015.01.004

Galvagno, M., Wohlfahrt, G., Cremonese, E., Rossini, M., Colombo, R., Filippa, G., Julitta, T., Manca, G., Siniscalco, C., Morra Di Cella, U., Migliavacca, M., 2013. Phenology and carbon dioxide source/sink strength of a subalpine grassland in response to an exceptionally short snow season. Environ. Res. Lett. 8. https://doi.org/10.1088/1748-9326/8/2/025008

Gitelson, A.A., Viña, A., Verma, S.B., Rundquist, D.C., Arkebauer, T.J., Keydan, G., Leavitt, B., Ciganda, V., Burba, G.G., Suyker, A.E., 2006. Relationship between gross primary production and chlorophyll content in crops: Implications for the synoptic monitoring of vegetation productivity. J. Geophys. Res. Atmos. 111, 1–13. https://doi.org/10.1029/2005JD006017

Gong, Z., Kawamura, K., Ishikawa, N., Goto, M., Wulan, T., Alateng, D., Yin, T., Ito, Y., 2015. MODIS normalized difference vegetation index (NDVI) and vegetation phenology dynamics in the Inner Mongolia grassland. Solid Earth 6, 1185–1194. https://doi.org/10.5194/se-6-1185-2015

Gonsamo, A., Chen, J.M., David, T.P., Kurz, W.A., Wu, C., 2012. Land surface phenology from optical satellite measurement and CO 2 eddy covariance technique. J. Geophys. Res. Biogeosciences 117, 1–18. https://doi.org/10.1029/2012JG002070

Grippa, M., Kergoat, L., Toan, T. Le, Mognard, N.M., Delbart, N., Hermitte, J.L., 2005. The impact of snow depth and snowmelt on the vegetation variability over central Siberia 32, 2–5. https://doi.org/10.1029/2005GL024286

Gu, L., Post, W., Baldocchi, D.D., Black, T., Suyker, A., Verma, S., Vesala, T., Wofsy, S., 2009. Characterizing the Seasonal Dynamics of Plant Community Photosynthesis Across a Range of Vegetation Types, in: Phenology of Ecosystem Processes. pp. 35–58.

Hao, R., Yu, D., Liu, Yupeng, Liu, Yang, Qiao, J., Wang, X., Du, J., 2017. Impacts of changes in

climate and landscape pattern on ecosystem services. Sci. Total Environ. 579, 718–728. https://doi.org/10.1016/j.scitotenv.2016.11.036

Hock, R., Rasul, G., Adler, C., Cáceres, B., Gruber, S., Hirabayashi, Y., Jackson, M., Kääb, A., Kang, S., Kutuzov, S., Milner, A., Molau, U., Morin, S., Orlove, B., Steltzer, H.I., 2019. Chapter 2: High Mountain Areas. IPCC Special Report on the Ocean and Cryosphere in a Changing Climate. IPCC Spec. Rep. Ocean Cryosph. a Chang. Clim. 131–202.

Hou, X., Gao, S., Niu, Z., Xu, Z., 2014. Extracting grassland vegetation phenology in North China based on cumulative SPOT-VEGETATION NDVI data. Int. J. Remote Sens. 35, 3316–3330. https://doi.org/10.1080/01431161.2014.903437

Hua, X., Sirguey, P., Ohlemüller, R., 2021. Recent trends in the timing of the growing season in New Zealand's natural and semi-natural grasslands. GIScience Remote Sens. 58, 1090–1111. https://doi.org/10.1080/15481603.2021.1969629

Imer, D., Merbold, L., Eugster, W., Buchmann, N., 2013. Temporal and spatial variations of soil CO2, CH4 and N2O fluxes at three differently managed grasslands. Biogeosciences 10, 5931–5945. https://doi.org/10.5194/bg-10-5931-2013

IPCC, 2014. Climate Change 2014: Synthesis Report. Contribution of Working Groups I, II and III to the Fifth Assessment Report of the Intergovernmental Panel on Climate Change.

Jerome, D.K., Petry, W.K., Mooney, K.A., Iler, A.M., 2021. Snow melt timing acts independently and in conjunction with temperature accumulation to drive subalpine plant phenology 5054–5069. https://doi.org/10.1111/gcb.15803

Jin, H., Eklundh, L., 2014. A physically based vegetation index for improved monitoring of plant phenology. Remote Sens. Environ. 152, 512–525. https://doi.org/10.1016/j.rse.2014.07.010

Jin, H., Jönsson, A.M., Bolmgren, K., Langvall, O., Eklundh, L., 2017. Disentangling remotely-sensed plant phenology and snow seasonality at northern Europe using MODIS and the plant phenology index. Remote Sens. Environ. 198, 203–212. https://doi.org/10.1016/j.rse.2017.06.015

Julitta, T., Cremonese, E., Migliavacca, M., Colombo, R., Galvagno, M., Siniscalco, C., Rossini, M., Fava, F., Cogliati, S., Morra di Cella, U., Menzel, A., 2014. Using digital camera images to analyse snowmelt and phenology of a subalpine grassland. Agric. For. Meteorol. 198–199, 116–125. https://doi.org/10.1016/j.agrformet.2014.08.007

Klein, G., 2018. Unchanged risk of frost exposure for subalpine and alpine plants after snowmelt in Switzerland despite climate warming 1755–1762.

Kline, M., 1998. Calculus: An Intuitive and Physical Approach (Google eBook), (Second Ed. ed. Dover Publications.

Klosterman, S.T., Hufkens, K., Gray, J.M., Melaas, E., Sonnentag, O., Lavine, I., Mitchell, L., Norman, R., Friedl, M.A., Richardson, A.D., 2014. Evaluating remote sensing of deciduous forest phenology at multiple spatial scales using PhenoCam imagery. Biogeosciences 11, 4305–4320. https://doi.org/10.5194/bg-11-4305-2014

Körner, C., 2021. Life under and in snow: protection and limitation, Alpine Plant Life. https://doi.org/10.1007/978-3-030-59538-8_5

Lara, B., Gandini, M., 2016. Assessing the performance of smoothing functions to estimate land surface phenology on temperate grassland. Int. J. Remote Sens. 37, 1801–1813. https://doi.org/10.1080/2150704X.2016.1168945

Li, X., Guo, W., Li, S., Zhang, J., Ni, X., 2021. The different impacts of the daytime and nighttime land surface temperatures on the alpine grassland phenology. Ecosphere 12. https://doi.org/10.1002/ecs2.3578

Lieth, H., 1974. Phenology and Seasonality Modelling. Springer-Verlag, New York.

Liu, Y., Hill, M.J., Zhang, X., Wang, Z., Richardson, A.D., Hufkens, K., Filippa, G., Baldocchi, D.D., Ma, S., Verfaillie, J., Schaaf, C.B., 2017. Using data from Landsat, MODIS, VIIRS and PhenoCams to monitor the phenology of California oak/grass savanna and open grassland across spatial scales. Agric. For. Meteorol. 237–238, 311–325. https://doi.org/10.1016/j.agrformet.2017.02.026

Marcolla, B., Cescatti, A., Manca, G., Zorer, R., Cavagna, M., Fiora, A., Gianelle, D., Rodeghiero, M., Sottocornola, M., Zampedri, R., 2011. Climatic controls and ecosystem responses drive the inter-annual variability of the net ecosystem exchange of an alpine meadow. Agric. For. Meteorol. 151, 1233–1243. https://doi.org/10.1016/j.agrformet.2011.04.015

Medlyn, B.E., 1998. Physiological basis of the light use efficiency model. Tree Physiol. 18, 167–176. https://doi.org/10.1093/treephys/18.3.167

Menzel, A., Yuan, Y., Matiu, M., Sparks, T., Scheifinger, H., Gehrig, R., Estrella, N., 2020. Climate change fingerprints in recent European plant phenology 2599–2612. https://doi.org/10.1111/gcb.15000

Merbold, L., Eugster, W., Stieger, J., Zahniser, M., Nelson, D., Buchmann, N., 2014. Greenhouse gas budget (CO2, CH4 and N2O) of intensively managed grassland following restoration. Glob. Chang. Biol. 20, 1913–1928. https://doi.org/10.1111/gcb.12518

Migliavacca, M., Galvagno, M., Cremonese, E., Rossini, M., Meroni, M., Sonnentag, O., Cogliati, S., Manca, G., Diotri, F., Busetto, L., Cescatti, A., Colombo, R., Fava, F., Morra di Cella, U., Pari, E., Siniscalco, C., Richardson, A.D., 2011. Using digital repeat photography and eddy covariance data to model grassland phenology and photosynthetic CO2 uptake. Agric. For. Meteorol. 151, 1325–1337. https://doi.org/10.1016/j.agrformet.2011.05.012

Mutanga, O., Shoko, C., 2018. Monitoring the spatio-temporal variations of C3/C4 grass species using multispectral satellite data. Int. Geosci. Remote Sens. Symp. 2018-July, 8988–8991. https://doi.org/10.1109/IGARSS.2018.8517685

Ni, J., 2002. Carbon storage in grasslands of China. J. Arid Environ. 50, 205–218. https://doi.org/10.1006/jare.2001.0902

Pastorello, G., Trotta, C., Canfora, E., Chu, H., Christianson, D., Cheah, Y.W., Poindexter, C., Chen, J., Elbashandy, A., Humphrey, M., Isaac, P., Polidori, D., Ribeca, A., van Ingen, C., Zhang, L., Amiro, B., Ammann, C., Arain, M.A., Ardö, J., Arkebauer, T., Arndt, S.K., Arriga, N., Aubinet, M., Aurela, M., Baldocchi, D., Barr, A., Beamesderfer, E., Marchesini, L.B., Bergeron, O., Beringer, J., Bernhofer, C., Berveiller, D., Billesbach, D., Black, T.A., Blanken, P.D., Bohrer, G., Boike, J., Bolstad, P. V., Bonal, D., Bonnefond, J.M., Bowling, D.R., Bracho, R., Brodeur, J., Brümmer, C., Buchmann, N., Burban, B., Burns, S.P., Buysse, P.,

Cale, P., Cavagna, M., Cellier, P., Chen, S., Chini, I., Christensen, T.R., Cleverly, J., Collalti, A., Consalvo, C., Cook, B.D., Cook, D., Coursolle, C., Cremonese, E., Curtis, P.S., D'Andrea, E., da Rocha, H., Dai, X., Davis, K.J., De Cinti, B., de Grandcourt, A., De Ligne, A., De Oliveira, R.C., Delpierre, N., Desai, A.R., Di Bella, C.M., di Tommasi, P., Dolman, H., Domingo, F., Dong, G., Dore, S., Duce, P., Dufrêne, E., Dunn, A., Dušek, J., Eamus, D., Eichelmann, U., ElKhidir, H.A.M., Eugster, W., Ewenz, C.M., Ewers, B., Famulari, D., Fares, S., Feigenwinter, I., Feitz, A., Fensholt, R., Filippa, G., Fischer, M., Frank, J., Galvagno, M., Gharun, M., Gianelle, D., Gielen, B., Gioli, B., Gitelson, A., Goded, I., Goeckede, M., Goldstein, A.H., Gough, C.M., Goulden, M.L., Graf, A., Griebel, A., Gruening, C., Grünwald, T., Hammerle, A., Han, S., Han, X., Hansen, B.U., Hanson, C., Hatakka, J., He, Y., Hehn, M., Heinesch, B., Hinko-Najera, N., Hörtnagl, L., Hutley, L., Ibrom, A., Ikawa, H., Jackowicz-Korczynski, M., Janouš, D., Jans, W., Jassal, R., Jiang, S., Kato, T., Khomik, M., Klatt, J., Knohl, A., Knox, S., Kobayashi, H., Koerber, G., Kolle, O., Kosugi, Y., Kotani, A., Kowalski, A., Kruijt, B., Kurbatova, J., Kutsch, W.L., Kwon, H., Launiainen, S., Laurila, T., Law, B., Leuning, R., Li, Yingnian, Liddell, M., Limousin, J.M., Lion, M., Liska, A.J., Lohila, A., López-Ballesteros, A., López-Blanco, E., Loubet, B., Loustau, D., Lucas-Moffat, A., Lüers, J., Ma, S., Macfarlane, C., Magliulo, V., Maier, R., Mammarella, I., Manca, G., Marcolla, B., Margolis, H.A., Marras, S., Massman, W., Mastepanov, M., Matamala, R., Matthes, J.H., Mazzenga, F., McCaughey, H., McHugh, I., McMillan, A.M.S., Merbold, L., Meyer, W., Meyers, T., Miller, S.D., Minerbi, S., Moderow, U., Monson, R.K., Montagnani, L., Moore, C.E., Moors, E., Moreaux, V., Moureaux, C., Munger, J.W., Nakai, T., Neirynck, J., Nesic, Z., Nicolini, G., Noormets, A., Northwood, M., Nosetto, M., Nouvellon, Y., Novick, K., Oechel, W., Olesen, J.E., Ourcival, J.M., Papuga, S.A., Parmentier, F.J., Paul-Limoges, E., Pavelka, M., Peichl, M., Pendall, E., Phillips, R.P., Pilegaard, K., Pirk, N., Posse, G., Powell, T., Prasse, H., Prober, S.M., Rambal, S., Rannik, Ü., Raz-Yaseef, N., Reed, D., de Dios, V.R., Restrepo-Coupe, N., Reverter, B.R., Roland, M., Sabbatini, S., Sachs, T., Saleska, S.R., Sánchez-Cañete, E.P., Sanchez-Mejia, Z.M., Schmid, H.P., Schmidt, M., Schneider, K., Schrader, F., Schroder, I., Scott, R.L., Sedlák, P., Serrano-Ortíz, P., Shao, C., Shi, P., Shironya, I., Siebicke, L., Šigut, L., Silberstein, R., Sirca, C., Spano, D., Steinbrecher, R., Stevens, R.M., Sturtevant, C., Suyker, A., Tagesson, T., Takanashi, S., Tang, Y., Tapper, N., Thom, J., Tiedemann, F., Tomassucci, M., Tuovinen, J.P., Urbanski, S., Valentini, R., van der Molen, M., van Gorsel, E., van Huissteden, K., Varlagin, A., Verfaillie, J., Vesala, T., Vincke, C., Vitale, D., Vygodskaya, N., Walker, J.P., Walter-Shea, E., Wang, H., Weber, R., Westermann, S., Wille, C., Wofsy, S., Wohlfahrt, G., Wolf, S., Woodgate, W., Li, Yuelin, Zampedri, R., Zhang, J., Zhou, G., Zona, D., Agarwal, D., Biraud, S., Torn, M., Papale, D., 2020. The FLUXNET2015 dataset and the ONEFlux processing pipeline for eddy covariance data. Sci. data 7, 225. https://doi.org/10.1038/s41597-020-0534-3

Peng, D., Wang, Y., Xian, G., Huete, A.R., Huang, W., Shen, M., Wang, F., Yu, L., Liu, Liangyun, Xie, Q., Liu, Lingling, Zhang, X., 2021. Investigation of land surface phenology detections in shrublands using multiple scale satellite data. Remote Sens. Environ. 252. https://doi.org/10.1016/j.rse.2020.112133

Peng, D., Zhang, X., Wu, C., Huang, W., Gonsamo, A., Huete, A.R., Didan, K., Tan, B., Liu, X., Zhang, B., 2017. Intercomparison and evaluation of spring phenology products using National Phenology Network and AmeriFlux observations in the contiguous United States. Agric. For. Meteorol. 242, 33–46. https://doi.org/10.1016/j.agrformet.2017.04.009

Ponzetta, M.P., Cervasio, F., Crocetti, C., Messeri, A., Argenti, G., 2010. Habitat improvements with wildlife purposes in a grazed area on the Apennine Mountains. Ital. J. Agron. 5, 233–238. https://doi.org/10.4081/ija.2010.233

Post, H., Hendricks Franssen, H.J., Graf, A., Schmidt, M., Vereecken, H., 2015. Uncertainty analysis of eddy covariance CO2 flux measurements for different EC tower distances using an extended two-tower approach. Biogeosciences 12, 1205–1221. https://doi.org/10.5194/bg-12-1205-2015

Prescher, A.K., Grünwald, T., Bernhofer, C., 2010. Land use regulates carbon budgets in eastern Germany: From NEE to NBP. Agric. For. Meteorol. 150, 1016–1025. https://doi.org/10.1016/j.agrformet.2010.03.008

Ren, S., Li, Y., Peichl, M., 2020. Diverse effects of climate at different times on grassland phenology in mid-latitude of the Northern Hemisphere. Ecol. Indic. 113. https://doi.org/10.1016/j.ecolind.2020.106260

Ren, S., Vitasse, Y., Chen, X., Peichl, M., An, S., 2022. Assessing the relative importance of sunshine, temperature, precipitation, and spring phenology in regulating leaf senescence timing of herbaceous species in China. Agric. For. Meteorol. 313, 108770. https://doi.org/10.1016/j.agrformet.2021.108770

Richardson, A.D., Keenan, T.F., Migliavacca, M., Ryu, Y., Sonnentag, O., Toomey, M., 2013. Climate change, phenology, and phenological control of vegetation feedbacks to the climate system. Agric. For. Meteorol. 169, 156–173. https://doi.org/10.1016/j.agrformet.2012.09.012

Running, S.W., Nemani, R.R., Heinsch, F.A., Zhao, M., Reeves, M., Hashimoto, H., 2004. A continuous satellite-derived measure of global terrestrial primary production. Bioscience 54, 547–560. https://doi.org/10.1641/0006-3568(2004)054[0547:ACSMOG]2.0.CO;2

Sadras, V.O., Moran, M.A., 2013. Agricultural and Forest Meteorology Nonlinear effects of elevated temperature on grapevine phenology. Agric. For. Meteorol. 173, 107–115. https://doi.org/10.1016/j.agrformet.2012.10.003

Singh, R.K., Svystun, T., AlDahmash, B., Jönsson, A.M., Bhalerao, R.P., 2017. Photoperiod- and temperature-mediated control of phenology in trees – a molecular perspective. New Phytol. 213, 511–524. https://doi.org/10.1111/nph.14346

Sonobe, R., Yamaya, Y. classification from S.-2-derived vegetation indices using ensemble learningki, Tani, H., Wang, X., Kobayashi, N., Mochizuki, K., 2018. Crop classification from Sentinel-2-derived vegetation indices using ensemble learning. J. Appl. Remote Sens. 12, 1. https://doi.org/10.1117/1.jrs.12.026019

Sparks, T., Menzel, A., 2013. Plant Phenology Changes and Climate Change, in: Encyclopedia of Biodiversity. Academic Press, pp. 103–108. https://doi.org/10.1016/B978-0-12-384719-5.00229-X

Stöckli, R., Vidale, P.L., 2004. European plant phenology and climate as seen in a 20-year AVHRR land-surface parameter dataset. Int. J. Remote Sens. 25, 3303–3330. https://doi.org/10.1080/01431160310001618149

Templ, B., Koch, E., Bolmgren, K., Ungersböck, M., Paul, A., Scheifinger, H., Rutishauser, T., Busto, M., Chmielewski, F.M., Hájková, L., Hodzić, S., Kaspar, F., Pietragalla, B., Romero-Fresneda, R., Tolvanen, A., Vučetič, V., Zimmermann, K., Zust, A., 2018. Pan European Phenological database (PEP725): a single point of access for European data. Int. J. Biometeorol. 62, 1109–1113. https://doi.org/10.1007/s00484-018-1512-8

Tian, F., Cai, Z., Jin, H., Hufkens, K., Scheifinger, H., Tagesson, T., Smets, B., Van Hoolst, R., Bonte, K., Ivits, E., Tong, X., Ardö, J., Eklundh, L., 2021. Calibrating vegetation phenology from Sentinel-2 using eddy covariance, PhenoCam, and PEP725 networks across Europe. Remote Sens. Environ. 260. https://doi.org/10.1016/j.rse.2021.112456

Vitasse, Y., Ursenbacher, S., Klein, G., Bohnenstengel, T., Chittaro, Y., Delestrade, A., Monnerat, C., Rebetez, M., Rixen, C., Strebel, N., Schmidt, B.R., Wipf, S., Wohlgemuth, T., Yoccoz, N.G., Lenoir, J., 2021. Phenological and elevational shifts of plants , animals and fungi under climate change in the European Alps 41, 1816–1835. https://doi.org/10.1111/brv.12727

Vorkauf, M., Kahmen, A., Körner, C., Hiltbrunner, E., 2021. Flowering phenology in alpine grassland strongly responds to shifts in snowmelt but weakly to summer drought. Alp. Bot. 131, 73–88. https://doi.org/10.1007/s00035-021-00252-z

Wang, J., Wu, C., Zhang, C., Ju, W., Wang, X., Chen, Z., Fang, B., 2018. Improved modelling of gross primary productivity (GPP) by better representation of plant phenological indicators from remote sensing using a process model. Ecol. Indic. 88, 332–340. https://doi.org/10.1016/j.ecolind.2018.01.042

Watson, C.J., Restrepo-Coupe, N., Huete, A.R., 2019. Multi-scale phenology of temperate grasslands: Improving monitoring and management with near-surface phenocams. Front. Environ. Sci. 7, 1–18. https://doi.org/10.3389/fenvs.2019.00014

Weil, G., Lensky, I.M., Levin, N., 2017. Using ground observations of a digital camera in the VIS-NIR range for quantifying the phenology of Mediterranean woody species. Int. J. Appl. Earth Obs. Geoinf. 62, 88–101. https://doi.org/10.1016/j.jag.2017.05.016

Weisberg, P.J., Dilts, T.E., Greenberg, J.A., Johnson, K.N., Pai, H., Sladek, C., Kratt, C., Tyler, S.W., Ready, A., 2021. Phenology-based classification of invasive annual grasses to the species level. Remote Sens. Environ. 263, 112568. https://doi.org/10.1016/j.rse.2021.112568

White, M.A., de Beurs, K.M., Didan, K., Inouye, D.W., Richardson, A.D., Jensen, O.P., O'Keefe, J., Zhang, G., Nemani, R.R., van Leeuwen, W.J.D., Brown, J.F., de Wit, A., Schaepman, M., Lin, X., Dettinger, M., Bailey, A.S., Kimball, J., Schwartz, M.D., Baldocchi, D.D., Lee, J.T., Lauenroth, W.K., 2009. Intercomparison, interpretation, and assessment of spring phenology in North America estimated from remote sensing for 1982-2006. Glob. Chang. Biol. 15, 2335–2359. https://doi.org/10.1111/j.1365-2486.2009.01910.x

Wohlfahrt, G., Hammerle, A., Haslwanter, A., Bahn, M., Tappeiner, U., Cernusca, A., 2008. Seasonal and inter-annual variability of the net ecosystem CO2 exchange of a temperate mountain grassland: Effects of weather and management. J. Geophys. Res. Atmos. 113, 1–14. https://doi.org/10.1029/2007JD009286

Wu, C., Peng, D., Soudani, K., Siebicke, L., Gough, C.M., Arain, M.A., Bohrer, G., Lafleur, P.M., Peichl, M., Gonsamo, A., Xu, S., Fang, B., Ge, Q., 2017. Land surface phenology derived from normalized difference vegetation index (NDVI) at global FLUXNET sites. Agric. For. Meteorol. 233, 171–182. https://doi.org/10.1016/j.agrformet.2016.11.193

Xie, J., Hüsler, F., Jong, R. De, Chimani, B., Asam, S., 2021. Spring Temperature and Snow Cover Climatology Drive the Advanced Springtime Phenology (1991 – 2014) in the European Alps Journal of Geophysical Research : Biogeosciences. https://doi.org/10.1029/2020JG006150

Xu, H., Twine, T.E., Yang, X., 2014. Evaluating remotely sensed phenological metrics in a dynamic ecosystem model. Remote Sens. 6, 4660–4686. https://doi.org/10.3390/rs6064660

Xu, L., Zhang, X., Wang, Y., Fu, Y., Yan, H., Qian, S., Cheng, L., 2021. Drivers of phenology shifts and their effect on productivity in northern grassland of China during 1984–2017—evidence from long-term observational data. Int. J. Biometeorol. 65, 527–539. https://doi.org/10.1007/s00484-020-02046-0

Xu, X., Zhou, G., Du, H., Mao, F., Xu, L., Li, X., Liu, L., 2020. Combined MODIS land surface temperature and greenness data for modelling vegetation phenology, physiology, and gross primary production in terrestrial ecosystems. Sci. Total Environ. 726, 137948. https://doi.org/10.1016/j.scitotenv.2020.137948

Zhang, Q., Cheng, Y. Ben, Lyapustin, A.I., Wang, Y., Xiao, X., Suyker, A., Verma, S., Tan, B., Middleton, E.M., 2014. Estimation of crop gross primary production (GPP): I. impact of MODIS observation footprint and impact of vegetation BRDF characteristics. Agric. For. Meteorol. 191, 51–63. https://doi.org/10.1016/j.agrformet.2014.02.002

Zhang, X., Jayavelu, S., Liu, L., Friedl, M.A., Henebry, M., Liu, Y., Schaaf, C.B., Richardson, A.D., Gray, J., 2018. Agricultural and Forest Meteorology Evaluation of land surface phenology from VIIRS data using time series of PhenoCam imagery 257, 137–149. https://doi.org/10.1016/j.agrformet.2018.03.003

Zheng, Z., Zhu, W., 2017. Uncertainty of remote sensing data in monitoring vegetation phenology: A comparison of MODIS C5 and C6 vegetation index products on the Tibetan Plateau. Remote Sens. 9. https://doi.org/10.3390/rs9121288

Chapter 5.

Opportunities for adaptation to climate change of extensively grazed pastures in the Central Apennines (Italy)

Chapter 5 has been based on the study:
Bellini, E., Martin R., Argenti G., Staglianò N., Dibari C., Moriondo M. and Bellocchi G. 2023. Opportunities for adaptation to climate change of extensively grazed pastures in the Central Apennines (Italy). (*Published*) *Land*.

PhD candidate's contribution:

Edoardo Bellini developed the model for simulating grass growth with the collaboration of Moriondo M. He collected on-field data with co-authors, produced the results and wrote the sections of the chapter under the supervision of the other co-authors.

5. Opportunities for adaptation to climate change of extensively grazed pastures in the Central Apennines (Italy)

Edoardo Bellini [1], Raphael Martin [2], Giovanni Argenti [1,*], Nicolina Staglianò [1], Sergi Costafreda-Aumedes [3], Camilla Dibari [1], Marco Moriondo [3], Gianni Bellocchi [2]

[1] Department of Agriculture, Food, Environment and Forestry (DAGRI), University of Florence, 50144 Florence, Italy. edoardo.bellini@unifi.it (E.B.), nicolina.stagliano@unifi.it (N.S.), camilla.dibari@unifi.it (C.D.)
[2] Université Clermont Auvergne, INRAE, VetAgro Sup, UREP, 63000 Clermont-Ferrand, France. raphael.martin@inrae.fr (R.M.), gianni.bellocchi@inrae.fr (G.B.)
[3] Institute of BioEconomy, Italian National Research Council (IBE-CNR), 50019 Sesto Fiorentino, Italy. sergi.costafreda@ibe.cnr.it (S.C.), marco.moriondo@cnr.it (M.M.)
***** Correspondence: giovanni.argenti@unifi.it (G.A.); 055 2755747

Abstract: Future climate change is expected to significantly alter the growth of vegetation in grassland systems, in terms of length of the growing season, forage production and climate-altering gas emissions. The main objective of this work was therefore to simulate the future impacts of foreseen climate change in the context of two pastoral systems in the central Italian Apennines and test different adaptation strategies to cope with these changes. The PaSim simulation model was therefore used for this purpose. After calibration by comparison with observed data of aboveground biomass (AGB) and leaf area index (LAI), the model was able to produce different future outputs, such as length of growing season, AGB, greenhouse gas (GHG) emissions for two time-windows (i.e. 2011-2040 and 2041-2070) using 14 global climate models (GCMs) for the generation of future climate data, according to RCP (Representative Concentration Pathways) 4.5 and 8.5 scenarios under business as usual management (BaU). As a result of increasing temperatures, the fertilizing effect of CO2 and a similar trend in water content between present and future, simulations showed a lengthening of the season (i.e. mean increase: +8.5 and 14 days under RCP4.5 and 8.5 for the period 2011-2040, +19 and 31.5 days under RCP4.5 and 8.5 for the period 2041-2070) and a rise in forage production (i.e. mean biomass peak increase of the two test sites under BaU: +53.7% and 62.75% for RCP 4.5. and 8.5 in the 2011-2040 period, +115.3% and 176.9% in RCP4.5 RCP8.5 in 2041-2070). Subsequently, three different alternative management strategies were tested: a 20% rise in animal stocking rate (+20 GI), a 15% increase in grazing length (+15 GL) and a combination of these two management factors (+20 GI×15 GL). Simulation results on alternative management strategies suggest that the favorable conditions for forage production could support the increase in animal stocking rate and grazing length of alternative management strategies (i.e. +20 GI, +15 GL, +20 GI×15 GL). Under future projections Net Ecosystem Exchange (NEE) and nitrogen oxide (N2O) emissions decreased, whereas methane (CH4) rose. The simulated GHG future changes varied in magnitude according to the different adaptation strategies tested. The development and assessment

of adaptation strategies for extensive pastures of the Central Apennines provide a basis for appropriate agricultural policy and optimal land management in response to the ongoing climate change.

Keywords: grasslands, modelling, PaSim, climatic scenarios, aboveground biomass

---

1. Introduction

With an herbage production potential up to ~ 15 t DM ha^{-1} (Dillon, 2018), grasslands contribute significantly to global food security by providing fodder for ruminants used in the production of protein-rich foods, such as meat and milk (Barbour et al., 2022; Mara, 2012). In Italy, grassland areas (i.e., permanent meadows and pastures) cover approximately 3.6 Mha (ISTAT, 2022), roughly 12% of the entire Italian territory, and are located mainly along the Alpine and Apennine mountain ranges and on the islands (Burrascano et al., 2010). Differing in climate and land use, factors that influence productivity and botanical composition, Italian grasslands can be divided into three different biogeographic regions: Alpine, Apennine, and Mediterranean (Dibari et al., 2021). They are mostly large-scale rainfed pastoral systems, with permanent pastures dominant in the mountains and hilly areas and fodder crops also dominant in the Mediterranean region. Generally, these systems provide forage for only short periods of time during spring and summer, exhibiting great inter-annual variability in production (Argenti et al., 2011; Cavallero et al., 2007). With regard to mountain areas (i.e., Alps and Apennines), grasslands are often located in areas with nutrient-poor soils and/or extreme climate conditions that make vegetation growth, and consequently forage production, reliant on seasonal dynamics (Orlandi et al., 2016). Focusing specifically on Apennine mountain pastures, forage quality is generally lower than in Alpine pasturelands (Targetti et al., 2013), due mainly to the great variability in pedo-climatic conditions that can be found along the latitudinal gradient of Italy (Metzger et al., 2005).

In addition to forage production, grasslands provide several other ecosystem services important for human well-being, such as water and nutrient regulation and protection from soil erosion (Bengtsson et al., 2019; Hao et al., 2017; Ponzetta et al., 2010; Tamburini et al., 2022; Wepking et al., 2022). Particularly important is the role that these systems can play in climate-changing emissions (Renáta Sándor et al., 2018), as they can stock/emit carbon dioxide CO_2 (Oates and Jackson, 2014; Smith et al., 2008) and emit non-CO_2 greenhouse gases, such as methane (CH_4) and nitrous oxide (N_2O) (Franzluebbers, 2020). According to Guillaume et al. (2022), soil organic C stock measured from surface to 50 cm depth in permanent grasslands is approximately 7 kg C m^{-2}, and evidence from European grasslands shows that soil C sequestration rates can reach 0.77 g C m^{-2} yr^{-1} (Soussana et

al., 2007). Compared with other ecosystems, grasslands are, in fact, an important store of C (Dass et al., 2018), and management (grazing in particular) is an important regulator of C and N fluxes (Steinfeld and Wassenaar, 2007). Grasslands have the advantage of potentially acting as C and N sinks, compared with croplands, and can mitigate GHG emissions in livestock production systems, as C and N sequestration can offset GHG emission (Barthel et al., 2018; Sándor et al., 2018, Soussana et al., 2007)

Pastoral resources in the Apennines during the last decades have shown fragility in the face of changes induced by recent global warming. There was a shift in air temperature distribution towards warmer values in all seasons (especially for minimum temperature, while maximum temperature shows a more intense warming and a pronounced peak in summer) since the 1980s, with an acceleration in the 2000s (Toreti and Desiato, 2008), and it is projected to increase in the future (Tomozeiu et al., 2018). In view of the expected increase in temperatures associated with a decrease in precipitation during the summer period, forage production is assumed to change in terms of quantity and quality (Chelli et al., 2017; Scocco et al., 2016). Moreover, evolution of the distribution of species in herbaceous communities and changes in the botanical composition of semi-natural grasslands are highlighted (Petriccione and Bricca, 2019). In fact, rising temperatures and summer droughts tend to promote the predominance of thermophilic communities or species more adapted to xeric environments, which now grow in environments at lower altitudes, as was already observed in the Alps (Dibari et al., 2020) and Apennines (Alberto Evangelista et al., 2016; Stanisci et al., 2016).

In this view, simulation models, through the reproduction of system biophysical processes, can help stakeholders in decision-making by assessing the impacts of climate change and/or testing different management strategies under current (Bebeley et al., 2022; Kamilaris et al., 2020) or future scenarios (Fullman et al., 2017; Kalaugher et al., 2017; L. Ma et al., 2019; Moore and Ghahramani, 2014; Snow et al., 2014). In this context, appropriate management (e.g., stocking rate and grazing period) can preserve grassland biodiversity, maintain socio-ecological systems, and counteract the effects of climate change. On the basis of assessment of the previous literature, it can be said that a very small number of modelling exercises have examined the effect of foreseen climate changes on pasture production characteristics in the Apennine area (Dibari et al., 2021), as almost all works have analyzed the effects on vegetation features and biodiversity (e.g., Dibari et al., 2015; Ferrarini et al., 2017; Frate et al., 2018). Therefore, the present research aims to analyze the expected effect of climatic changes mainly from an agronomic perspective, providing an approach that can be repeated in other contexts and that is aimed at evaluating the impacts on productive features of forage resources and the possible adaptation strategies of some of the main pasture management characteristics .

This perspective forms the basis for the design and implementation of this study initiated in 2020 on two pastoral farms in the Apennines territory of central Italy, based on field observations and model-based simulations. Modelling the performance of pastoral systems is helpful in defining management strategies that maximize pastoral production and minimize environmental impacts (Vigan et al., 2017). Field data support the modelling exercises by providing detailed on-farm information on the spatial and temporal variation of important canopy state variables, which are often difficult to obtain (Insua et al., 2019b). Simulation results under future climate change scenarios were the key tools for the design and assessment of the analytical framework concerning climate change adaptation strategies, pivotal factors for the conservation of grassland resources (Gao et al., 2014). Based on the hypothesis that future climate change will significantly affect extensive grazing systems of the Central Apennines, the specific objectives of this study were: (1) to inform the modelling via calibration with field data; (2) to use the calibrated models to project the impacts of climate change; and (3) to assess a set of adaptation options for pastoral management identified locally.

2. Materials and Methods

The study was initially conducted by calibrating the grassland simulation model PaSim (Riedo et al., 1998) with observed data collected on two specific farms in the Italian Apennines (Suite 1). The parameterization obtained was subsequently used, together with the climate models, to simulate the impacts of climate change on grasslands (Suite 2). In parallel, a sensitivity analysis was performed with specific attention to biomass production (Suite 3). Finally, on the basis of the results obtained in the impact analysis, possible adaptation strategies were identified and tested (Suite 4). A general outline of the methodology used can be seen in Figure 1.

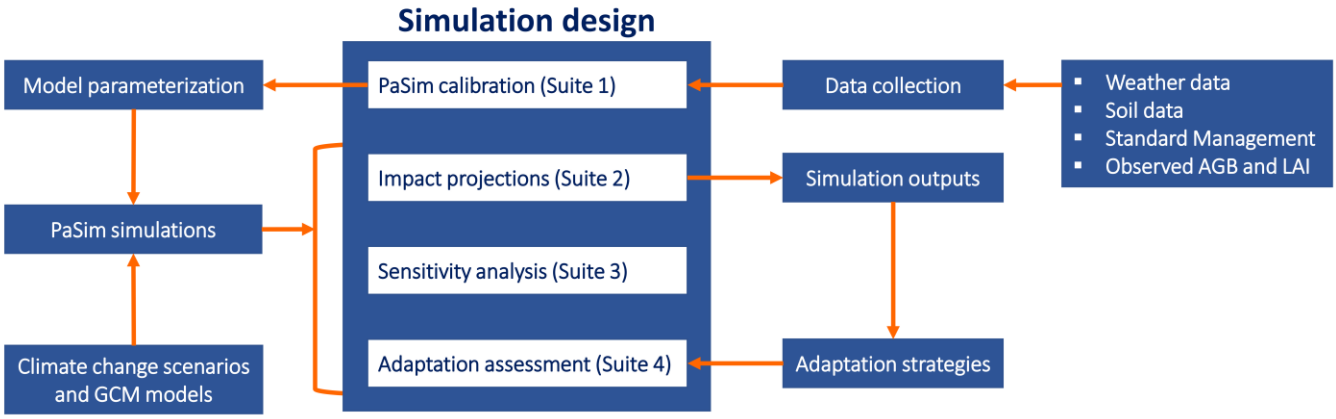

Figure 1. Workflow of the methodology applied in this study. PaSim is the grassland simulation model used for the analysis.

2.1. Study Sites, Experimental Layout, and Data Collection

The study considered two pastoral farms (Figure 2) located at different altitudes in the Tuscan Apennines (Table 1), both managed under continuous grazing system of Limousin cattle (Table 2).

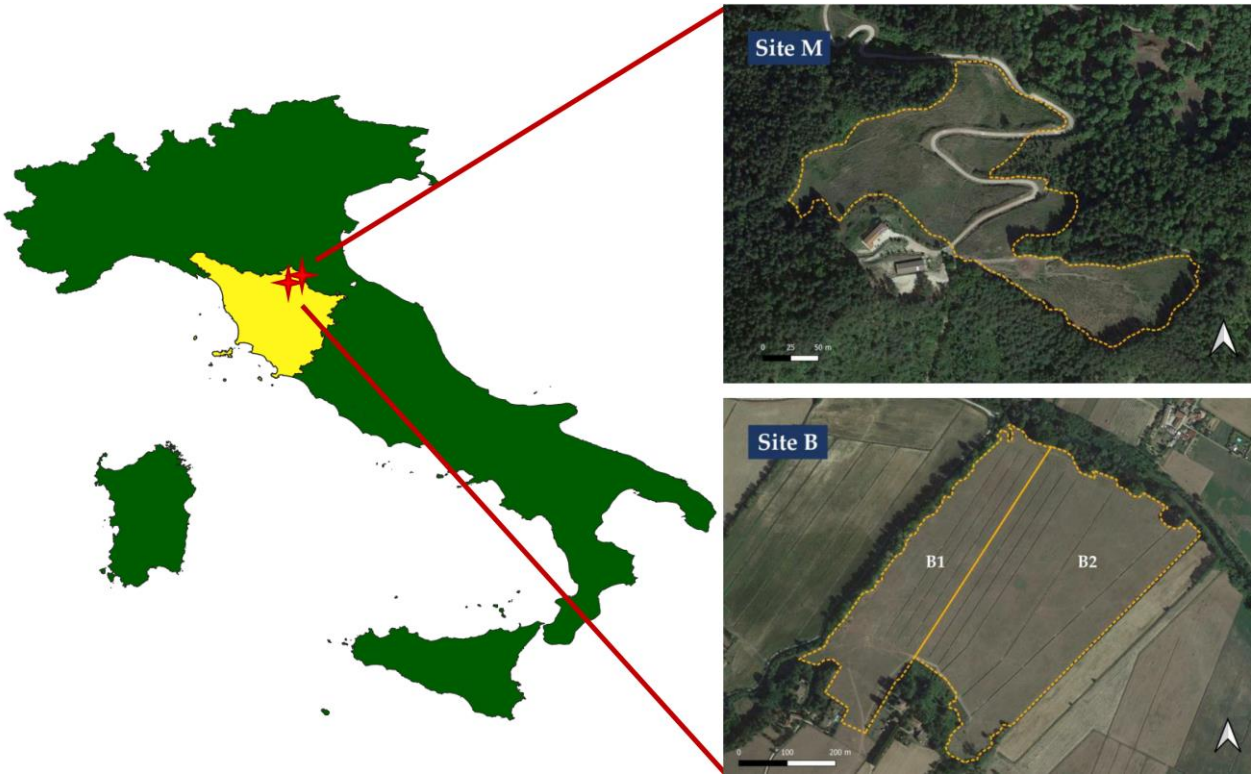

Figure 2. Aerial view of the study sites of Marradi (M, left) and Borgo San Lorenzo (B, right). Satellite images of the sites were obtained from Google Earth.

The Marradi study site (M) covers more than 5 ha of upland sown pasture that tends towards a re-naturalization, usually grazed from May to July. The Borgo San Lorenzo study site (B) covers 30 ha of lowland sown pasture. For the purpose of the trial, Site B was divided in 2020 into two differently managed sub-areas, B1 (approx. 10 ha) and B2 (approx. 20 ha). Specifically, in sub-area B1 the pasture was grazed by Limousin cattle from April until the end of October, while sub-area B2 was managed under a mixed utilization: mowed in May and grazed from June until the end of October.

Table 1. Description of the study sites.

Description	Unit	Site M (Marradi)	Site B (Borgo San Lorenzo)
Location			
Latitude (WGS84)	degree N	44.08°	43.95°
Longitude (WGS84)	degree E	11.63°	11.35°
Elevation	m a.s.l.	600	200

Climate			
Mean annual temperature[1]	°C	12.4	13.4
Mean annual precipitation[2]	mm	1330	990
Soil[3]			
Depth	m	1	1
Clay	%	37	37
Silt	%	42	36
Sand	%	21	27
Total organic carbon	g kg^{-1}	33.6	23.5
Total nitrogen	g kg^{-1}	3.0	2.5
Soil pH	-	6.6	7.4
Bulk density	g cm^{-3}	1.29	1.44
Saturated soil water content	m^3 m^{-3}	0.52	0.51
Field capacity	m^3 m^{-3}	0.36	0.35
Wilting point	m^3 m^{-3}	0.21	0.21
Dominant vegetation	-	*Dactylis glomerata*, *Lolium* sp., *Festuca arundinacea*, *Phleum pratense*, and *Onobrychis viciifolia*, with other minor forbs and a large presence in some sectors of shrubs, such as *Rubus ulmifolius*.	*Lolium* sp., *Dactylis glomerata*, *Trifolium pratense*, *Trifolium repens*, *Lotus corniculatus*, and *Festuca arundinacea*, with other minor forbs.

[1] Site M: mean of 2016, 2017, and 2020; Site B: mean of 1951–2020.

[2] Site M: mean of 2001–2020; Site B: mean of 2001–2020.

Data collected from regional weather stations of Tuscany Region (SIR, Servizio Idrologico Regionale, https://www.sir.toscana.it/index.php). Distance from sites <10 km.

[3] 1 m soil profile mean.

Table 2. Management of the two study sites. Livestock Standard Unit (LSU) refers to a dairy cow producing 3,000 kg of milk per year, without additional concentrated feed (EC, 2008).

Management	**Unit**	**Site M (Marradi)**		**Site B (Borgo San Lorenzo)**			
				B1		**B2**	
		2020	**2021**	**2020**	**2021**	**2020**	**2021**
Surface	ha	5.4		10		20	10
Cut	day of year	-	-		-	125	-

Grazing period	days of year (start, end)	139–244[a]; 244–267[b]	135–176[a]; 176–276[b]	100–180[a]; 186–300[b]	100–145[a]; 145–306[b]	180–186[a]; 186–300[b]	110–145[a]; 145–306[b]
Stocking rate	LSU ha^{-1} d^{-1}	4.0[a]; 3.4[b]	3.3[a]; 2.0[b]	2.9[a]; 1.0[b]		1.5[a]; 1.0[b]	0.9; 1.2[b]

[a] and [b] represent two distinctive grazing periods during the season in terms of stocking rate.

Samples of aboveground dry matter (DM) biomass (AGB, kg DM m^{-2}) and measurements of leaf area index (LAI, m^2 m^{-2}) were collected during field surveys conducted in spring/summer (2020 and 2021) at both sites and used for the modelling work (Table S1). Field data were collected in 16 randomly arranged samples in an area of 1 m^2 each (eight in M, four in B1, and four in B2). The sampling position was changed from time to time, taking care to choose areas that represented the general situation. The AccuPAR PAR/LAI Ceptometer Model LP-80 (Decagon Devices, 2017) was used to measure LAI in each plot.

2.2. Climate Scenarios and Models

Daily-downscaled (bias-corrected) weather data were selected to map a broad range of climate outputs for impact modelling (Wilcke and Bärring, 2016) (Table S2).

In order to take into account the uncertainties of the different climate models in the projected simulations (Pierce et al., 2009), the outputs of an ensemble of models were considered for the modelling exercise under the future scenarios RCP4.5 (intermediate scenario) and RCP8.5 (extreme scenario). The climate change scenario ensemble included 14 members deriving from the combination of 14 Global Climate Models (GCMs) downscaled to six high-resolution (~0.12°) Regional Climate Models (RCMs) in the framework of the Med-CORDEX project (Ruti et al., 2016). Daily climate outputs (minimum and maximum temperatures and cumulative rainfall) obtained from the 14 GCMs (available at https://www.medcordex.eu/index.php/) were then bias-corrected over the study sites according to Cornes et al. (2018) and Lange (2019) in order to drive the relevant simulations in future periods. Daily global radiation and relative humidity were retrieved from daily temperature according to Bristow-Campbell (Bristow and Campbell, 1984) and the FAO Irrigation and Drainage paper (Allen et al., 1998), respectively. CO_2 annual concentrations (ppm) for past, current, and future projections were calculated from the IPCC report (IPCC, 2021).

2.3. The Grassland Model

The Pasture Simulation model (PaSim) was chosen for this study because it can describe in detail the dynamic biogeochemical responses of a grassland system under altered climate and management. Originally developed by Riedo et al. (1998), PaSim simulates the cycling of water, C, and N in

grassland systems at a sub-daily time step (1/50th of a day) or, as in this work, at a daily time step. Microclimate, soil biophysics, vegetation, herbivores, and management practices are interacting modules. The simulations are not spatially resolved (e.g., inhomogeneity is not taken into account) and input/output data are assumed to be representative of the entire field. The assimilated photosynthetic C is dynamically allocated to a root and three shoot compartments (each composed of four age classes) or lost through animal metabolism (ecosystem respiration). Accumulated aboveground biomass is cut, grazed, or relocated to the litter pool. Management includes the application of organic and mineral N fertilizers, mowing, and grazing. Details on the model processes are provided in published articles (L. Ma et al., 2019; Vigan et al., 2017), which have contributed to the recognition of PaSim as a suitable tool to reproduce biophysical and biogeochemical processes in managed grasslands and its inclusion in international modelling exercises (Ehrhardt et al., 2018b; Renáta Sándor et al., 2018).

2.4. Simulation Design

The modelling work was performed in four simulation suites: Suite 1 with observational data (calibration), Suite 2 with projected climate change scenarios with CO_2 fertilization effect (impact projections), Suite 3 with projected climate change scenarios without CO_2 fertilization effect (sensitivity), and Suite 4 with modified management under projected climate change scenarios with CO_2 fertilization effect (adaptation assessment).

For Suite 1, the simulations setup included weather, soil, vegetation variables and management implementation in the studied years (2020 and 2021). The weather variables included daily minimum and maximum air temperatures, precipitation, and solar radiation. Temperature, precipitation, and wind speed data for 2020 and 2021 were collected from the regional weather stations of Tuscany Region (SIR, Servizio Idrologico Regionale, https://www.sir.toscana.it/index.php) located near the study sites. Daily global solar radiation data were generated from the R package “sirad”, developed by Bojanowski et al. (Bojanowski et al., 2013), based on the model of Bristow and Campbell (1984). The soil data were extracted from the SoilgridsTM dataset (https://soilgrids.org), described in Poggio et al. (2021). The actual management practices (grazing intensity and periods) are described in Table 2. Model calibration was not applied separately to each site. The model was calibrated on all datasets to obtain more realistic and robust parameter values for application on a larger scale, as in (Ma et al., 2015). The availability of detailed LAI and AGB data from two grassland sites offered the possibility of a genuine (multi-location and multi-output) calibration of the model, on the assumption that a unique calibration across sites is appropriate under these conditions. We assumed that a common set of eco-physiological model parameters can be established to simulate C3 grasslands (including grass,

forb, and legume species) under contrasting climatic and management regimes (e.g., Site M represents hill situations, and Site B represents plain situations), while site-specific climatic and management conditions provide the local drivers of actual grassland biomass and foliage production.

In particular, PaSim calibration (Suite 1) was performed against LAI and AGB data collected in the years 2020 and 2021 by modifying the values of a set of parameters (Table S3) to which model sensitivity was determined in previous studies (Ma et al., 2015; Pulina et al., 2018; R. Sándor et al., 2018; Touhami et al., 2013). Parameter values were modified (with the generation of 1000 sets of values using the random Latin hypercube method) within their plausible ranges (Riedo et al., 1998) to ensure satisfactory performance, which is a realistic representation of both outputs. The sets of parameter values resulting from the model calibration were used to compare the PaSim outputs (AGB and LAI) with the observations in each study site. The agreement between simulated and observed AGB and LAI was assessed by inspection of time-series plots (fluctuations of output variables over time) and numerically, through two performance metrics commonly used in model evaluation (Richter et al., 2012): relative root mean square error (best, $0 \leq RRMSE < +\infty$, worst) and coefficient of determination (worst, $0 \leq R2 \leq 1$, best).

For Suites 2, 3, and 4, simulated pastoral outputs were obtained by forcing the calibrated PaSim with the downscaled (bias-corrected) daily weather data described in Section 2.2, Climate Scenarios and Models. Projected PaSim responses to climate change forcing options were calculated on changes in a set of agro-ecosystem outputs related to growing season length, fodder production, water cycle, and C-N fluxes (Table 3). At both sites, we assessed the sensitivity of the grassland model to climate change (RCP4.5 and RCP8.5 for the ongoing and mid-future periods) under business-as-usual (BaU) management (Suites 2 and 3) and alternative management scenarios (Suite 4).

For Suite 2 (impact projections) and Suite 4 (adaptation assessment), grassland modelling results were obtained with a climate forcing based on atmospheric CO_2 concentration set at 363 ppm, on average, for the baseline scenario (near past: 1981–2010). In this way, the year 2010 was taken as the end of the time horizon used in this study to emulate the near-past climate, i.e., 30-year time span until the late 2000s, which includes the limit of the historical period (1765–2005) of the atmospheric observations used to drive the climate models (Meinshausen et al., 2011). Then, mean atmospheric CO_2 concentrations were prescribed according to the selected RCPs (middle impact: 4.5; extreme impact: 8.5) and timeframes (ongoing: 2011–2040; mid-future: 2041–2070): 431 (ongoing) and 523 (mid-future) mean ppm under RCP4.5; and 438 (ongoing) and 613 (mid-future) mean ppm under RCP8.5. The results related to the pasture system obtained in Suite 2 were then used in the choice of the possible future adaptation strategies (e.g., increase or decrease in animal load and/or length of grazing season).

For Suite 3 (sensitivity), any fertilization effect from the additional CO_2 emitted during the period from 2011 to 2070 was eliminated. What has been carried out here is, in effect, a test of the sensitivity of PaSim to alterations in weather inputs, this exercise being ultimately focused on understanding the grassland modelling process (not on assessing impacts of climate change and elevated CO_2).

Table 3. Climate change impact metrics.

Type	Output	Acronym	Unit	Description
Date	Growing season start	GSs	day of year (doy)	Day after seven consecutive days with a mean air temperature ≥8 °C from 1 January onwards (Movedi et al., 2019a)
	Growing season end	GSe		Day after seven consecutive days with a mean air temperature <8 °C from 1 July onwards (Movedi et al., 2019a)
	Biomass peak date	BPd		Day of the year with the highest value of aboveground biomass
Count	Growing season length	GS	days	Number of days between the GSs and GSe
Amount	Biomass peak	BP	kg DM m^{-2}	Aboveground biomass value at the peak date
	Aboveground biomass	AGB	kg DM m^{-2}	Aboveground biomass values
	Net ecosystem exchange	NEE	kg C m^{-2} yr^{-1}	C-N fluxes (annual balance)
	Methane	CH_4	kg C m^{-2} yr^{-1}	(These include emissions from ecosystem respiration, RECO = plant + soil + animal respiration, as well as estimates of the plant production of organic compounds from atmospheric CO_2 (GPP: gross primary production) and other system variables: NEE = RECO - GPP, enteric emissions of CH_4 from grazing animals and N_2O emissions from the N cycle)
	Nitrous oxide	N_2O	kg N m^{-2} yr^{-1}	
	Soil water content	SWC	m^3 m^{-3}	Annual mean of daily soil water content values (0.35-m topsoil). In supplementary materials.

3. Results

3.1. Climate Analysis

The monthly distribution of air temperatures at the two study sites (Figure 3), averaged from the outputs of 14 climate models, showed an overall increase in temperature towards the mid-future,

similar for both sites, with the highest increases in summer (roughly +2.6 °C at both sites under the warmest scenario) and the lowest in autumn–winter (roughly +2.1 °C at both sites under the warmest scenario).

Analysis of simulated rainfall data (Figure 3) showed increases in the November-March period relative to the baseline in both scenarios and sites (Site M: +3.1% and +5.1%; Site B: +6.0% and +8.2%, for RCP4.5 and RCP8.5, respectively), while between April and October there was a sharp decrease in rainfall at both sites (−7.0% and −8.9% at M and −9.4% and −8.9% at B for RCP4.5 and RCP8.5, respectively).

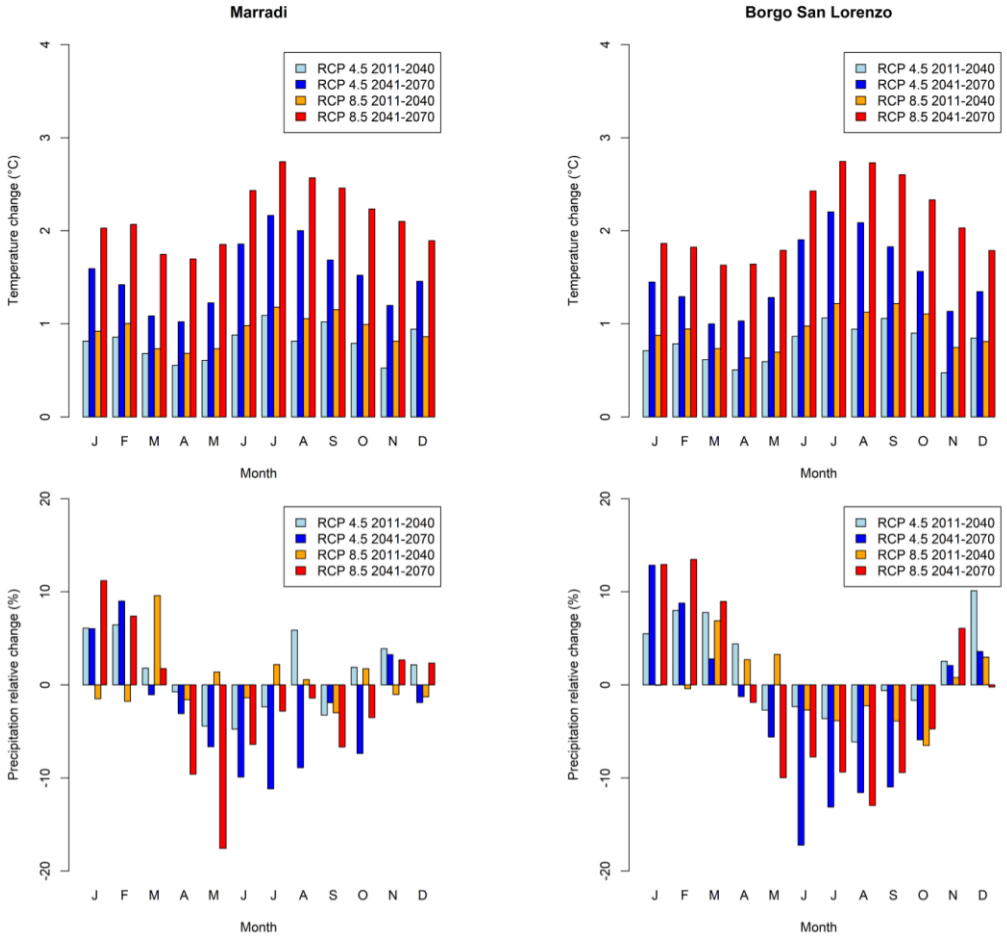

Figure 3. Absolute change (°C) in monthly mean air temperature (top graphs) and relative change (%) of monthly cumulated rainfall (bottom graphs) generated in the two study sites with the RCM ensemble (14 models) for two climate scenarios (RCP4.5, RCP8.5) and two periods – 2011–2040 (ongoing) and 2041–2070 (mid-future)—over the baseline period 1981–2010 (near past).

3.2. Suite 1 of Simulations: Evaluation of the Model Against Observed Data

AGB simulations (Figure 4, Table 4) indicate that estimates substantially reflect patterns of vegetation dynamics (R^2~0.70) although some departures from observed data are noted. The RRMSE values (<15%), in particular, suggest that the model has strong predictive ability for biomass production.

This was also obtained with the LAI, with R^2<0.50 only in sub-area B1 of Site B, where the RRMSE of ~25% was acceptable.

Table 4. Model performance for the two study sites (M: Marradi; B: Borgo San Lorenzo, sub-areas B1 and B2) based on two performance metrics: R^2, coefficient of determination of the linear regression between estimates and observations; and RRMSE (%), Relative Root Mean Square Error. AGB: aboveground biomass; LAI: Leaf Area Index.

Output	Site M		Site B			
			B_1		B_2	
	R^2	RRMSE	R^2	RRMSE	R^2	RRMSE
AGB	0.76	14.9	0.66	13.5	0.68	10.0
LAI	0.96	9.6	0.47	24.5	0.71	12.6

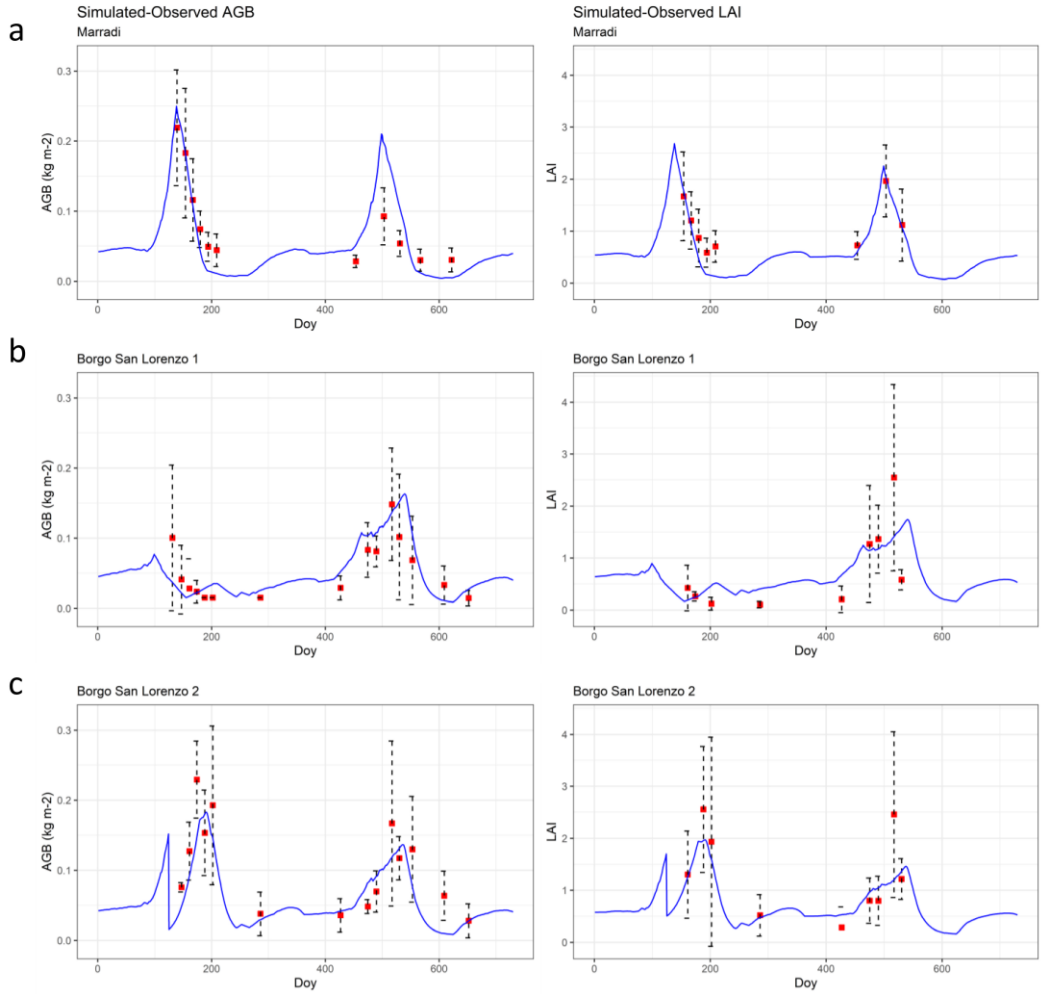

Figure 4. Simulated (blue line) and observed (red square dots) patterns of aboveground biomass (AGB) and leaf area index (LAI) at Sites M (a), B1 (b), and B2 (c) for the period 2020–2021.

3.3. Suites 2, 3, and 4 of Simulations: Impacts of Future Scenarios, Sensitivity to Weather Inputs, and Adaptation Strategies

For both sites, we assessed the response of the grassland model to climate change (RCP4.5 and RCP8.5 for the ongoing and mid-future periods) with business-as-usual (BaU) management (Suite 2) and to different management options (Suite 4). Multi-year mean responses for growing season length (GS), biomass production (AGB), and biogeochemical (C-N fluxes) were calculated. Sensitivity analysis was performed without the CO_2 fertilization (Suite 3) effect by observing future AGB trends over the season for the different RCPs and time periods.

3.4. Growing Season

Under the climate change scenarios, the estimated length of the growing season increases at both sites because optimal thermal conditions for vegetation growth occur earlier and later in the season. This leads to an earlier onset (GSs) and later end (GSe) of the growing season (GS) in both sites, especially in the mid-future (i.e., 2041–2070) (Figure 5). Specifically, for RCP4.5, GSs was advanced by 4 and 8 days, on average, in Site M and by 6 and 12 days in Site B for the periods 2011–2040 and 2041–2070, respectively. In addition, GSe was delayed by 3 and 9 days, on average, for the periods 2011–2040 and 2041–200, respectively, at Site M and by 4 and 9 days, on average, at Site B for the periods 2011–2040 and 2041–2070, respectively. The most pronounced differences from the baseline are visible for the RCP8.5 scenario. Earlier onsets of 4 and 17 days for Site M and 11 and 15 days for Site B under the periods 2011–2040 and 2041–2070, respectively, are accompanied by delays in GSe (5 and 18 days for Site M and 8 and 13 days for site B under the periods 2011–2040 and 2041–2070, respectively).

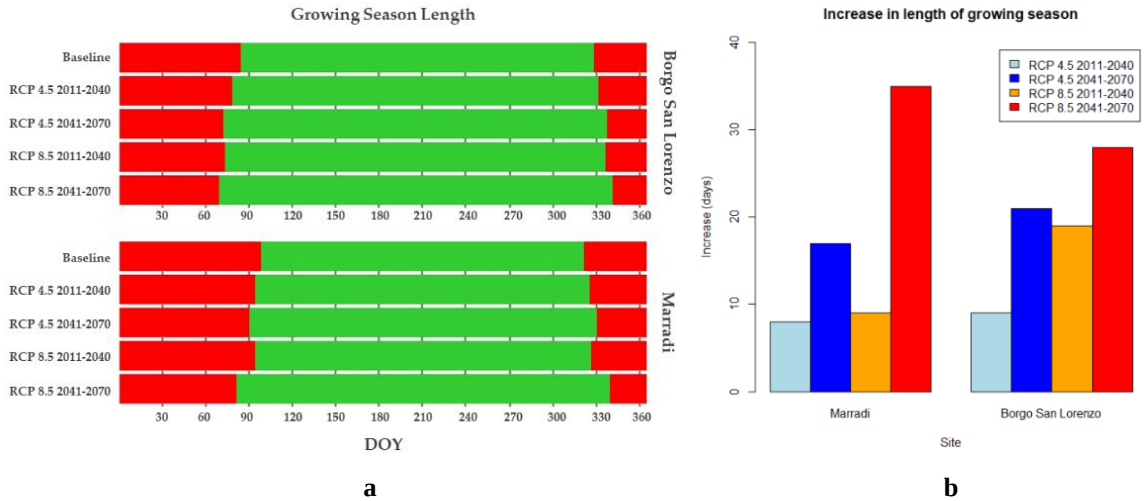

a **b**

Figure 5. Estimated durations (30-year mean values) of vegetation growing seasons (green bars) for baseline and climate change scenarios under business-as-usual management at both study sites (**a**). On the right, increases of growing season length compared with the baseline (**b**).

3.5. Aboveground Biomass

Figure 6 shows the AGB production patterns under BaU management in both sites for the baseline and future projections, while the AGB patterns obtained with all alternative management options can be found in the Supplementary material (Figures S2-S5).

The main differences in AGB patterns among alternative management and climate scenarios were assessed from changes in peak biomass dates (BPd) and corresponding AGB values (BP), which strongly influence stakeholders' and farmers' decisions in choosing the most suitable periods for grazing.

With the baseline climate scenarios, PaSim reported peak biomass on days 138 (Site M) and 157 (Site B). With the future climate scenarios, the model indicated the same BPd at Site M (day 138) with both scenarios and time slices, as grazing starts on day 139, while Site B showed a general delay in BPd, specifically 1 to 5 days in RCP4.5 and 3 to 10 days in RCP8.5.

In the baseline scenarios, the peak biomass production (BP) is 0.13 (±0.03 standard deviation) kg DM m^{-2} at Site M and 0.09 (±0.02 standard deviation) kg DM m^{-2} at Site B. With the climate change patterns, PaSim estimated higher BP values with both RCP4.5 (by 48.4 and 90.8% at Site M and 58.9 and 139.7% at Site B, for 2011–2040 and 2041–2070, respectively) and RCP8.5 (by 52.1 and 136.9% at Site M and 73.4 and 216.8% at Site B, respectively), mainly due to the fertilizing role of CO_2 in the selected emission scenarios and the absence of sensible water deficits simulated by PaSim (Figure S1). With respect to SWC, in fact, although the simulated patterns suggest that, with drier summer conditions, grassland growth may be limited by some water stress in the future, differences between the baseline and climate change scenarios are limited at both sites. In particular, no significant changes in SWC are evident during the spring period, when plant growth activity is the greatest.

To assess the effect of CO_2 fertilization (Suite 3), we tested the same climate change scenarios using the mean baseline CO_2 concentration (i.e., 363 ppm recorded, on average, during 1981–2010), showing that BP values under the baseline CO_2 concentration did not increase to the same extent as observed for the future scenarios with higher CO_2 concentration (Figure 7). Specifically, compared with the baseline, the BP increased by 24.8 and 29.5% at Site M and 10.5 and 16.5% at Site B for RCP4.5 (for 2011–2040 and 2041–2070, respectively) and by 25.2 and 50.0% at Site M and 15.4 and 27.0% at Site B for RCP8.5 (for 2011–2040 and 2041–2070, respectively).

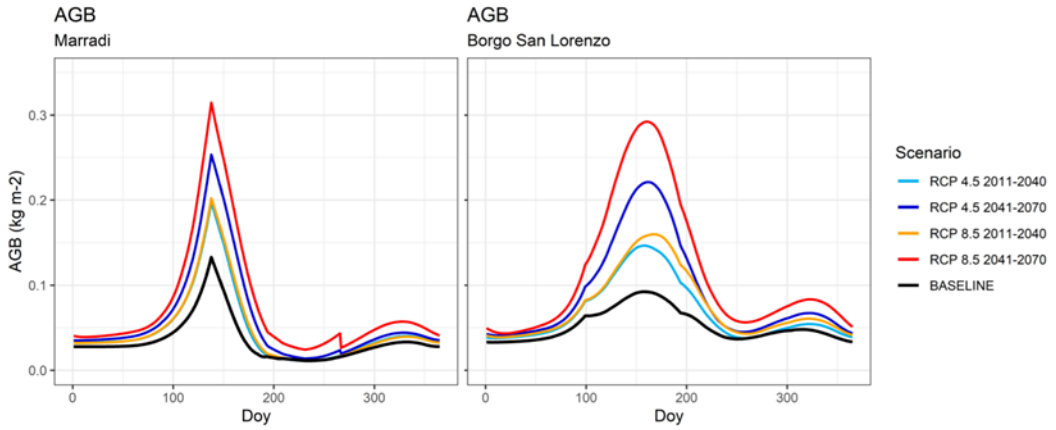

Figure 6. Daily simulation (30-year mean) of aboveground biomass (AGB) with PaSim for baseline and climate change scenarios under business-as-usual management at both study sites.

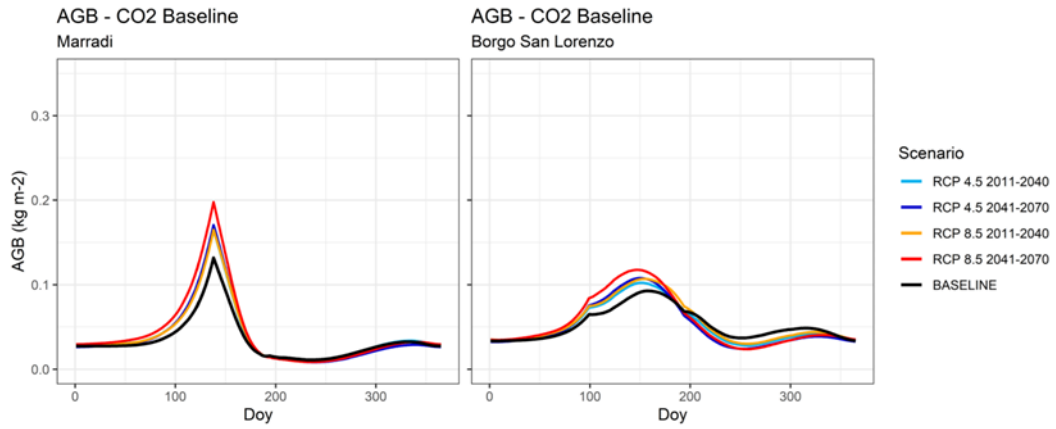

Figure 7. Daily simulation (30-year mean) of aboveground biomass (AGB) with PaSim for baseline and climate change scenarios (no CO_2 fertilization) under business-as-usual management at both study sites.

Considering the results of Suite 2, alternative management practices (Suite 4) included: (1) livestock grazing intensity increased by 20% (i.e., +20 GI); (2) extension of the grazing period length by 15% (i.e., +15 GL), specifically 7 days earlier start and 7 days later end at Marradi, 16 days earlier start and 16 days later end at Borgo San Lorenzo; (3) combination of (1) and (2) (i.e., +20GI x 15GL). For the impact of adaptation strategies, the value of the peak biomass obtained with alternative management practices (i.e., BaU and adaptation management options) was compared with the peak biomass from business-as-usual (BaU) management under the projected scenarios (Figure 8).

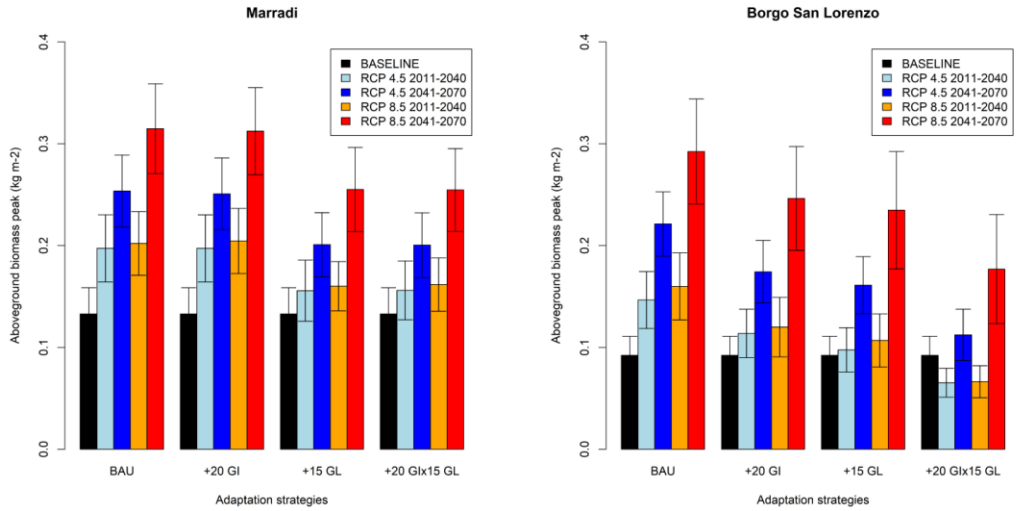

Figure 8. Changes in peak aboveground biomass (kg DM m^{-2}) among business-as-usual management (BaU) under the baseline climate (black histogram) and all alternative management options under RCP4.5 (cyan and blue histograms) and RCP8.5 (orange and red histograms) in both sites as provided by PaSim. Vertical bars are standard deviations.

According to model's outputs, the aboveground peak (Figure 8) and the trends over the season (Figures S2-S5), obtained using the different adaptation strategies, show that future biomass availability will reach higher values when compared with the baseline, even by increasing the animal stocking rate (i.e., +20 GI) and/or the number of grazing days (i.e., +15 GL or +20 GI x 15 GL).

3.6. Carbon–nitrogen Fluxes

Under current climate and management conditions, PaSim shows limited non-CO_2 emissions at both sites, i.e., ~2 g C m^{-2} yr^{-1} for CH_4 and 4.6–4.7 g N m^{-2} yr^{-1} for N_2O emissions, while the C exchanges reflect that both sites are sources of C (NEE≥ 350 g C m^{-2} yr^{-1}).

Table 4. C-N emissions (NEE: net ecosystem CO_2 exchange; CH_4: methane; and N_2O: nitrous oxide) from the two study sites (baseline climate), estimated (30-year mean with standard deviation) using PaSim. The estimated components of the C budget (GPP: gross primary production; RECO: ecosystem respiration) can be found in Supplementary material (Table S4).

Site	**NEE**	**CH_4**	**N_2O**
	g C m^{-2} yr^{-1}		**g N m^{-2} yr^{-1}**
Site M	381.3 ± 245.6	2.2 ± 0.3	4.6 ± 3.4
Site B	350.1 ± 236.1	1.8 ± 0.2	4.7 ± 3.2

Heatmaps of the % differences between current conditions (i.e., baseline climate and BaU management) and combinations of alternative climate and management scenarios allow the impact of altered climate and management changes on gas emissions at the two study sites to be assessed (Figure 9). For NEE, in particular, the PaSim heatmaps show overall trends towards C uptake (more negative

NEE values) in both study sites by moving towards extreme climate conditions (i.e., RCP8.5 and time-frame 2041–2070), with all management options. This reflects the AGB pattern (Figure 6) resulting from a higher photosynthetic plant production from atmospheric CO_2, even with increased animal respiration under the option of increased livestock density (GPP and RECO values in Table S4).

As for CH_4 emissions, the PaSim heatmap indicates that emissions are higher with the warmest scenario and as livestock density increases (up to <100%). Finally, the N_2O emissions estimated by PaSim tend to be lower under future climate and alternative management scenarios.

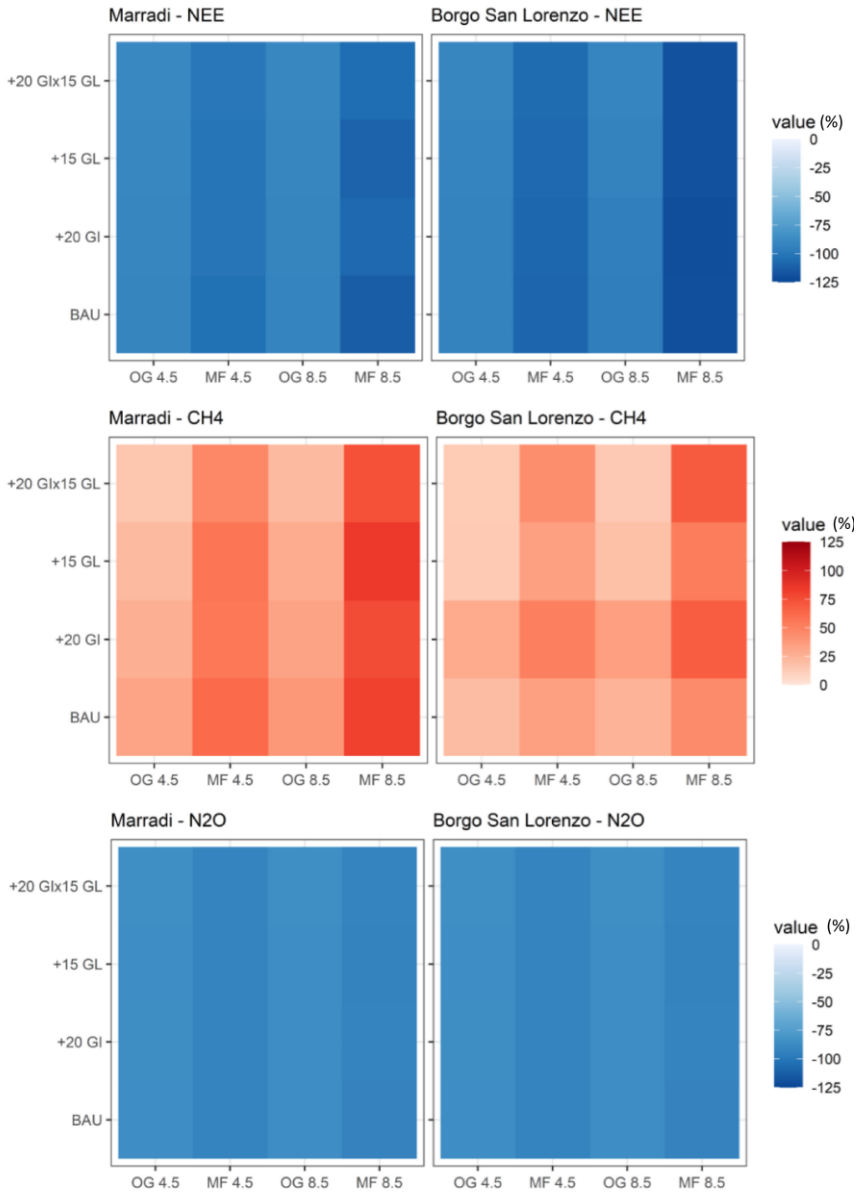

Figure 9. Heatmap visualization of the relative differences (%) of the three main greenhouse gas emissions (NEE: net ecosystem exchange; CH_4: methane; and N_2O: nitrous oxide), estimated using PaSim, for alternative management and climate change scenarios compared with current climate and management in the two study sites. OG: ongoing period, MF: mid-future period, 4.5: RCP4.5, 8.5: RCP8.5, GI: grazing intensity; and GL: grazing length, 20: +20%, 15: +15%.

4. Discussion

4.1. Model Parameterisation

The great deal of fundamental research incorporated into the mechanistic PaSim model has ensured satisfactory estimates, which are also comparable to published grassland modelling studies (R Sándor et al., 2017; Schucknecht et al., 2022). This is relevant considering that simulations for grasslands are generally less accurate compared with arable crops (Kollas et al., 2015) since large uncertainties in biomass and LAI measurements cause simulation of grassland vegetation dynamics to be difficult to perform (Movedi et al., 2019b; Vuichard et al., 2007).

This was obtained with calibrated parameter values (Table S3) that do not deviate substantially from those obtained in previous studies on continental and Mediterranean grasslands. For instance, the maximum specific leaf area, slam=27.2 m^2 kg^{-1}, is similar to slam=29 m^2 kg^{-1} obtained in the Europe-wide calibration of Ma et al. (2015). Light-saturated leaf photosynthetic rates for reproductive (pmco2rep=12.88 μmol C m^{-2} s^{-1}) and vegetative (pmco2veg=9.49 μmol C m^{-2} s^{-1}) stages are similar to the values obtained for Mediterranean grasslands (pmco2rep=14.0 μmol C m^{-2} s^{-1} and pmco2veg=10.0 μmol C m^{-2} s^{-1}) from Pulina et al. (2018). The root and shoot turnover rates at 20 °C, kturnrt20=0.0155 d^{-1} and kturnsh20=0.0468 d^{-1}, respectively, exceed those estimated by Pulina et al. (2018) for grasslands dominated by annual self-seeding plant species: 0.0144 d^{-1} and 0.0250 d^{-1}, respectively. With the obtained calibration, the shoot turnover parameter dwindled to approximately 21 days (1/0.0144 d^{-1}), which is lower than 40 days (1/0.0250 d^{-1}), as in Pulina et al. (2018). In fact, perennial plants tend to invest mainly in long-lived and competitive adult individuals, and, consequently, shoot turnover tends to be faster in perennial plants than in annual species, as the former allocate more resources for new leaf growth to maximize photosynthetic efficiency (Schippers et al., 2001).

4.2. Uncertainties in Climate Change Impacts and Adaptation Strategies

The adopted impact model was widely applied in various contexts (Fuchs et al., 2020; Ma et al., 2015; Pulina et al., 2018; Touhami et al., 2013; Vital et al., 2013), dealing with multifaceted territorial and vegetation structures and extreme weather conditions, which are often difficult to parameterize (Wang et al., 2022) due to the complex response of the vegetation growth with respect to critical thresholds (e.g., air temperatures, water requirements, and radiation use efficiency) for mixed plant communities (Renáta Sándor et al., 2018). In this study, PaSim represented the effects of climate change and management options on the timing and extent of the growing season and C-N fluxes, together with biomass production and peaks. The longer growing season length was due to the extension of the potential growing season in both spring and autumn, as already observed in grasslands during the last

decades (Bellini et al., 2023; Ren et al., 2022). The mean plant growth trend simulated with the model (30-year means) mirrors the observed pattern of vegetation growth during the growing season, indicating that the overall pattern of response to elevated atmospheric CO_2 concentration significantly stimulates leaf photosynthesis (Ainsworth and Long, 2005; Ellsworth et al., 2004). Sensitivity analysis performed in Suite 2 highlighted this fertilization effect of increased CO_2 concentration simulated by PaSim; nevertheless, it must be underlined that similar trends of increased aboveground biomass in both future climate change scenarios and time periods are visible also with steady CO_2 concentration (i.e., baseline concentration, 363 ppm), albeit to a lesser extent. In addition, although a down-regulation strategy can be useful to limit the effect of increased CO_2 concentration on plant growth (Ainsworth and Rogers, 2007), it is worth emphasizing that the production increases projected for the mid-future (2041–2070) resulted in being particularly high when compared with a baseline that reflects a situation of the near past (period 1981–2010). When compared, instead, with the ongoing period (2011–2040), which reflects average aboveground biomass values similar to the present and to the calibration period, the increases are smaller, comparable to those found in other studies (Shrestha et al., 2015; Zarrineh et al., 2020). The CO_2 positive effect is reflected in the higher C uptake estimated by PaSim as a result of increased productivity, also with higher stocking rates (i.e., higher C losses due to higher animal respiration), which confirms the increased worldwide productivity of grasslands exposed to increased CO_2 (Chang et al., 2021).

PaSim estimated increasing CH_4 emissions and decreasing N_2O emissions with climate scenarios. The former logically reflects evidence that grasslands emit more CH_4 at higher temperatures (Zhu et al., 2020). Although the latter does not reflect the direct effect of temperature on the enzymatic processes involved in N_2O production, N_2O emissions are controlled mainly by soil properties and current soil N levels (Butterbach-Bahl et al., 2013), which may have been reduced with increased plant demand due to higher biomass production under climate scenarios. This increase in future biomass production, driven by the higher average annual GPP (gross primary production), also led to a consequent decrease in simulated NEE over the years.

4.3. Consequences for Grassland Sustainability

Herders depend on pasture and water resources for their livestock and are among the groups most vulnerable to climate change impacts in dry regions (Cullen et al., 2009; Moore and Ghahramani, 2014; Murphy et al., 2002; Ouled Belgacem and Louhaichi, 2013; Parton et al., 1994). Although there are reasons to be concerned, some impacts of climate change are expected to be positive. Foreseen climate variability can be an opportunity for effective management, as actions could be timed to the most effective conditions, and climate change could be a motivation to develop a broader and more

responsive and collaborative management paradigm. We showed that increases in plant productivity and longer growing seasons in central Italy may support more livestock and increase economic benefits. Rising air temperatures simulated by climatic models, combined with increasing concentrations of CO_2 in the atmosphere in RCP4.5 and RCP8.5 scenarios, are expected to offer important opportunities in terms of forage production for livestock systems in central Italy. This is possible if future water availability is not a limiting factor, as stressed by various research studies on grassland potential production (He et al., 2022). Indeed, as seen from the results of climatic models, precipitations are expected to decrease in the future, mostly in summer months but not particularly in spring. The availability of water in the soil, therefore, does not vary significantly over time and future climate change scenarios, as is visible from the soil water content simulated by PaSim (Figure S1). These trends on future pasture productivity are consistent with other studies, originating also from different geographical sectors. Already in the understanding of Rounsevell et al. (1996), it seemed unlikely that climate change would have a negative impact on grasslands in England and Wales, while Riedo et al. (1998) predicted a positive effect on grassland productivity in central Europe. Additionally, in the case of grasslands in the United States, pasture production is generally expected to increase under projected climate scenarios (Edmonds and Rosenberg, 2005). Moreover, Morales et al. (2007) predicted an increase in grassland productivity in Europe, albeit with significant regional variability. In this regard, it should be emphasised that the impacts of climate change on grazing systems may be region-specific (Harrison et al., 2016).

Adaptation strategies must face different and opposite effects on rangeland productivity, as already previously pointed out (Cheng et al., 2022; Joyce et al., 2013), and in some cases, it is foreseen that climate change can produce a positive effect, being able to support greater livestock numbers (Briske et al., 2015) and to lengthen the duration of the grazing season due to a higher herbage availability early in the year (Hristov et al., 2018). In our study, we provided clues for increasing stocking rates and extending grazing periods (mainly by putting animals out to pasture earlier) to take advantage of the change in seasonality and increased forage production compared with the baseline (1981–2010), especially in the mid-future (i.e., 2041–2070). The possibility of having an earlier vegetative recovery that prolongs the duration of the grazing season allows, along with the higher productivity assumed, an increase in animal density, and, in this way, a biomass intake more consistent with the forage availability. Consequently, these conditions allow a more efficient management of the resource (Xu et al., 2016) with less waste and a more adequate stocking rate, a factor that ensures less degradation of the pasture itself (Allen et al., 2011). Results confirm these opportunities also comparing mid-future aboveground biomass under adaptation strategies (peak and trend, Figure 8 and Figures S2–S5) with those of the ongoing period under BaU (i.e., 2011–2040), which is the condition most similar

to the one of calibration. In this view, it is, however, important to emphasize that in the simulation of adaptation strategies, the model does not specifically consider the role of increased animal stocking rate and/or duration of the grazing season on soil compaction, a condition that may disadvantage forage quality, vegetation regrowth, and biodiversity (Li et al., 2017; Liu et al., 2022). In addition, warming and altered rainfall patterns may reduce the forage quality and palatability of Italian grasslands (Dibari et al., 2021). Indeed, climatic changes, as well as land-use changes, have already strongly modified the botanical composition, species distribution, and size of grasslands in the central Italian massifs since the 1950s (Frate et al., 2018). The observed floral, ecological, and structural variations confirm that grassland ecosystems in mountainous environments in Italy have undergone a process of thermophilization, with an evolutionary trend towards more nutrient-demanding vegetation (Alberto Evangelista et al., 2016; Ferrarini et al., 2017). Variations in vegetation composition in response to increased competition for environmental factors indicate, at higher altitudes, less displacement of plant species from higher slopes as well as dispersal of species from south-facing to north-facing slopes, with greater presence of grass- and shrub-dominated communities replacing rare and cold-tolerant species (Porro et al., 2019). This reflects the narrower thermal niche of mountain plant species, which makes short-term adaptation/acclimation more difficult (Löffler and Pape, 2020). As a narrow thermal niche prevents plant species from adapting quickly to high altitudes, site elevation explains the response of species richness to warming (Piseddu et al., 2021). Indeed, although changes in species cover and plant community composition indicate an accelerated transformation to more heat-demanding vegetation, this colonization process may occur at a slower rate than the continued decline of cryophilic species, favoring periods of accelerated species decline (Lamprecht et al., 2018).

The analyses performed in this study identified the possible impacts of climate change on a typical grazing system of the Apennines in Central Italy, highlighting future trends of different system characteristics, such as length of the growing season, pasture productivity, soil water conditions, and gas emissions, as well as possible alternative management strategies in a context of future climate change. In fact, the results obtained in this study highlight the potential of employing specific models for simulating the behavior of pastoral resources under actual utilization and different future scenarios (i.e., RCP4.5 and RCP8.5), testing adaptation management options. In this sense, the study has produced a significant step forward compared with previous studies that analyzed climate change impacts on Apennine grasslands, mainly with regard to the botanical evolution of the plant communities, by providing insights on future agronomic conditions and possible adaptation strategies. The modelling approach used has, thus, been demonstrated to be a useful tool to support the management decisions that breeders will have to make in the near future.

5. Conclusions

The results of this study represent a step forward in the knowledge of the impacts of future climate change on a typical pasture system in the central Apennines. Specifically, this study fills a lack of information on future grassland development, as well as providing detailed information on the length of the growing season, GHG emissions, water conditions, and the effectiveness of different adaptation strategies in response to the increase in forage production simulated by PaSim in future scenarios. In particular, the analysis of adaptation strategies investigated possible management changes to cope with climate change impacts, providing useful indications to stakeholders and policy-makers for appropriate agricultural policy and optimal land management strategies for ongoing climate change. However, while modelling approaches capture distinct aspects of the adaptive process, they have done so in relative isolation from the use of other technological supports (e.g., remote sensing and precision farming) and participatory approaches, without producing improved unified representations. As well, management options to sustain grassland ecosystems under global change are many and need to be tested for their ability to maintain or enhance resource values in the future. Social impact assessment studies are, thus, needed to examine how the impacts, i.e., the effects of climatic anomalies on the performance of Apennine pastures, propagate through the socio-economic and political systems. This type of integrated approach, which would include the potential for adaptation and adjustment to climate pressure, would reflect the reality of pastoral communities much better than the modelling used and raises fruitful research questions regarding the vulnerability of Apennine territories and their adaptive capacity.

Author Contributions: Conceptualization, G.B. and E.B.; methodology, G.B., E.B., R.M. and S.C.; software, R.M. and G.B; validation, E.B., G.A., M.M. and C.D.; formal analysis, R.M and E.B.; investigation, G.A., C.D., N.S., E.B., S.C. and M.M.; resources, G.A. and N.S.; data curation, C.D., G.A, N.S.; writing—original draft preparation, G.B, E.B.; writing—review and editing, G.A., M.M., C.D., S.C. and N.S.; visualization, E.B. and G.B.; supervision, R.M, G.A, G.B, M.M.; project administration, C.D. and G.B.; funding acquisition, G.A., C.D. and G.B. All authors have read and agreed to the published version of the manuscript.

Funding: The study was developed in the framework of E.B.'s PhD thesis, supported by the VISTOCK project funded by GAL-START Mugello (Tuscany Region), grant number 853175. It falls within the thematic area of the French government IDEX-ISITE initiative (reference: 16-IDEX-0001; project CAP 20-25).

Data Availability Statement: Not applicable

Acknowledgments: We thank the farms involved in the study for the practical support.

Conflicts of Interest: The authors declare no conflict of interest.

References

Ainsworth, E.A., Long, S.P., 2005. What have we learned from 15 years of free-air CO2 enrichment (FACE)? A meta-analytic review of the responses of photosynthesis, canopy properties and plant production to rising CO2. New Phytol. 165, 351–372. https://doi.org/10.1111/j.1469-8137.2004.01224.x

Ainsworth, E.A., Rogers, A., 2007. The response of photosynthesis and stomatal conductance to rising [CO 2]: Mechanisms and environmental interactions. Plant, Cell Environ. 30, 258–270. https://doi.org/10.1111/j.1365-3040.2007.01641.x

Allen, R.G., Pereira, L.S., Raes, D., Smith, M., 1998. FAO Irrigation and Drainage Paper No. 56 - Crop Evapotranspiration.

Allen, V.G., Batello, C., Berretta, E.J., Hodgson, J., Kothmann, M., Li, X., McIvor, J., Milne, J., Morris, C., Peeters, A., Sanderson, M., 2011. An international terminology for grazing lands and grazing animals. Grass Forage Sci. 66, 2–28. https://doi.org/10.1111/j.1365-2494.2010.00780.x

Argenti, G., Bottai, L., Chiesi, M., Maselli, F., Staglianò, N., Targetti, S., 2011. Analisi e valutazione di pascoli montani attraverso l'integrazione di dati multispettrali e ausiliari. Riv. Ital. di Telerilevamento 43, 45-57 (in italian).

Barbour, R., Young, R.H., Wilkinson, J.M., 2022. Production of Meat and Milk from Grass in the United Kingdom. Agronomy 12, 1–9. https://doi.org/10.3390/agronomy12040914

Barthel, M., Buchmann, N., Eugster, W., Butterbach-bahl, K., Eugenio, D., Zeeman, M., Lu, H., Kiese, R., Bahn, M., Hammerle, A., 2018. Greenhouse gas fluxes over managed grasslands in Central Europe s 1843–1872. https://doi.org/10.1111/gcb.14079

Bebeley, J.F., Kamara, A.Y., Jibrin, J.M., Akinseye, F.M., Tofa, A.I., Adam, A.M., 2022. Evaluation and application of the CROPGRO - soybean model for determining optimum sowing windows of soybean in the Nigeria savannas. Sci. Rep. 1–15. https://doi.org/10.1038/s41598-022-10505-4

Bellini, E., Moriondo, M., Dibari, C., Leolini, L., Staglian, N., Stendardi, L., Filippa, G., Galvagno, M., Argenti, G., 2023. Impacts of Climate Change on European Grassland Phenology : A 20-Year Analysis of MODIS Satellite Data 1–22.

Bengtsson, J., Bullock, J.M., Egoh, B., Everson, C., Everson, T., O'Connor, T., O'Farrell, P.J., Smith, H.G., Lindborg, R., 2019. Grasslands—more important for ecosystem services than you might think. Ecosphere 10, 1–20. https://doi.org/10.1002/ecs2.2582

Bojanowski, J.S., Donatelli, M., Skidmore, A.K., Vrieling, A., 2013. An auto-calibration procedure for empirical solar radiation models. Environ. Model. Softw. 49, 118–128.

https://doi.org/10.1016/j.envsoft.2013.08.002

Briske, D.D., Joyce, L.A., Polley, H.W., Brown, J.R., Wolter, K., Morgan, J.A., McCarl, B.A., Bailey, D.W., 2015. Climate-change adaptation on rangelands: Linking regional exposure with diverse adaptive capacity. Front. Ecol. Environ. 13, 249–256. https://doi.org/10.1890/140266

Bristow, K.L., Campbell, G.S., 1984. On the relationship between incoming solar radiation and daily maximum and minimum temperature. Agric. For. Meteorol. 31, 159–166. https://doi.org/https://doi.org/10.1016/0168-1923(84)90017-0

Burrascano, S., Caccianiga, M., Gigante, D., 2010. Dry grasslands habitat types in Italy, Bulletin of the European Dry Grasslands Group 9.

Butterbach-Bahl, K., Baggs, E.M., Dannenmann, M., Kiese, R., Zechmeister-Boltenstern, S., 2013. Nitrous oxide emissions from soils: How well do we understand the processes and their controls? Philos. Trans. R. Soc. B Biol. Sci. 368. https://doi.org/10.1098/rstb.2013.0122

Cavallero, A., Aceto, P., Gorlier, A., Lombardi, G., Lonati, M., Martinasso, B., Tagliatori, C., 2007. I tipi pastorali delle Alpi piemontesi. Bologna, Italy.

Chang, J., Ciais, P., Gasser, T., Smith, P., Herrero, M., Havlík, P., Obersteiner, M., Guenet, B., Goll, D.S., Li, W., Naipal, V., Peng, S., Qiu, C., Tian, H., Viovy, N., Yue, C., Zhu, D., 2021. Climate warming from managed grasslands cancels the cooling effect of carbon sinks in sparsely grazed and natural grasslands. Nat. Commun. 12, 1–10. https://doi.org/10.1038/s41467-020-20406-7

Chelli, S., Wellstein, C., Campetella, G., Canullo, R., Tonin, R., Zerbe, S., Gerdol, R., 2017. Climate change response of vegetation across climatic zones in Italy. Clim. Res. 71, 249–262. https://doi.org/10.3354/cr01443

Cheng, M., Mccarl, B., Fei, C., 2022. Climate Change and Livestock Production : A Literature Review.

Cornes, R.C., van der Schrier, G., van den Besselaar, E.J.M., Jones, P.D., 2018. An Ensemble Version of the E-OBS Temperature and Precipitation Data Sets. J. Geophys. Res. Atmos. 123, 9391–9409. https://doi.org/10.1029/2017JD028200

Cullen, B.R., Johnson, I.R., Eckard, R.J., Lodge, G.M., Walker, R.J., Rawnsley, R.P., McCaskillF, M.R., 2009. Climate change effects on pasture systems in south-eastern Australia. Crop Pasture Sci. 60, 933–942.

Dass, P., Houlton, B.Z., Wang, Y., Warlind, D., n.d. Grasslands may be more reliable carbon sinks than forests in California OPEN ACCESS Grasslands may be more reliable carbon sinks than forests in California.

Dibari, C., Argenti, G., Catolfi, F., Moriondo, M., Staglianò, N., Bindi, M., 2015. Pastoral suitability driven by future climate change along the apennines. Ital. J. Agron. 10, 109–116. https://doi.org/10.4081/ija.2015.659

Dibari, C., Costafreda-Aumedes, S., Argenti, G., Bindi, M., Carotenuto, F., Moriondo, M., Padovan, G., Pardini, A., Staglianò, N., Vagnoli, C., Brilli, L., 2020. Expected changes to alpine pastures in extent and composition under future climate conditions. Agronomy 10, 1–21. https://doi.org/10.3390/agronomy10070926

Dibari, C., Pulina, A., Argenti, G., Aglietti, C., Bindi, M., Moriondo, M., Mula, L., Pasqui, M., Seddaiu, G., Roggero, P.P., 2021. Climate change impacts on the alpine, continental and mediterranean grassland systems of italy: A review. Ital. J. Agron. 16, 1843.

Dillon, P., 2018. The evolution of grassland in the European Union in terms of utilisation, productivity, food security and the importance of adoption of technical innovations in increasing sustainability of pasture-based ruminant production systems. Grassl. Sci. Eur. Vol. 23, 3-15.

Edmonds, J.A., Rosenberg, N.J., 2005. Climate change impacts for the conterminous USA: An integrated assessment summary. Clim. Chang. Impacts Conterminous USA An Integr. Assess. 151–162. https://doi.org/10.1007/1-4020-3876-3_9

Ehrhardt, F., Soussana, J.F., Bellocchi, G., Grace, P., McAuliffe, R., Recous, S., Sándor, R., Smith, P., Snow, V., de Antoni Migliorati, M., Basso, B., Bhatia, A., Brilli, L., Doltra, J., Dorich, C.D., Doro, L., Fitton, N., Giacomini, S.J., Grant, B., Harrison, M.T., Jones, S.K., Kirschbaum, M.U.F., Klumpp, K., Laville, P., Léonard, J., Liebig, M., Lieffering, M., Martin, R., Massad, R.S., Meier, E., Merbold, L., Moore, A.D., Myrgiotis, V., Newton, P., Pattey, E., Rolinski, S., Sharp, J., Smith, W.N., Wu, L., Zhang, Q., 2018. Assessing uncertainties in crop and pasture ensemble model simulations of productivity and N2O emissions. Glob. Chang. Biol. 24, e603–e616. https://doi.org/10.1111/gcb.13965

Ellsworth, D.S., Reich, P.B., Naumburg, E.S., Koch, G.W., Kubiske, M.E., Smith, S.D., 2004. Photosynthesis, carboxylation and leaf nitrogen responses of 16 species to elevated pCO2 across four free-air CO2 enrichment experiments in forest, grassland and desert. Glob. Chang. Biol. 10, 2121–2138. https://doi.org/10.1111/j.1365-2486.2004.00867.x

Evangelista, A., Frate, L., Carranza, M.L., Attorre, F., Pelino, G., Stanisci, A., 2016. Changes in composition, ecology and structure of high-mountain vegetation: A re-visitation study over 42 years. AoB Plants 8, 1–11. https://doi.org/10.1093/aobpla/plw004

Ferrarini, A., Alatalo, J.M., Gervasoni, D., Foggi, B., 2017. Exploring the compass of potential changes induced by climate warming in plant communities. Ecol. Complex. 29, 1–9. https://doi.org/10.1016/j.ecocom.2016.11.003

Franzluebbers, A.J., 2020. Cattle grazing effects on the environment: Greenhouse gas emissions and carbon footprint, Management Strategies for Sustainable Cattle Production in Southern Pastures. Elsevier Inc. https://doi.org/10.1016/B978-0-12-814474-9.00002-5

Frate, L., Carranza, M.L., Evangelista, A., Stinca, A., Schaminée, J.H.J., Stanisci, A., 2018. Climate and land use change impacts on mediterranean high-mountain vegetation in the apennines since the 1950s. Plant Ecol. Divers. 11, 85–96. https://doi.org/10.1080/17550874.2018.1473521

Fuchs, K., Merbold, L., Buchmann, N., Bellocchi, G., Bindi, M., Brilli, L., Conant, R.T., Dorich, C.D., Ehrhardt, F., Fitton, N., Grace, P., Klumpp, K., Liebig, M., Lieffering, M., Martin, R., McAuliffe, R., Newton, P.C.D., Rees, R.M., Recous, S., Smith, P., Soussana, J.F., Topp, C.F.E., Snow, V., 2020. Evaluating the Potential of Legumes to Mitigate N2O Emissions From Permanent Grassland Using Process-Based Models. Global Biogeochem. Cycles 34. https://doi.org/10.1029/2020GB006561

Fullman, T.J., Bunting, E.L., Kiker, G.A., Southworth, J., 2017. Predicting shifts in large herbivore distributions under climate change and management using a spatially-explicit ecosystem model. Ecol. Modell. 352, 1–18. https://doi.org/10.1016/j.ecolmodel.2017.02.030

Gao, Q. zhu, Li, Y., Xu, H. mei, Wan, Y. fan, Jiangcun, W. zha, 2014. Adaptation strategies of climate variability impacts on alpine grassland ecosystems in Tibetan Plateau. Mitig. Adapt. Strateg. Glob. Chang. 19, 199–209. https://doi.org/10.1007/s11027-012-9434-y

Guillaume, T., Makowski, D., Libohova, Z., Elfouki, S., Fontana, M., Leifeld, J., Bragazza, L., Sinaj, S., 2022. Geoderma Carbon storage in agricultural topsoils and subsoils is promoted by including temporary grasslands into the crop rotation. Geoderma 422, 115937. https://doi.org/10.1016/j.geoderma.2022.115937

Hao, R., Yu, D., Liu, Yupeng, Liu, Yang, Qiao, J., Wang, X., Du, J., 2017. Impacts of changes in climate and landscape pattern on ecosystem services. Sci. Total Environ. 579, 718–728. https://doi.org/10.1016/j.scitotenv.2016.11.036

Harrison, M.T., Cullen, B.R., Rawnsley, R.P., 2016. Modelling the sensitivity of agricultural systems to climate change and extreme climatic events. Agric. Syst. https://doi.org/10.1016/j.agsy.2016.07.006

He, P., Ma, X., Sun, Z., Han, Z., Ma, S., Xiaoyu, M., 2022. Compound drought constrains gross primary productivity in Chinese grasslands. Environ. Res. Lett. 17(10).

Hristov, A.N., Degaetano, A.T., Rotz, C.A., Hoberg, E., Skinner, R.H., Felix, T., Li, H., Patterson, P.H., Roth, G., Hall, M., Ott, T.L., Baumgard, L.H., Staniar, W., Hulet, R.M., Dell, C.J., Brito, A.F., Hollinger, D.Y., 2018. Climate change effects on livestock in the Northeast US and strategies for adaptation. Clim. Change 146, 33–45. https://doi.org/10.1007/s10584-017-2023-z

Insua, J.R., Utsumi, S.A., Basso, B., 2019. Estimation of spatial and temporal variability of pasture growth and digestibility in grazing rotations coupling unmanned aerial vehicle (UAV) with crop simulation models. PLoS One 14, 1–21. https://doi.org/10.1371/journal.pone.0212773

IPCC, 2021. Annex III: Tables of historical and projected well-mixed greenhouse gas mixing ratios and effective radiative forcing of all climate forcers [Dentener F.J., B. Hall, C. Smith (eds.)]. In Climate Change 2021: The Physical Science Basis. Contribution of Wor. Cambridge University Press, Cambridge, United Kingdom and New York, NY, USA, pp. 2139–2152. https://doi.org/doi:10.1017/9781009157896.017

ISTAT, 2022. http://dati.istat.it/index.aspx?queryid=33704 (access date 05-12-2022).

Joyce, L.A., Briske, D.D., Brown, J.R., Polley, H.W., McCarl, B.A., Bailey, D.W., 2013. Climate change and North American rangelands: Assessment of mitigation and adaptation strategies. Rangel. Ecol. Manag. 66, 512–528. https://doi.org/10.2111/REM-D-12-00142.1

Kalaugher, E., Beukes, P., Bornman, J.F., Clark, A., Campbell, D.I., 2017. Modelling farm-level adaptation of temperate, pasture-based dairy farms to climate change. Agric. Syst. 153, 53–68. https://doi.org/10.1016/j.agsy.2017.01.008

Kamilaris, C., Dewhurst, R.J., Sykes, A.J., Alexander, P., 2020. Modelling alternative management scenarios of economic and environmental sustainability of beef fi nishing systems. J. Clean. Prod. 253, 119888. https://doi.org/10.1016/j.jclepro.2019.119888

Kollas, C., Kersebaum, K.C., Nendel, C., Manevski, K., Müller, C., Palosuo, T., Armas-Herrera, C.M., Beaudoin, N., Bindi, M., Charfeddine, M., Conradt, T., Constantin, J., Eitzinger, J., Ewert, F., Ferrise, R., Gaiser, T., Cortazar-Atauri, I.G. de, Giglio, L., Hlavinka, P., Hoffmann, H.,

Hoffmann, M.P., Launay, M., Manderscheid, R., Mary, B., Mirschel, W., Moriondo, M., Olesen, J.E., Öztürk, I., Pacholski, A., Ripoche-Wachter, D., Roggero, P.P., Roncossek, S., Rötter, R.P., Ruget, F., Sharif, B., Trnka, M., Ventrella, D., Waha, K., Wegehenkel, M., Weigel, H.J., Wu, L., 2015. Crop rotation modelling-A European model intercomparison. Eur. J. Agron. 70, 98–111. https://doi.org/10.1016/j.eja.2015.06.007

Lamprecht, A., Semenchuk, P.R., Steinbauer, K., Winkler, M., Pauli, H., 2018. Climate change leads to accelerated transformation of high-elevation vegetation in the central Alps. New Phytol. 220, 447–459. https://doi.org/10.1111/nph.15290

Lange, S., 2019. Trend-preserving bias adjustment and statistical downscaling with ISIMIP3BASD (v1.0). Geosci. Model Dev. 12, 3055–3070. https://doi.org/10.5194/gmd-12-3055-2019

Li, W., Cao, W., Wang, J., Li, X., Xu, C., Shi, S., 2017. Effects of grazing regime on vegetation structure, productivity, soil quality, carbon and nitrogen storage of alpine meadow on the Qinghai-Tibetan Plateau. Ecol. Eng. 98, 123–133. https://doi.org/10.1016/j.ecoleng.2016.10.026

Liu, J., Isbell, F., Ma, Q., Chen, Y., Xing, F., Sun, W., Wang, L., Li, J., Wang, Y., Hou, F., Xin, X., Nan, Z., Eisenhauer, N., Wang, D., 2022. Overgrazing, not haying, decreases grassland topsoil organic carbon by decreasing plant species richness along an aridity gradient in Northern China. Agric. Ecosyst. Environ. 332, 107935. https://doi.org/10.1016/j.agee.2022.107935

Löffler, J., Pape, R., 2020. Thermal niche predictors of alpine plant species. Ecology 101, 1–18. https://doi.org/10.1002/ecy.2891

Ma, L., Derner, J.D., Harmel, R.D., Tatarko, J., Moore, A.D., Rotz, C.A., Augustine, D.J., Boone, R.B., Coughenour, M.B., Beukes, P.C., van Wijk, M.T., Bellocchi, G., Cullen, B.R., Wilmer, H., 2019. Application of grazing land models in ecosystem management: Current status and next frontiers. Adv. Agron. 158, 173–215. https://doi.org/10.1016/bs.agron.2019.07.003

Ma, S., Lardy, R., Graux, A.I., Ben Touhami, H., Klumpp, K., Martin, R., Bellocchi, G., 2015. Regional-scale analysis of carbon and water cycles on managed grassland systems. Environ. Model. Softw. 72, 356–371. https://doi.org/10.1016/j.envsoft.2015.03.007

Mara, F.P.O., 2012. The role of grasslands in food security and climate change 1263–1270. https://doi.org/10.1093/aob/mcs209

Meinshausen, M., Smith, S.J., Calvin, K., Daniel, J.S., Kainuma, M.L.T., Lamarque, J., Matsumoto, K., Montzka, S.A., Raper, S.C.B., Riahi, K., Thomson, A., Velders, G.J.M., van Vuuren, D.P.P., 2011. The RCP greenhouse gas concentrations and their extensions from 1765 to 2300. Clim. Change 109, 213–241. https://doi.org/10.1007/s10584-011-0156-z

Metzger, M.J., Bunce, R.G.H., Jongman, R.H.G., Mücher, C.A., Watkins, J.W., 2005. A climatic stratification of the environment of Europe. Glob. Ecol. Biogeogr. 14, 549–563. https://doi.org/10.1111/j.1466-822X.2005.00190.x

Moore, A.D., Ghahramani, A., 2014. Climate change and broadacre livestock production across southern Australia. 3. Adaptation options via livestock genetic improvement. Anim. Prod. Sci. 54, 111–124. https://doi.org/10.1071/AN13052

Morales, P., Hickler, T., Rowell, D.P., Smith, B., Sykes, M.T., 2007. Changes in European ecosystem

productivity and carbon balance driven by regional climate model output. Glob. Chang. Biol. 13, 108–122. https://doi.org/10.1111/j.1365-2486.2006.01289.x

Movedi, E., Bellocchi, G., Argenti, G., Paleari, L., Vesely, F., Staglianò, N., Dibari, C., Confalonieri, R., 2019a. Development of generic crop models for simulation of multi-species plant communities in mown grasslands. Ecol. Modell. 401, 111–128. https://doi.org/10.1016/j.ecolmodel.2019.03.001

Movedi, E., Bellocchi, G., Argenti, G., Paleari, L., Vesely, F., Staglianò, N., Dibari, C., Confalonieri, R., 2019b. Development of generic crop models for simulation of multi-species plant communities in mown grasslands. Ecol. Modell. 401, 111–128. https://doi.org/10.1016/j.ecolmodel.2019.03.001

Murphy, K.L., Burke, I.C., Vinton, M.A., Lauenroth, W.K., Aguiar, M.R., Wedin, D.A., Virginia, R.A., Lowe, P.N., 2002. Regional analysis of litter quality in the central grassland region of North America. J. Veg. Sci. 13, 395–402. https://doi.org/10.1111/j.1654-1103.2002.tb02063.x

Oates, L.G., Jackson, R.D., 2014. Livestock management strategy affects net ecosystem carbon balance of subhumid pasture. Rangel. Ecol. Manag. 67, 19–29. https://doi.org/10.2111/REM-D-12-00151.1

Orlandi, S., Probo, M., Sitzia, T., Trentanovi, G., Garbarino, M., Lombardi, G., Lonati, M., 2016. Environmental and land use determinants of grassland patch diversity in the western and eastern Alps under agro-pastoral abandonment. Biodivers. Conserv. 25, 275–293. https://doi.org/10.1007/s10531-016-1046-5

Ouled Belgacem, A., Louhaichi, M., 2013. The vulnerability of native rangeland plant species to global climate change in the West Asia and North African regions. Clim. Change 119, 451–463. https://doi.org/10.1007/s10584-013-0701-z

Parton, W.J., Ojima, D.S., Cole, C. V., Schimel, D.S., 1994. A general model for soil organic matter dynamics: sensitivity to litter chemistry, texture and management. Quant. Model. soil Form. Process. Proc. Symp. Minneapolis, 1992 147–167. https://doi.org/10.2136/sssaspecpub39.c9

Petriccione, B., Bricca, A., 2019. Thirty years of ecological research at the Gran Sasso d'Italia LTER site: Climate change in action. Nat. Conserv. 34, 9–39. https://doi.org/10.3897/natureconservation.34.30218

Pierce, D.W., Barnett, T.P., Santer, B.D., Gleckler, P.J., 2009. Selecting global climate models for regional climate change studies. Proc. Natl. Acad. Sci. U. S. A. 106, 8441–8446. https://doi.org/10.1073/pnas.0900094106

Piseddu, F., Bellocchi, G., Picon-Cochard, C., 2021. Mowing and warming effects on grassland species richness and harvested biomass: meta-analyses. Agron. Sustain. Dev. 41, 1–21. https://doi.org/10.1007/s13593-021-00722-y

Poggio, L., De Sousa, L.M., Batjes, N.H., Heuvelink, G.B.M., Kempen, B., Ribeiro, E., Rossiter, D., 2021. SoilGrids 2.0: Producing soil information for the globe with quantified spatial uncertainty. Soil 7, 217–240. https://doi.org/10.5194/soil-7-217-2021

Ponzetta, M.P., Cervasio, F., Crocetti, C., Messeri, A., Argenti, G., 2010. Habitat improvements with wildlife purposes in a grazed area on the Apennine Mountains. Ital. J. Agron. 5, 233–238.

https://doi.org/10.4081/ija.2010.233

Porro, F., Tomaselli, M., Abeli, T., Gandini, M., Gualmini, M., Orsenigo, S., Petraglia, A., Rossi, G., Carbognani, M., 2019. Could plant diversity metrics explain climate-driven vegetation changes on mountain summits of the GLORIA network? Biodivers. Conserv. 28, 3575–3596. https://doi.org/10.1007/s10531-019-01837-1

Pulina, A., Lai, R., Salis, L., Seddaiu, G., Roggero, P.P., Bellocchi, G., 2018. Modelling pasture production and soil temperature, water and carbon fluxes in Mediterranean grassland systems with the Pasture Simulation model. Grass Forage Sci. 73, 272–283. https://doi.org/10.1111/gfs.12310

Ren, S., Vitasse, Y., Chen, X., Peichl, M., An, S., 2022. Assessing the relative importance of sunshine, temperature, precipitation, and spring phenology in regulating leaf senescence timing of herbaceous species in China. Agric. For. Meteorol. 313, 108770. https://doi.org/10.1016/j.agrformet.2021.108770

Richter, K., Atzberger, C., Hank, T.B., Mauser, W., 2012. Derivation of biophysical variables from Earth observation data: validation and statistical measures. J. Appl. Remote Sens. 6, 063557–1. https://doi.org/10.1117/1.jrs.6.063557

Riedo, M., Grub, A., Rosset, M., 1998. A pasture simulation model for dry matter production , and fluxes of carbon , nitrogen , water and energy 105, 141–183.

Rounsevell, M.D.A., Brignall, A.P., Siddons, P.A., 1996. Potential climate change effects on the distribution of agricultural grassland in England and Wales. Soil Use Manag. 44–51. https://doi.org/10.1111/j.1475-2743.1996.tb00528.x

Ruti, P.M., Somot, S., Giorgi, F., Dubois, C., Flaounas, E., Obermann, A., Dell'Aquila, A., Pisacane, G., Harzallah, A., Lombardi, E., Ahrens, B., Akhtar, N., Alias, A., Arsouze, T., Aznar, R., Bastin, S., Bartholy, J., Béranger, K., Beuvier, J., Bouffies-Cloché, S., Brauch, J., Cabos, W., Calmanti, S., Calvet, J.C., Carillo, A., Conte, D., Coppola, E., Djurdjevic, V., Drobinski, P., Elizalde-Arellano, A., Gaertner, M., Galàn, P., Gallardo, C., Gualdi, S., Goncalves, M., Jorba, O., Jordà, G., L'Heveder, B., Lebeaupin-Brossier, C., Li, L., Liguori, G., Lionello, P., Maciàs, D., Nabat, P., Önol, B., Raikovic, B., Ramage, K., Sevault, F., Sannino, G., Struglia, M. V., Sanna, A., Torma, C., Vervatis, V., 2016. Med-CORDEX initiative for Mediterranean climate studies. Bull. Am. Meteorol. Soc. 97, 1187–1208. https://doi.org/10.1175/BAMS-D-14-00176.1

Sándor, R., Barcza, Z., Acutis, M., Doro, L., Hidy, D., Köchy, M., Minet, J., Lellei-kovács, E., Ma, S., Perego, A., Rolinski, S., Ruget, F., Sanna, M., Seddaiu, G., Wu, L., Bellocchi, G., 2017. Multi-model simulation of soil temperature , soil water content and biomass in Euro-Mediterranean grasslands : Uncertainties and ensemble performance 88, 22–40. https://doi.org/10.1016/j.eja.2016.06.006

Sándor, Renáta, Ehrhardt, F., Brilli, L., Carozzi, M., Recous, S., Smith, P., Snow, V., Soussana, J.F., Dorich, C.D., Fuchs, K., Fitton, N., Gongadze, K., Klumpp, K., Liebig, M., Martin, R., Merbold, L., Newton, P.C.D., Rees, R.M., Rolinski, S., Bellocchi, G., 2018. The use of biogeochemical models to evaluate mitigation of greenhouse gas emissions from managed grasslands. Sci. Total Environ. 642, 292–306. https://doi.org/10.1016/j.scitotenv.2018.06.020

Sándor, R., Picon-Cochard, C., Martin, R., Louault, F., Klumpp, K., Borras, D., Bellocchi, G., 2018. Plant acclimation to temperature: Developments in the Pasture Simulation model. F. Crop. Res.

222, 238–255. https://doi.org/10.1016/j.fcr.2017.05.030

Schippers, P., Van Groenendael, J.M., Vleeshouwers, L.M., Hunt, R., 2001. Herbaceous plant strategies in disturbed habitats. Oikos 95, 198–210. https://doi.org/10.1034/j.1600-0706.2001.950202.x

Schucknecht, A., Seo, B., Krämer, A., Asam, S., Atzberger, C., Kiese, R., 2022. Estimating dry biomass and plant nitrogen concentration in pre-Alpine grasslands with low-cost UAS-borne multispectral data-a comparison of sensors, algorithms, and predictor sets. Biogeosciences 19, 2699–2727. https://doi.org/10.5194/bg-19-2699-2022

Scocco, P., Piermarteri, K., Malfatti, A., Tardella, F.M., Catorci, A., 2016. Increase of drought stress negatively affects the sustainability of extensive sheep farming in sub-Mediterranean climate. J. Arid Environ. 128, 50–58. https://doi.org/10.1016/j.jaridenv.2016.01.006

Shrestha, S., Abdalla, M., Hennessy, T., Forristal, D., Jones, M.B., 2015. Irish farms under climate change - Is there a regional variation on farm responses? J. Agric. Sci. 153, 385–398. https://doi.org/10.1017/S0021859614000331

Smith, P., Martino, D., Cai, Z., Gwary, D., Janzen, H., Kumar, P., McCarl, B., Ogle, S., O'Mara, F., Rice, C., Scholes, B., Sirotenko, O., Howden, M., McAllister, T., Pan, G., Romanenkov, V., Schneider, U., Towprayoon, S., Wattenbach, M., Smith, J., 2008. Greenhouse gas mitigation in agriculture. Philos. Trans. R. Soc. B Biol. Sci. 363, 789–813. https://doi.org/10.1098/rstb.2007.2184

Snow, V.O., Rotz, C.A., Moore, A.D., Martin-Clouaire, R., Johnson, I.R., Hutchings, N.J., Eckard, R.J., 2014. The challenges - and some solutions - to process-based modelling of grazed agricultural systems. Environ. Model. Softw. 62, 420–436. https://doi.org/10.1016/j.envsoft.2014.03.009

Soussana, J.F., Allard, V., Pilegaard, K., Ambus, P., Amman, C., Campbell, C., Raschi, A., Baronti, S., Rees, R.M., Skiba, U., Stefani, P., Manca, G., 2007. Full accounting of the greenhouse gas (CO 2 , N 2 O , CH 4) budget of nine European grassland sites 121, 121–134. https://doi.org/10.1016/j.agee.2006.12.022

Stanisci, A., Frate, L., Morra Di Cella, U., Pelino, G., Petey, M., Siniscalco, C., Carranza, M.L., 2016. Short-term signals of climate change in Italian summit vegetation: observations at two GLORIA sites. Plant Biosyst. 150, 227–235. https://doi.org/10.1080/11263504.2014.968232

Steinfeld, H., Wassenaar, T., 2007. The Role of Livestock Production in Carbon and Nitrogen Cycles 271–296. https://doi.org/10.1146/annurev.energy.32.041806.143508

Tamburini, G., Aguilera, G., Öckinger, E., 2022. Grasslands enhance ecosystem service multifunctionality above and below-ground in agricultural landscapes. J. Appl. Ecol. 3061–3071. https://doi.org/10.1111/1365-2664.14302

Targetti, S., Messeri, A., Staglianò, N., Argenti, G., 2013. Leaf functional traits for the assessment of succession following management in semi-natural grasslands: A case study in the North Apennines, Italy. Appl. Veg. Sci. 16, 325–332. https://doi.org/10.1111/j.1654-109X.2012.01223.x

Tomozeiu, R., Pasqui, M., Quaresima, S., 2018. Future changes of air temperature over Italian

agricultural areas: a statistical downscaling technique applied to 2021–2050 and 2071–2100 periods. Meteorol. Atmos. Phys. 130, 543–563. https://doi.org/10.1007/s00703-017-0536-7

Toreti, A., Desiato, F., 2008. Temperature trend over Italy from 1961 to 2004. Theor. Appl. Climatol. 91, 51–58. https://doi.org/10.1007/s00704-006-0289-6

Touhami, H. Ben, Lardy, R., Barra, V., Bellocchi, G., 2013. Screening parameters in the Pasture Simulation model using the Morris method. Ecol. Modell. 266, 42–57. https://doi.org/10.1016/j.ecolmodel.2013.07.005

Vigan, A., Lasseur, J., Benoit, M., Mouillot, F., Eugène, M., Mansard, L., Vigne, M., Lecomte, P., Dutilly, C., 2017. Evaluating livestock mobility as a strategy for climate change mitigation: Combining models to address the specificities of pastoral systems. Agric. Ecosyst. Environ. 242, 89–101. https://doi.org/10.1016/j.agee.2017.03.020

Vital, J.A., Gaurut, M., Lardy, R., Viovy, N., Soussana, J.F., Bellocchi, G., Martin, R., 2013. High-Performance computing for climate change impact studies with the Pasture Simulation model. Comput. Electron. Agric. 98, 131–135. https://doi.org/10.1016/j.compag.2013.08.004

Vuichard, N., Soussana, J.F., Ciais, P., Viovy, N., Ammann, C., Calanca, P., Clifton-Brown, J., Fuhrer, J., Jones, M., Martin, C., 2007. Estimating the greenhouse gas fluxes of European grasslands with a process-based model: 1. Model evaluation from in situ measurements. Global Biogeochem. Cycles 21, 1–14. https://doi.org/10.1029/2005GB002611

Wang, Z., Ma, Y., Zhang, Y., Shang, J., 2022. Review of remote sensing applications in grassland monitoring. Remote Sens. 14.

Wepking, C., Mackin, H.C., Raff, Z., Shrestha, D., Orfanou, A., Booth, E.G., Kucharik, C.J., Gratton, C., Jackson, R.D., 2022. Perennial grassland agriculture restores critical ecosystem functions in the U.S. Upper Midwest. Front. Sustain. Food Syst. 6. https://doi.org/10.3389/fsufs.2022.1010280

Wilcke, R.A.I., Bärring, L., 2016. Selecting regional climate scenarios for impact modelling studies. Environ. Model. Softw. 78, 191–201. https://doi.org/10.1016/j.envsoft.2016.01.002

Xu, C., Liu, H., Williams, A.P., Yin, Y., Wu, X., 2016. Trends toward an earlier peak of the growing season in Northern Hemisphere mid-latitudes. Glob. Chang. Biol. 2852–2860, 2852–2860. https://doi.org/10.1111/gcb.13224

Zarrineh, N., Abbaspour, K.C., Holzkämper, A., 2020. Integrated assessment of climate change impacts on multiple ecosystem services in Western Switzerland. Sci. Total Environ. 708, 135212. https://doi.org/10.1016/j.scitotenv.2019.135212

Zhu, Y., Purdy, K.J., Eyice, Ö., Shen, L., Harpenslager, S.F., Yvon-Durocher, G., Dumbrell, A.J., Trimmer, M., 2020. Disproportionate increase in freshwater methane emissions induced by experimental warming. Nat. Clim. Chang. 10, 685–690.

Chapter 6.

General conclusions

Chapter 6 reports the general conclusions of the work carried out during the PhD, analyzing the results in light of the research questions.

PhD candidate's contribution:

Edoardo Bellini wrote all sections of the chapter.

6. General conclusions

The streamline of this doctoral research was grasslands monitoring and prediction by using different approaches (remote sensing and crop modelling), considering different contexts (natural and extensively managed grasslands), spatial scales (local, regional and continental), and timelines (present and future). The outcomes deriving from the different approaches were critically analysed, achieving important results through the development of new methodologies and the identification of key information for grassland knowledge and management. These results enabled the achievement of the main objective concerning the use of these technologies and methodologies to maintain the productive and ecosystem functionalities of the grassland system through optimized management, the estimation of already visible and future climate change impacts, and the identification of possible adaptation strategies.

As previously reported, the objectives pursued during the PhD course reported in this thesis were: (i) the development of a simplified grassland-specific simulation model that, through the use of remotely collected information, could faithfully reproduce the dynamics of the system and, potentially, take advantage of the spatial resolution offered by different optical sensors to obtain detailed information of the area under study; (ii) the identification of a methodology for extracting the start, peak, and end dates of the season from sets of satellite images and the quantification of the changes that have occurred in grassland phenology at the continental level over the past few decades; (iii) the analysis of the impacts of future climate on extensive grazing systems of the central Italian Apennines and the identification of management strategies to be adopted to cope with these changes.

Specifically, the first objective was achieved by developing a simplified simulation model based on the concept of light use efficiency, capable of using information collected in the form of vegetation indices from proximal or satellite instruments for data integration. The simplification provided by the NDVI index, which was used to directly estimate Leaf Area Index (LAI) through a relationship identified by correlating the index to LAI measured in the field, made it possible to obtain accurate results in the simulation of forage biomass and water dynamics of the system, particularly in the estimation of the fraction of transpirable water in soil (FTSW) and evapotranspiration. These results were achieved through a general calibration of a few parameters, obtained in a typical alpine grassland context, validated, with the exception of the parameters related to optimal growth temperatures, with forage biomass data collected in the field in two managed pastures in the central Apennines during two years of this PhD research activity.

In this way, the model developed can be used in diverse contexts and with the potential to exploit the spatial resolution provided by satellite imagery, thus prefiguring itself as a tool applicable by stakeholders for grassland management based on the principles of precision agriculture.

The second specific objective of this research thesis, aimed at studying the impacts of climate change already visible in grassland phenology, was investigated through the use of remote sensing technologies, specifically the use of vegetation indices (i.e. kNDVI) derived from satellite images. First, the methodology to be used to estimate the phenological dates of the beginning (SOS), peak (POS) and end (EOS) of the growing season was identified. Specific grasslands were used to compare phenological dates estimated from seasonal curves of vegetation indices and Gross Primary Production (GPP) data, a proxy for plant photosynthetic activity, extracted using different fitting models and extraction methods. The identified methodology, effective in detecting SOS and POS, but not EOS, was then applied on long time series of MODIS satellite images in 31 European grasslands, different in altitude and latitude, during the period 2001-2021. The study carried out revealed a significant trend of advancement in the start and peak of the growing season, especially accentuated in the former case. In parallel, an analysis of the average seasonal temperatures, which tended to increase during the period analysed, made it possible to emphasise the role of temperatures in the anticipation of these phenological dates, an anticipation that was found to be greater with increasing latitude and decreasing altitude. This research work led to the obtaining of important information on the changes in the growth pattern of vegetation already visible as a result of rising temperatures in recent decades. The results, attained through the use of remote sensing technologies, provide a comprehensive methodological line for the analysis of phenology from satellites and, above all, quantify the early onset and peak of the growing season of different European grassland sites. This type of information is an important indication for assessing the current phenological trend, allowing for an estimation of future phenological trends and providing the necessary tools for policymakers and stakeholders to provide for the identification of effective adaptation strategies.

The third line of research, aimed at assessing future climate impacts, was carried out using the PaSim simulation model as an analysis tool. The simulation model was calibrated with observed values of aboveground biomass and LAI allowing for a region-specific calibration. The calibrated model was then applied using as input data the results of future climate simulations of 14 GCM climate models, downscaled and bias-corrected, according to different time windows (i.e. 2011-2040, 2041-2070) and climate scenarios (RCP4.5 and 8.5). The analysis carried out provided important information on the future trend of the forage biomass in an extensive grazing context in the Apennine environment, as well as indications on the length of the growing season and the emission of climate-altering gases.

The results of future projections showed an increase in the growing season and forage production for both time windows and scenarios, with higher magnitudes for the 2041-2070 window and for the RCP8.5 scenario. The improved growing conditions, favoured by an increase in temperature and CO_2 concentration not accompanied by a significantly more severe water deficit than in the baseline, were the starting point for the identification of possible adaptation strategies. In particular, this production increase simulated by PaSim was sufficient to support an increase in the grazing season (+15%) and animal load (+20%) without incurring in lower biomass production compared to the baseline values. With regard to greenhouse gases emissions, PaSim estimated a rise in CH_4 emissions and a decline in N_2O emissions with future projections. The former depended on the increasing values of air temperatures, while the second relied on soil N level, which may have been reduced with increased plant demand. This rise in future biomass production, driven by the higher average annual GPP (Gross Primary Production), also led to a consequent decrease in simulated future NEE (Net Ecosystem Exchange). The study represents a significant step forward compared to previous studies on climate change impacts on Apennine grasslands by providing insights on future agronomic conditions and possible adaptation strategies. The adopted modelling approach has thus been demonstrated to be a useful tool to support the decisions that breeders will have to make in the near future.

In conclusion, the combination of remote sensing and modelling, used as analytical tools for the study of grasslands, has allowed us to pursue different lines of research, but always aimed at understanding and finding information that could be useful for preserving the productivity and functionality of the system. As described above for each specific objective, the various research works led to important insights on multiple topics, with particular reference to the current and future conditions of the system. New lines of research and future perspectives that can bridge the remaining limits of grassland research through remote sensing and modelling approaches can be identified in Chapters 3, 4 and 5 within their respective “Discussions” and “Conclusions” sections. However, it must be emphasised that barriers still exist in the adoption of these methodologies as operational tools to be used to maximise the impacts of research in grassland management.

However, the collected results have already highlighted the potential of these systems and technologies, which are foreshadowed, with the advancement of the level of technology and the state of research, as increasingly important tools for researchers, stakeholders and policy-makers in understanding the grassland system in its complexity.

Supplementary Materials

Table S1. Aboveground dry matter biomass (AGB) and leaf area index (LAI) collected in 2020 and 2021 in the two study-sites (sample mean and standard deviation of eight sub-samples in Marradi and four sub-samples in Borgo San Lorenzo).

Var.	Site M (Marradi)				Site B (Borgo San Lorenzo)							
					B1				B2			
	2020		2021		2020		2021		2020		2021	
AGB	doy	kg m^{-2}	doy	kg m^{-2}	doy	kg m^{-2}	doy	kg m^{-2}	doy	kg m^{-2}	doy	kg m^{-2}
	139	0.22±0.08	89	0.03±0.01	131	0.10±0.10	62	0.03±0.02	147	0.08±0.01	62	0.04±0.02
	154	0.18±0.09	138	0.09±0.04	147	0.04±0.05	110	0.08±0.04	161	0.13±0.04	100	0.05±0.01
	167	0.12±0.06	166	0.05±0.02	161	0.03±0.04	125	0.08±0.02	174	0.23±0.06	125	0.08±0.03
	180	0.07±0.03	202	0.03±0.02	174	0.02±0.02	152	0.15±0.08	188	0.15±0.06	152	0.17±0.12
	194	0.05±0.02	257	0.03±0.02	188	0.02±~0.00	165	0.10±0.09	202	0.19±0.11	165	0.12±0.03
	209	0.04±0.02	-	-	202	0.02±~0.00	188	0.07±0.06	286	0.04±0.03	188	0.13±0.08
	-	-	-	-	286	0.02±~0.00	244	0.03±0.03	-	-	244	0.06±0.04
	-	-	-	-	-	-	287	0.01±0.01	-		287	0.03±0.02
LAI	doy	m^2 m^{-2}	doy	m^2 m^{-2}	doy	m^2 m^{-2}	doy	m^2 m^{-2}	doy	m^2 m^{-2}	doy	m^2 m^{-2}
	154	1.67±0.85	89	0.72±0.27	161	0.42±0.44	62	0.21±0.25	161	1.30±0.84	62	0.28±0.39
	167	1.20±0.55	138	1.97±0.69	174	0.26±0.09	110	1.27±1.12	-	-	110	0.80±0.44
	180	0.82±0.56	166	1.12±0.69	202	0.12±0.12	125	1.36±0.66	188	2.56±1.21	125	0.80±0.47
	194	0.58±0.28	-	-	286	0.10±0.06	152	2.55±1.79	202	1.93±2.01	152	2.46±1.59
	209	0.70±0.30	-	-	-	-	165	0.58±0.19	286	0.52±0.40	165	1.22±0.39

Table S2. Climate models used in this study, an indication of their origin (institute), version, realisation and frequency. The suffixes i and p of each realisation (r) indicate the initialisation and physics indices, respectively.

Institute	Global Climate Model (GCM)	Experiment	Realisation	Regional Climate Model (RCM)	Frequency
CLMcom	CNRM-CERFACS-CNRM-CM5	RCP4.5	r1i1p1	CLMcom-CCLM4-8-17	day
		RCP8.5	r1i1p1		day
	ICHEC-EC-EARTH	RCP4.5	r12i1p1		day
		RCP8.5	r12i1p1		day
	MOHC-HadGEM2-ES	RCP4.5	r1i1p1		day

		RCP8.5	r1i1p1		day
	MPI-M-MPI-ESM-LR	RCP4.5	r1i1p1		day
		RCP8.5	r1i1p1		day
DMI	NCC-NorESM1-M	RCP4.5	r1i1p1	DMI-HIRHAM5	day
		RCP8.5	r1i1p1		day
IPSL-INERIS	IPSL-IPSL-CM5A-MR	RCP4.5	r1i1p1	IPSL-INERIS-WRF331F	day
		RCP8.5	r1i1p1		day
KNMI	ICHEC-EC-EARTH	RCP4.5	r1i1p1	KNMI-RACMO22E	day
	MOHC-HadGEM2-ES	RCP4.5	r1i1p1		day
		RCP8.5	r1i1p1		day
MPI-CSC	MPI-M-MPI-ESM-LR	RCP4.5	r1i1p1	MPI-CSC-REMO2009	day
		RCP8.5	r1i1p1		day
	CNRM-CERFACS-CNRM-CM5	RCP4.5	r1i1p1		day
		RCP8.5	r1i1p1		day
SMHI	ICHEC-EC-EARTH	RCP4.5	r12i1p1	SMHI-RCA4	day
		RCP8.5	r12i1p1		day
	IPSL-IPSL-CM5A-MR	RCP4.5	r1i1p1		day
		RCP8.5	r1i1p1		day
	MOHC-HadGEM2-ES	RCP4.5	r1i1p1		day
		RCP8.5	r1i1p1		day
	MPI-M-MPI-ESM-LR	RCP4.5	r1i1p1		day
		RCP8.5	r1i1p1		day

Table S3. Summary of the PaSim parameters considered for the calibration.

Parameters			Value
Name	**Description**	**Unit**	
Canopy height parameter 1 (*hcanhalf*)	This parameter expresses the leaf area index for which the canopy corresponds to half the maximum height.	$m^2\ m^{-2}$	4
Canopy height parameter 2 (*hcanmax*)	This is the height of the flowering plant, the highest leaf not being elongated.	m	1.203

Maximum specific leaf area (*slam*)	The maximum value of the specific leaf area is the maximum ratio of leaf area to dry weight, used to derive the canopy leaf area from the leaf biomass.	$m^2\ kg^{-1}$	27.2
Light-saturated leaf photosynthetic rate for reproductive stage (*pmco2rep*)	They represent the influence of developmental stage on the photosynthetic rate of light-saturated leaves (defined under standard conditions of temperature and atmospheric CO_2 concentration), which is a component of the photosynthetic rate of the canopy.	$\mu mol\ C\ m^{-2}\ s^{-1}$	12.88
Light-saturated leaf photosynthetic rate for vegetative stage (*pmco2veg*)		$\mu mol\ C\ m^{-2}\ s^{-1}$	9.49
Root turnover parameter (*kturnrt20*)	It is the root turnover rate at 20 °C.	d^{-1}	0.0155
Shoot turnover parameter (*kturnsh20*)	It is the shoot turnover rate at 20 °C.	d^{-1}	0.0468
Parameter of the fractional N content of new plant structural dry matter (*fnref*)	This parameter is used to derive the nitrogen concentration of the newly produced structural dry matter.	kg N kg^{-1} DM	0.033
Temperature dependence factor of the soil respiration (*kfactor*)	It multiplies the temperature-dependent function to estimate soil respiration.	-	2
Relative root distribution (*froot*)	This is the relative dry matter of the roots in the different soil layers (one value per soil layer).	%	0.095 0.297 0.238 0.145 0.195 0.030
Base temperature (*Tbase*)	This is the air temperature below which plant growth and development are nil.	K	277.94
Normalisation factor for development (*tasumrep*)	This parameter (which divides the sum of the thermal units) normalises the developmental stage index in such a way that a value 1 marks the transition from the reproductive to the vegetative stage.	K-d	734.3

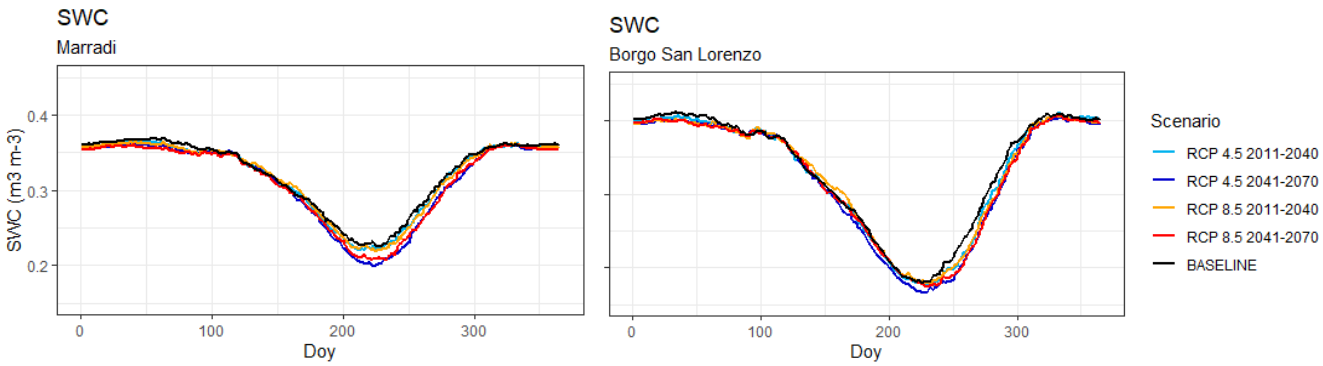

Figure S1. Daily simulation (30-year mean) of 0.35-m soil water content (SWC) with PaSim for baseline and climate-change scenarios under business-as-usual management at both study-sites. RCP4.5 and 8.5 are the different Representatives Concentration Pathways used in the simulations.

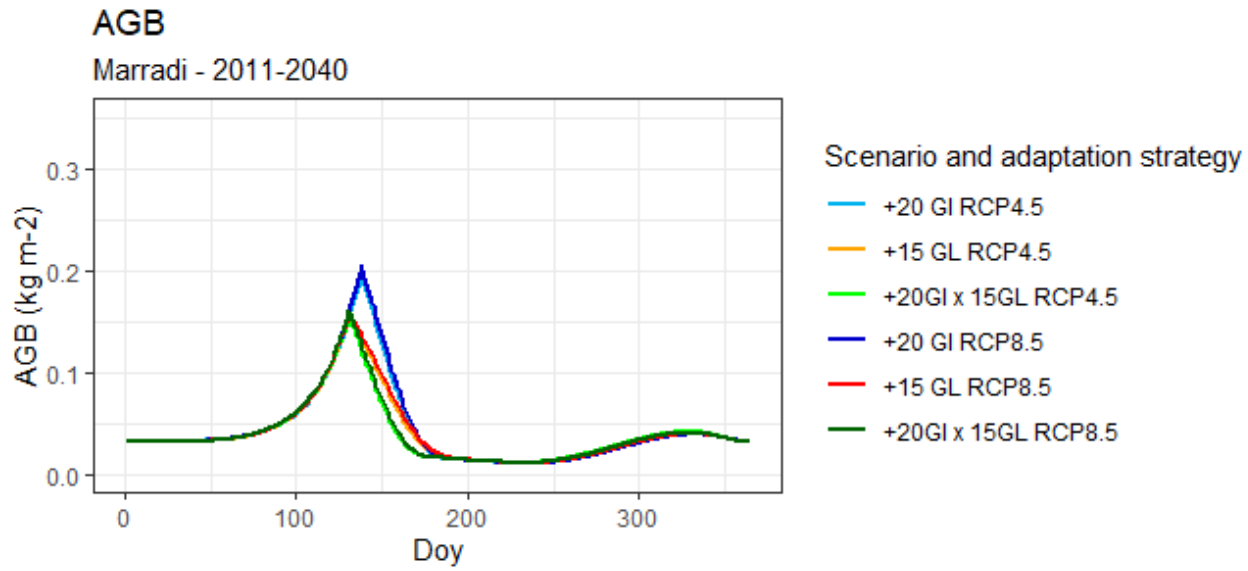

Figure S2. Daily simulation (30-year mean) of aboveground biomass (AGB) with PaSim for climate-change scenarios under different adaptation strategies at Marradi site for 2011-2040 period. +20 GI represent a 20% rise in animal stocking rate, 15 GL a 15% increase in grazing length and +20 GI×15 GL a combination of these two management factors. RCP4.5 and 8.5 are the different Representatives Concentration Pathways used in the simulations.

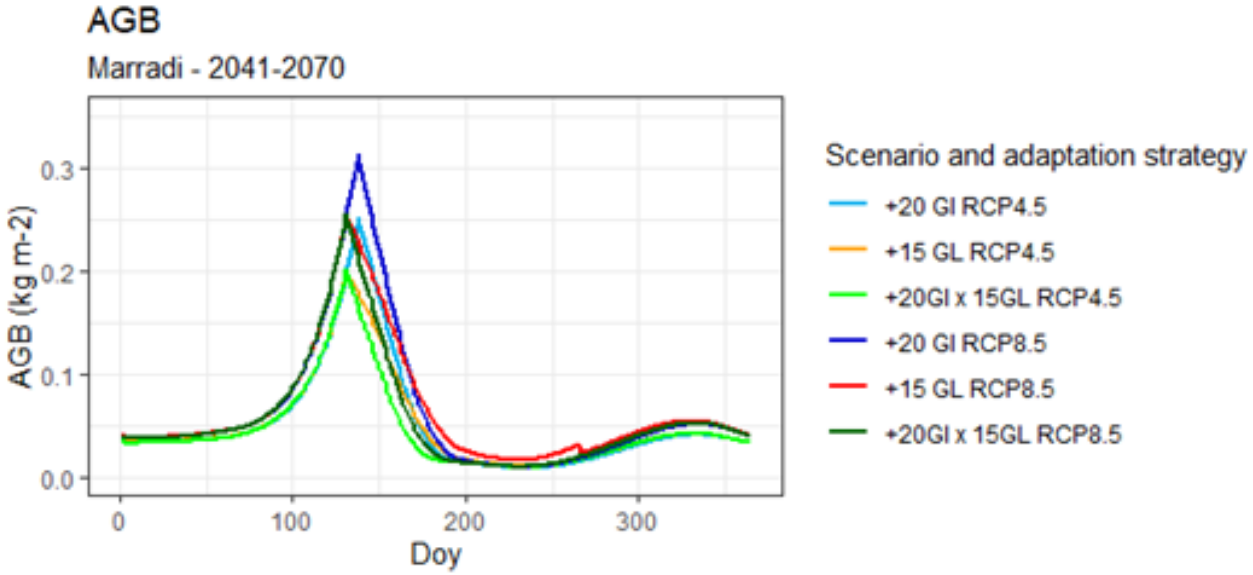

Figure S3. Daily simulation (30-year mean) of aboveground biomass (AGB) with PaSim for climate-change scenarios under different adaptation strategies at Marradi site for 2041-2070 period. +20 GI represent a 20% rise in animal stocking rate, 15 GL a 15% increase in grazing length and +20 GI×15 GL a combination of these two management factors. RCP4.5 and 8.5 are the different Representatives Concentration Pathways used in the simulations.

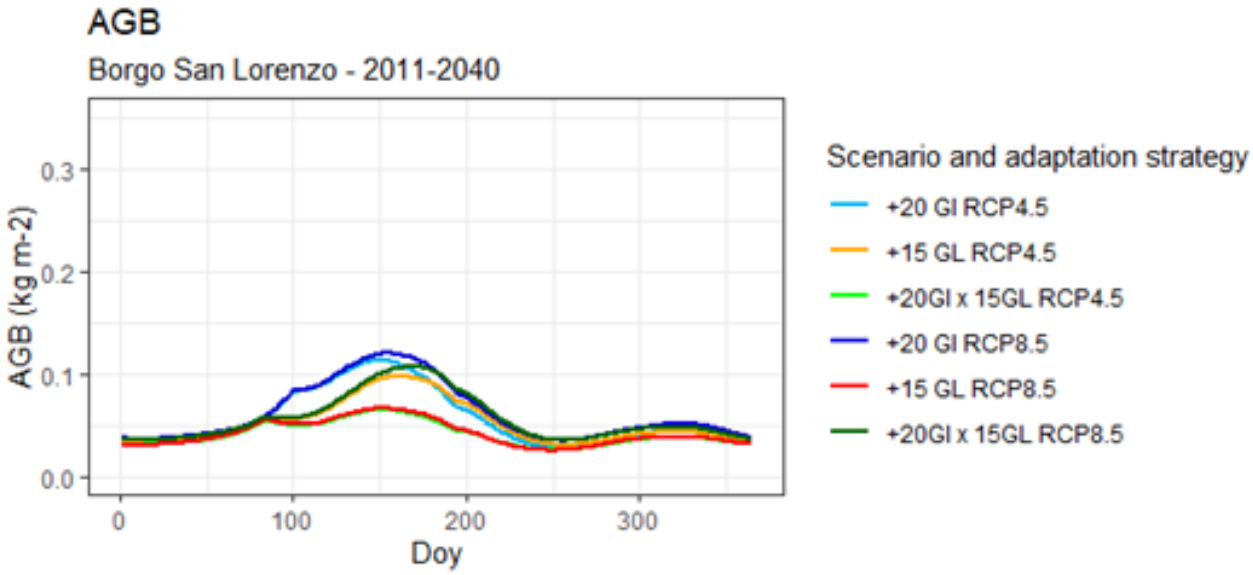

Figure S4. Daily simulation (30-year mean) of aboveground biomass (AGB) with PaSim for climate-change scenarios under different adaptation strategies at Borgo San Lorenzo site for 2011-2040 period. +20 GI represent a 20% rise in animal stocking rate, 15 GL a 15% increase in grazing length and +20 GI×15 GL a combination of these two management factors. RCP4.5 and 8.5 are the different Representatives Concentration Pathways used in the simulations.

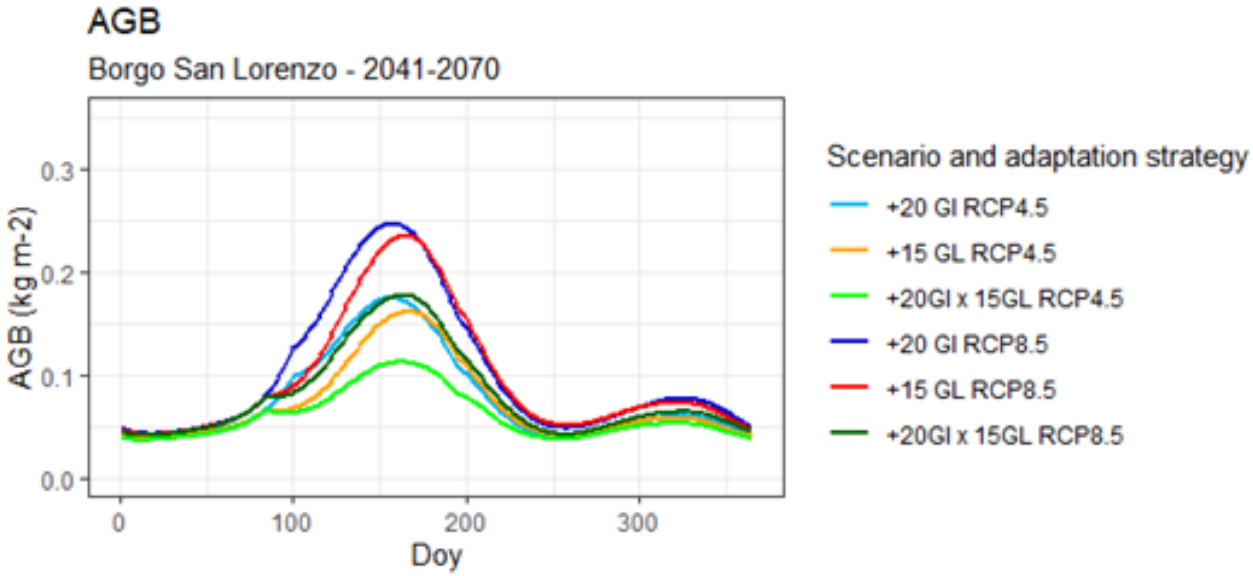

Figure S5. Daily simulation (30-year mean) of aboveground biomass (AGB) with PaSim for climate-change scenarios under different adaptation strategies at Borgo San Lorenzo site for 2041-2070 period. +20 GI represent a 20% rise in animal stocking rate, 15 GL a 15% increase in grazing length and +20 GI×15 GL a combination of these two management factors. RCP4.5 and 8.5 are the different Representatives Concentration Pathways used in the simulations.

Table S4. Simulated flux components (30-year mean) from the two study-sites for the baseline (1981-2010) and climate scenarios (RCP4.5 and RCP8.5) under different management options, estimated using PaSim (GPP: gross primary production; RECO: ecosystem respiration; NEE: net ecosystem exchange). +20 GI represent a 20% rise in animal stocking rate, 15 GL a 15% increase in grazing

length and +20 GI×15 GL a combination of these two management factors. RCP4.5 and 8.5 are the different Representatives Concentration Pathways used in the simulations.

Marradi		**CH_4**		**N_2O**		**GPP**		**RECO**		**NEE**	
		RCP4.5	RCP8.5	RCP4.5	RCP8.5	RCP4.5	RCP8.5	RCP4.5	RCP8.5	RCP4.5	RCP8.5
BAU	Baseline	2.2	2.2	4.7	4.7	337.3	337.3	718.7	718.7	381.3	381.3
	2011-2040	2.9	3.0	0.7	0.6	511.8	539.0	544.7	568.4	32.9	29.4
	2041-2070	3.5	3.9	0.4	0.3	716.5	962.4	701.3	911.2	-15.1	-51.2
+20 GI	2011-2040	2.7	2.9	0.7	0.7	469.5	491.3	505.0	523.9	35.5	32.6
	2041-2070	3.3	3.8	0.4	0.4	621.5	813.6	616.3	784.0	-5.2	-29.6
+ 15 GL	2011-2040	2.6	2.8	0.7	0.6	434.9	456.5	471.5	491.4	36.6	34.9
	2041-2070	3.4	4.0	0.4	0.3	602.1	837.0	595.4	797.0	-6.8	-39.9
+20 GI x 15 GL	2011-2040	2.5	2.6	0.7	0.7	404.2	422.2	443.1	459.6	38.9	37.3
	2041-2070	3.2	3.8	0.4	0.4	535.5	716.8	534.7	693.4	-0.8	-23.4

Borgo San Lorenzo		**CH_4**		**N_2O**		**GPP**		**RECO**		**NEE**	
		RCP4.5	RCP8.5	RCP4.5	RCP8.5	RCP4.5	RCP8.5	RCP4.5	RCP8.5	RCP4.5	RCP8.5
BAU	Baseline	1.8	1.8	4.6	4.6	509.4	509.4	859.5	859.5	350.1	350.1
	2011-2040	2.2	2.3	0.8	0.8	714.5	792.0	737.0	807.2	22.5	15.2
	2041-2070	2.5	2.7	0.4	0.4	965.0	1258.1	932.3	1187.9	-32.7	-70.3
+20 GI	2011-2040	2.4	2.5	0.7	0.7	610.3	679.6	632.9	695.8	22.6	16.2
	2041-2070	2.8	3.1	0.4	0.4	875.3	1185.0	844.7	1113.0	-30.5	-72.0
+ 15 GL	2011-2040	2.1	2.2	0.7	0.7	552.2	607.0	580.4	629.5	28.2	22.5
	2041-2070	2.5	2.8	0.4	0.4	807.3	1104.3	780.1	1036.3	-27.3	-68.0
+20 GI x 15 GL	2011-2040	2.1	2.1	0.7	0.7	445.4	459.0	477.8	489.5	32.4	30.5
	2041-2070	2.7	3.1	0.4	0.3	701.3	979.3	678.2	912.6	-23.1	-66.7

Acknowledgements

The writing of this PhD thesis represents the final work of a research activity carried out during my three years at the University of Florence. A certainly not easy path, which at the cost of great effort and commitment, however, has led to great satisfaction.

For the achievement of this important result, I would like to thank all the people who have been close to me, both in and outside of work.

First, I would like to thank Prof. Giovanni Argenti, Dr. Marco Moriondo, and Dr. Camilla Dibari for the opportunity I was given and the help and support they offered me during the course of my PhD.

Likewise, I would like to thank all the members of the EcoAgroMeteo research group, who have always assisted me whenever needed. Special thanks go to my friend Riccardo Rossi, who shared the PhD journey with me and helped me with constant support.

Many thanks also go to Prof. Gianni Bellocchi, for his welcome and help during my time abroad at the INRAE Institute of Clermont Ferrand, France.

In addition, I want to thank all the people who shared with me this PhD time outside the University, in particular my group of closest friends, Ander De Palas.

Finally, very great thanks to my family, especially my parents, Sauro and Rossella, who have always supported me in every possible way throughout all these years.

To all these people,

Grazie